Boronic Acids as Penicillinase Inhibitors

by

Juan F. Barquero

A dissertation submitted to the Graduate Faculty in Biochemistry in partial fulfillment of the requirements for the degree of Doctor of Philosophy, The City University of New York

2013

This manuscript has been read and accepted for the
Graduate Faculty in Biochemistry in satisfaction of the
dissertation requirement for the degree of Doctor of Philosophy.

Dr. Manfred Philipp_____
Chair of Examining Committee

_____ _____
Date

Dr. Edward Kennelly_____
Executive Officer

_____ _____
Date

Haiping Cheng, Ph.D._____

Miguel Cervantes-Cervantes, Ph.D._____

Richard Magliozzo, Ph.D._____

Susan Rotenberg, Ph.D._____

Supervisory Committee

THE CITY UNIVERSITY OF NEW YORK

Abstract

Boronic Acids as Penicillinase Inhibitors

by

Juan F. Barquero
Advisor: Dr. Manfred Philipp.

β-lactamases are enzymes produced by bacteria resistant to antibiotics. A common feature on beta lactam antibiotics is the beta-lactam ring. β-lactamases hydrolyze the β-lactam ring leaving the antibiotic inoperative. The advent of bacteria that are resistant to β-lactams has impelled researchers to find inhibitors for β-lactamases that mimic the lactam ring but do not get hydrolyzed. One group of these new antibiotics is the aryl boronic acids. The main reason the boronic acids have been chosen as potential drugs is their lack of toxicity and their easy excretion in the urine. One of the most important structural features of these compounds is their chemical and geometric fitness in the active site of β-lactamases. Boronic acids mimic the tetrahedral intermediate formed in the half-acylation reaction that occurs during the hydrolysis of the β-lactam ring. The major goal of the research presented here was to discover new aryl boronic acids inhibitors of penicillinases from the class A β-lactamases. To accomplish this goal, commercially available boronic acids that are manufactured for the Suzuki reaction were used. These compounds included fluorinated, chlorinated, brominated, carboxylated, nitrophenylated, pinacol-esterified and thiophene-carboxylated aryl boronic acid derivatives. Kinetic evaluations of each class of compounds were performed under pseudo first-order enzymatic reaction conditions and the inhibitory constants (Ki) were reported using nitrocefin as substrate for two enzymes: the in-house expressed β-lactamase BlaC and the β-lactamase from *Bacillus cereus* 569/H9 (Calbiochem) identified as TEM-116. The structure-activity relationship (SAR) showed

that the most potent inhibitors of BlaC β-lactamase were 2-carboxythiophene-5-boronic acid; 3,4,5-trifluorophenylboronic acid; 3-nitrophenytlboronic acid and 2,3,4,5-tetrafluorophenylboronic acid, Ki values of 1.2, 175.7, 213.9 and 228.6 micromolar respectively. In addition, SAR revealed that the most potent inhibitors for *Bacillus cereus* β-lactamase I were 2-carboxythiophen-5-boronic acid, 3-carboxyphenylboronic acid, 2-carboxythiophene-4-boronic acid, and 3-carboxy-4-fluorophenylboronic acid having Ki values of 1.1, 19.4, 46.5, and 47.1 micromolar respectively. To gain further insight into the molecular interactions between each class of inhibitors and their targeted enzymes docking experiments were performed using *Autodock Vina* program combined with *Sculpt* from MDL and followed by the molecular visualization of the protein-ligand complexes using *Swiss-PdbViewer* and *DiscoveryStudio* from Accelerys. The results conclusively show that some selective classes of aryl boronic acids are potent competitive inhibitors of BlaC and *Bacillus cereus* β-lactamase I and that they should be further considered for advanced drug discovery and improvement of treatment against antibiotic resistant bacteria. Furthermore, the discovery that 4,4'-DDT is an inhibitor of *Mycobacterium tuberculosis* β-lactamase, combined with *in silico* studies, suggests that further elaboration of this molecule may be one route to new inhibitors.

Acknowledgements

I would like to express my gratitude to Professor Manfred Philipp for having helped me throughout these years in the project. I would also like to thank my instructors at the Graduate School and University Center for their patient in my progress through the years. I would like to thank Dr. Lesley Davenport and Dr. Edward Kenelly, former and current directors of the Biochemistry Program, respectively, for their continuous encouragement to advance in my career. I would like to thank Judy Li for her patience and her diligence in remaining me of deadlines and requirements to get the job done. I would like to thank the members of the examining committee for their input during our meetings and their professionalism in the task at hand. I would like to thank my colleagues in the lab: Dr. Sheuli Sikder-Masiak, Dr. Janet González and Dr. Cristina Clement for all their help and insights in the subject matter.

I appreciate the support of the faculty at Lehman College since my undergraduate years. Big thank you to the crew at the stockroom at the Chemistry Department of Lehman College for helping me get what I needed in due time. Thank you all, thank you for being part of my journey.

Table of Contents

List of tables.

List of figures.

1. Introduction

1.1. β-Lactamases: Structure-function relationship and target for drug discoveries

It has come to the attention of the scientific community, the authorities and the public that infection by *Mycobacterium tuberculosis* is latent in approximately 2 billion people globally (Flores *et al.,* 2005); The incidence of tuberculosis has been increasing exponentially in the last decade, and that no new specific drug against tuberculosis has been found; After AIDS, the leading cause of mortality due to infection is tuberculosis, 2 to 3 million deaths per year on a global scale (Andries *et al,* 2005). The widespread use and misuse of antibiotics globally has aggravated the problem and has contributed to the emergence on new diseases and antibiotic resistant pathogens (Essack, 2001). Resistance to antibiotics by pathogens has been influenced by man in the last 60 years (Fisher *et al.,* 2005). β-lactam antibiotics have been known since the discovery of penicillin from *Penicillium notatum* by Alexander Fleming in 1927 (Deshpande *et al*., 2004). However, it is claimed that even before Fleming, Lister and Sanderson at Oxford utilized a fungal extract for localized wounds in 1911 (Deshpande *et al*., 2004). Soon after penicillin's clinical success, other antibiotics were developed such as streptomycin in 1943, chloramphenicol in 1947, chlortetracycline in 1948, neomycin in 1949, erythromycin in 1952 (Deshpande *et al*., 2004), and isoniazid in the 1950's. The first enzyme known to hydrolyze penicillin was the AmpC β-lactamase of *Escherichia coli* (Jacoby, 2009). Today 470 β-lactamases have been identified and classified into four groups from A to D (Verna *et al.,* 2013). The penicillins expanded to orally active penicillins, broad spectrum and enzymatically stable penicillins, and then the cephalosporins of three generations, the monobactams, carbapenems, β-

lactamase stable penicillins and cephalosporins, and β-lactamase inhibitors (Foye *et al.,* 1995). Commercially available penicillins are divided into groups (Foye *et al.,* 1995):

- Fermentation-derived penicillins: 6-aminopenicillin acid (6-APA), benzylpenincillin (penicillin G), phenoxymethylpenicillin (penicillin V).
- Penicillinase-resistant parenteral (administered by other channels than digestive track) penicillin: Methicillin.
- Penicillinase-resistant oral penicillins: Oxacillin, cloxacillin, dicloxacillin.
- Penicillinase-sensitive, broad-spectrum, parenteral penicillin: Carbenicillin, carindacillin, azlocillin, mezlocillin, ticarcillin, piperacillin, ampicillin, amoxicillin, and miscellaneus becamicillin, mecillinam.

Commercially-available β-lactamase inhibitors approved by the Food and Drug Administration (FDA) are: Sulbactam, tazobactam, clavulanate (Hugonnet and Blanchard, 2007), and cefepime (Barlow and Hall, 2003).

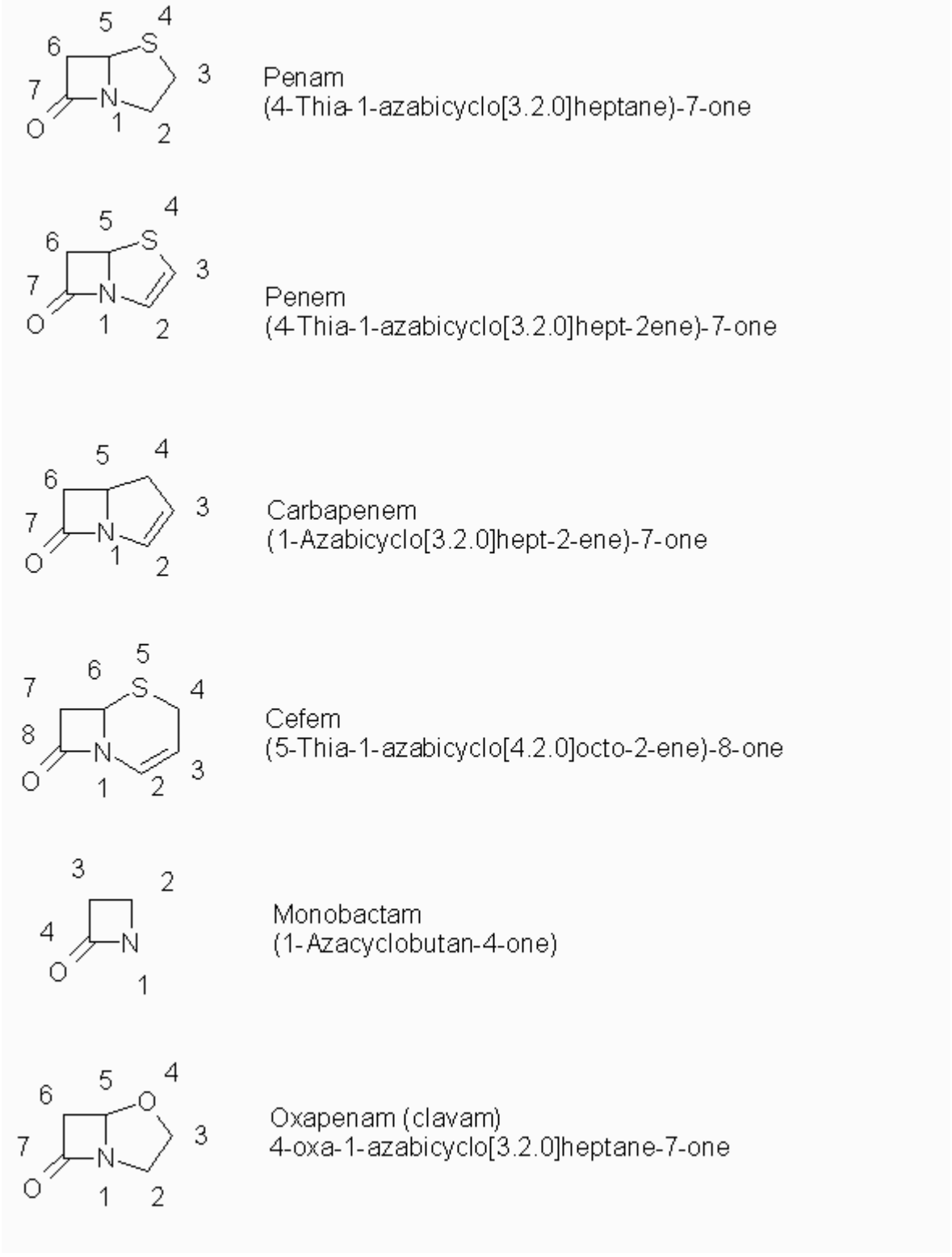

Figure 1: Core structure for clinically available β-lactams. (Foye, 1995). (Structures drawn in *IsisDraw*).

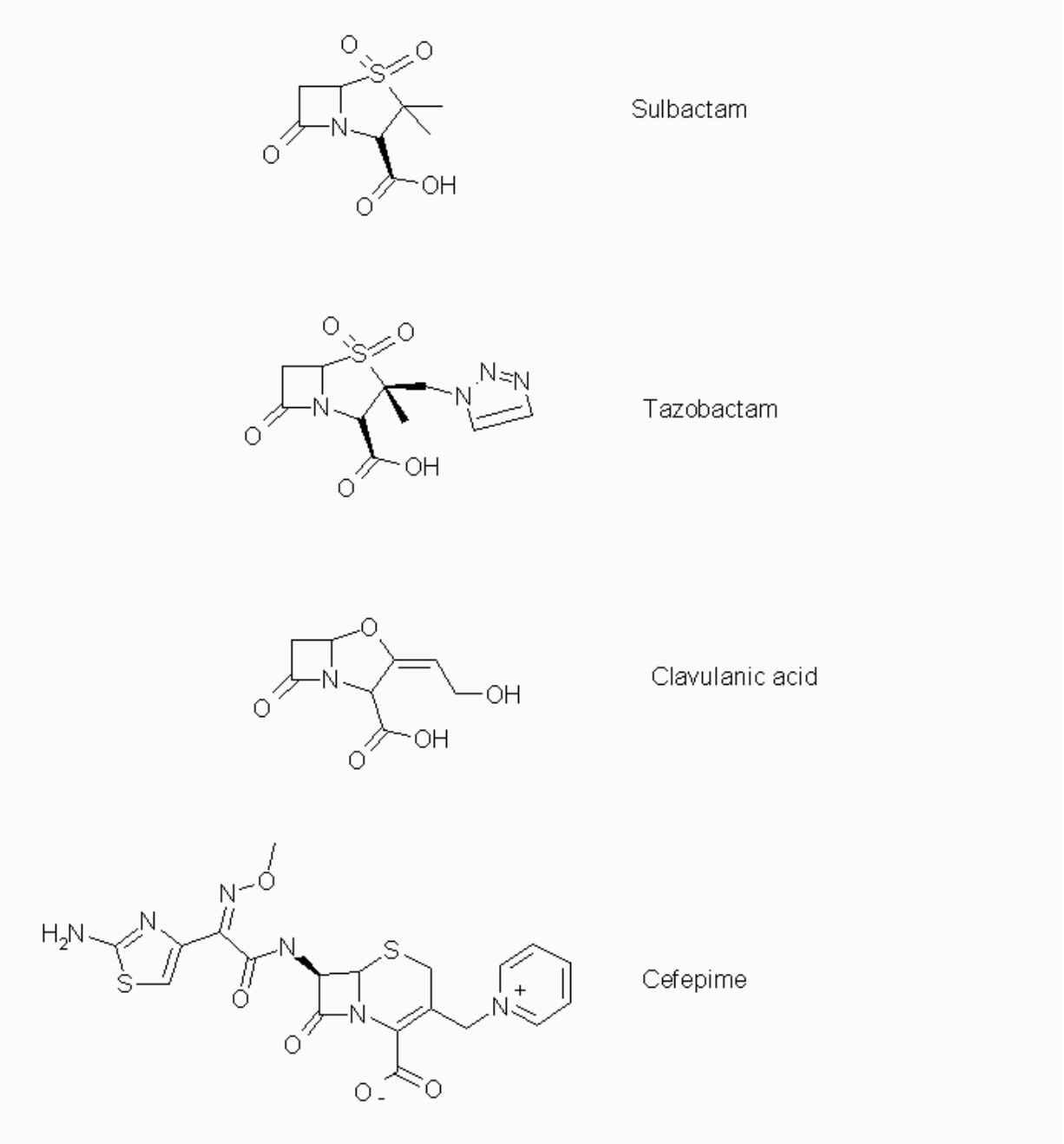

Figure 2: FDA-approved commercially available β-lactamase inhibitors. (Hugonnet and Blanchard, 2007, Barlow and Hall, 2003) (Structures drawn in *IsisDraw*)

β-lactamases are enzymes that hydrolyze the β-lactam ring, a common feature in antibiotics (Figure 1. b), rendering them inoperative. β-lactamases are the main cause of resistance to the attack of penicillin and the β-lactam in bacteria (Matagne *et al*., 1998). The growing numbers of bacteria that are becoming antibiotic-resistant are of major concern (World Health Organization,

2007). Their great adaptability makes them diverse and difficult to eliminate (Fisher *et al.,* 2005). The enzyme that bacteria produce, β-lactamase, disables β-lactams before they reach their target.

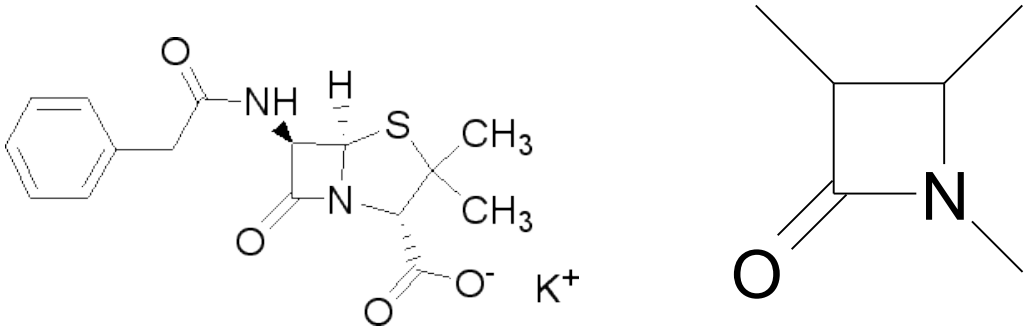

Figure 3: Penicillin-G and a β-lactam ring. a) Penicillin-G potassium salt. (From Sigma Aldrich.com website) (Lee, 2005). b) β-lactam ring. (Picture drawn in *Isis Draw* from MDL).

The cell wall

The cell wall in bacteria is a complex rigid structure, which function is to protect the cell from lysing when the water pressure increases inside the cytoplasm and to protect it from the environment. It is a macromolecular complex of peptidoglycan (also called murein).

The backbone of the peptidoglycan is formed by a disaccharide *N*-acetylglucosamine (NAG) and *N*-acetylmuramic acid (NAM) linked by a β-1,4 glycosidic bonds, in rows of 10 to 65 sugars. Adjacent rows are linked by polypeptides that may change in length, but always include tetrapeptides (Tortora, 1998). Depending on the structure of the cell wall bacteria have been classified as Gram-positive and Gram-negative bacteria. Gram-positive remain purple after alcohol is removed in the last step of the Gram stain procedure developed in 1884 by the Danish bacteriologist Hans Christian Gram (Tortora, 1998). Gram-positive cell wall contains several peptidoglycan layers making them susceptible to the attack of penicillin. Gram-negative cell wall

contains one or just a few layers of peptidoglycan in an intermembrane space, called periplasmic space, between an outer membrane and the cytoplasmic membrane. The outer membrane is impermeable to penicillin (Tortora, 1998). β-lactamase shows in the periplasmic space in Gram-negative bacteria and in the cell surface of Gram-positive bacteria (Foye, 1995).

β-lactamases are classified as Class A, B, C and D (Salverda *et al.*, 2010). R.P. Ambler from the Department of Molecular Biology, University of Edinburgh, proposed in 1980 the separation of β-lactamases into two groups, namely Class A and Class B. The properties he used to classify the β-lactamases were: "(1) isoelectric point, (2) molecular mass, (3) relative activity towards β-lactams, (4) interaction with inhibitors and inactivators, (5) the nature of the active site, (6) amino acid sequence, and (7) three-dimensional structure" (Ambler, 1980). In the Class A he included the β-lactamases with masses around 29,000 D, *Staphylococcus aureus* PC1, *Bacillus licheniformis* 749/C, *Bacillus cereus* 569/H β-lactamase I, and *Escherichia coli* R-TEM. In Class B β-lactamases he included *Bacillus cereus* II which is a Zn^{2+}-dependent enzyme, and with a lower molecular weight of around 23,000 (Ambler, 1980). Class A, C (AmpC β-lactamases), and D (Oxa β-lactamases) are serine enzymes, whereas Class B and its subgroups B1, B2, and B3 are metallo- enzymes (Hall and Barlow, 2005).

The evolutionary relationship among enzymes in this classification is depicted in figure 4, and a more detail phylogenic tree of class A β-lactamases is given in figure 5. The phylogenetic tree by Hall and Barlow (2004) indicates that divergence of Class C β-lactamase came before divergence of Class A and D β-lactamases and that they are relative to the DD-peptidases. Moreover, Class C has evolved in the same path without splitting into other classes. This tree
is based on homology of the amino acid at positions the 3D structure of the enzyme not the sequence, therefore, it is a structure-based tree (Hall and Barlow, 2004).

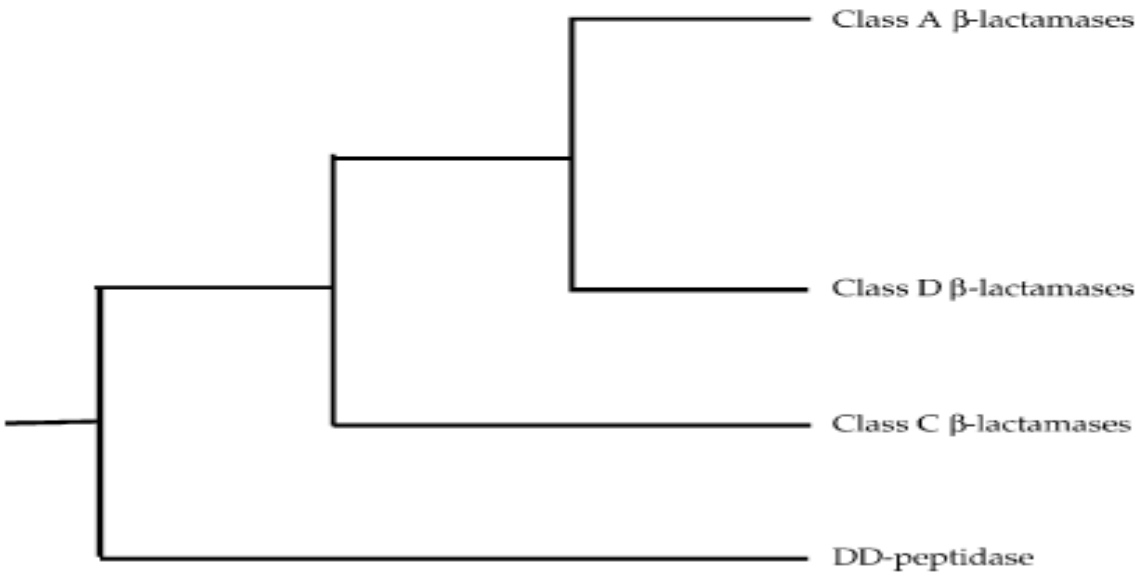

Figure 4: Phylogenetic tree for the evolution of β-lactamases (From Hall and Barlow, 2004). Line length does not represent time or nucleotide distance, it only represents the divergence to different paths by the different classes of β-lactamases.

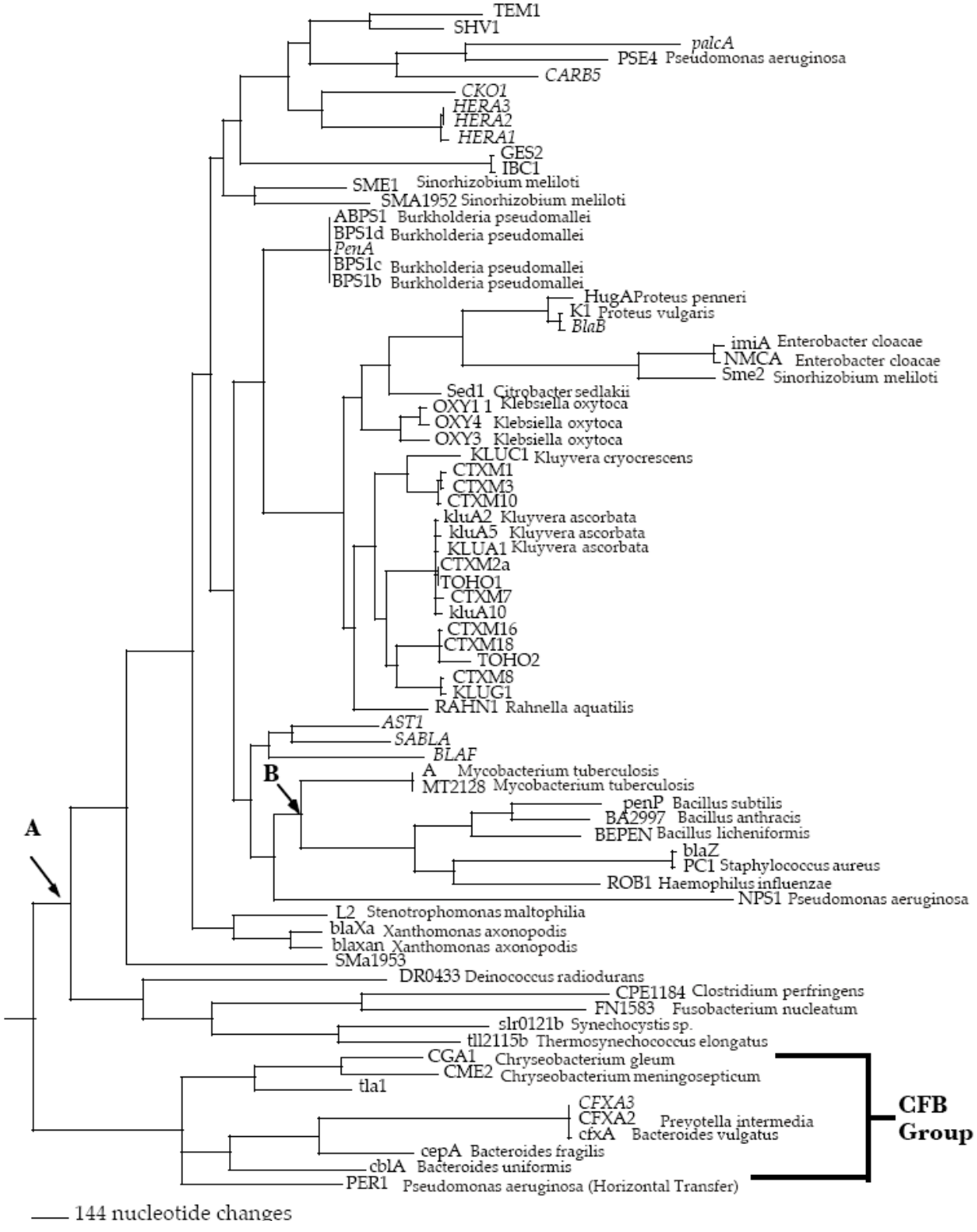

Figure 5: Phylogenetic tree of the class A β-lactamase (From Hall and Barlow, 2004).

Figure 5 shows the relationship among Class A β-lactamases. The scale is noted at 144 nucleotide change per length of bar. CFB group is *Cytophaga-Flexibacter-Bacteroides* which is the group containing the genes CGA1, CME2, and CFXA2. Node A indicated divergence of Gram-positive from Gram negative bacteria and then in B horizontal transfer from Gram-negative into Gram-positive bacteria. *Mycobacterium tuberculosis* is a Gram-positive bacterium, and *Haemophilus influenzae* a Gram-negative bacterium. The TEMs and their cousin SHV1 are from Gram-negative bacteria. TEM and the SHVs according to the tree diverged from each other 300 to 400 million years ago, the CTX-M 200 to 300 million years ago. Node A occurred 2.2 billion years ago and node B occurred 800 million years ago. Because these genes have been in the bacteria for millions of years shouldn't be of surprise, the fact that they are expressed as a response to the use of β-lactam antibiotics in medicine and in agriculture. (Hall and Barlow, 2004).

The need for β-lactamase production by the antibiotic resistant bacteria is due to the work of penicillin, as well as other β-lactams, in interfering with cell wall formation. This occurs in the last reaction in cross-linking of the two strands of peptidoglycans: the deacylation half reaction (Figure 5). The enzymes that catalyze the cross-linking of the peptidoglycans are penicillin binding protein or transpeptidases (PBP). An example of PBP is the structure with accession number 2BCF in Pubmed databases (Figure 32 a).

The sequence of events that led to this type of research is as follows: 1) Bacteria would build cell walls with the use of the PBPs. The PBPs cross link two peptidoglycan strands in which a D-Ala-D-Ala terminus is cleaved thus losing one D-Ala in a serine acylation half reaction, then in a deacylation half reaction this D-Ala terminus would be transferred to an amine substituent in a second peptidoglycan (Fisher *et al*., 2005). 2) Antibiotics, such as penicillin-G and the β-lactams

(Figure 1), inhibit PBPs (Figure 32 a). Penicillin and the beta lactams mimic the central portion of this newly formed peptide. The carbonyl on the C-terminus of D-Alanine is mimicked by the lactone carbonyl of the β-lactam ring in Penicillin. Transpeptidases then acylate the lactone carbonyl of the β-lactam ring instead of the carbonyl of the peptidoglycan (Fisher *et al*., 2005). 3) Bacteria respond to this attack by the β-lactams by expressing enzymes that mimic the PBPs active site and attack the lactone carbonyl of the β-lactams hydrolyzing the amide bond of the ring. The antibiotic would no longer resemble the junction of the peptidoglycans in the cell wall and the PBPs carry on with acylation-deacylation reactions to cross-link the peptidoglycans. These enzymes that mimic the PBPs are the β-lactamases (Figure 32b), and the bacteria producing them become antibiotic resistant (Fisher *et al*., 2005). 4) In response to the appearance of new β-lactamases, researchers are compelled to look for compounds that resemble the penicillin system, but would not be hydrolyzed by β-lactamases. Boronic acids are part of such compounds.

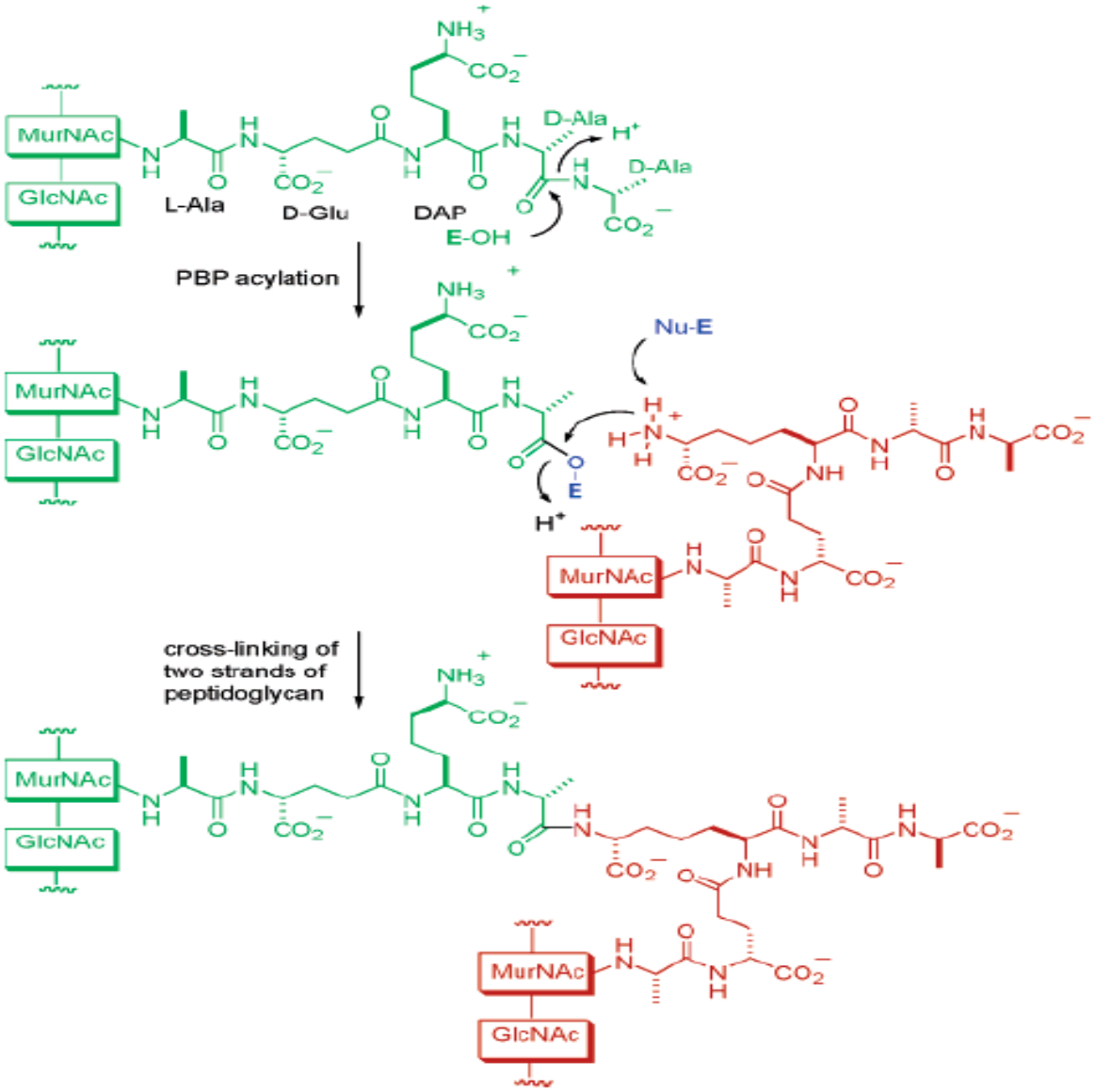

Figure 6: Schematics of PBP acylation reaction (From Fisher *et al.*, 2005). The scheme shows the acylation half reaction in which the enzyme reacts via nucleophilic attack of the C-*terminus* of a D-Ala in the pentapeptide *N*-acetylmuramic acid (NAM) assembled with *N*-acetylglucosamine (NAG) as NAG-NAM and hydrolyzes the peptide bond. The resulting acylated species is transferred to an amino group of the nearby chain. The structure in the junction of this new peptidoglycan the D-Ala-D-Ala portion of the first strand of the peptidoglycan and the diaminopimelate portion of the second strand is mimicked in part by β-lactams. (Fisher *et al*., 2005)

Because of ever-evolving pathogens, it is of the highest importance to find new compounds that would inhibit the β-lactamases.

The PBPs and class A β-lactamases share conserved positions; they have the same amino acid side chains in the same residue position, in the amino acid sequence (Figures 6, 7 and 8). For the structure BlaC (accession number 3CG5) the first 40 residues are missing as a truncated leading sequence (Tremblay *et al*., 2008). This is why Ser70 is Ser42 in 3CG5 (Table 5).

D-Ala-D-Ala-peptidases (DD-peptidases) or PBPs and class A β-lactamases share structural elements in the active site which are: 1st element, Ser-Xaa-Xaa-Lys; 2nd element, Ser-Xaa-Gly; 3rd element, Glu-Xaa-Glu-Leu-Asn, and the 4th element or Omega (Ω) loop, Glu-Xaa-Glu-Leu-Asn *(1)*. (Table 5, Figures 6, 7 and 8).

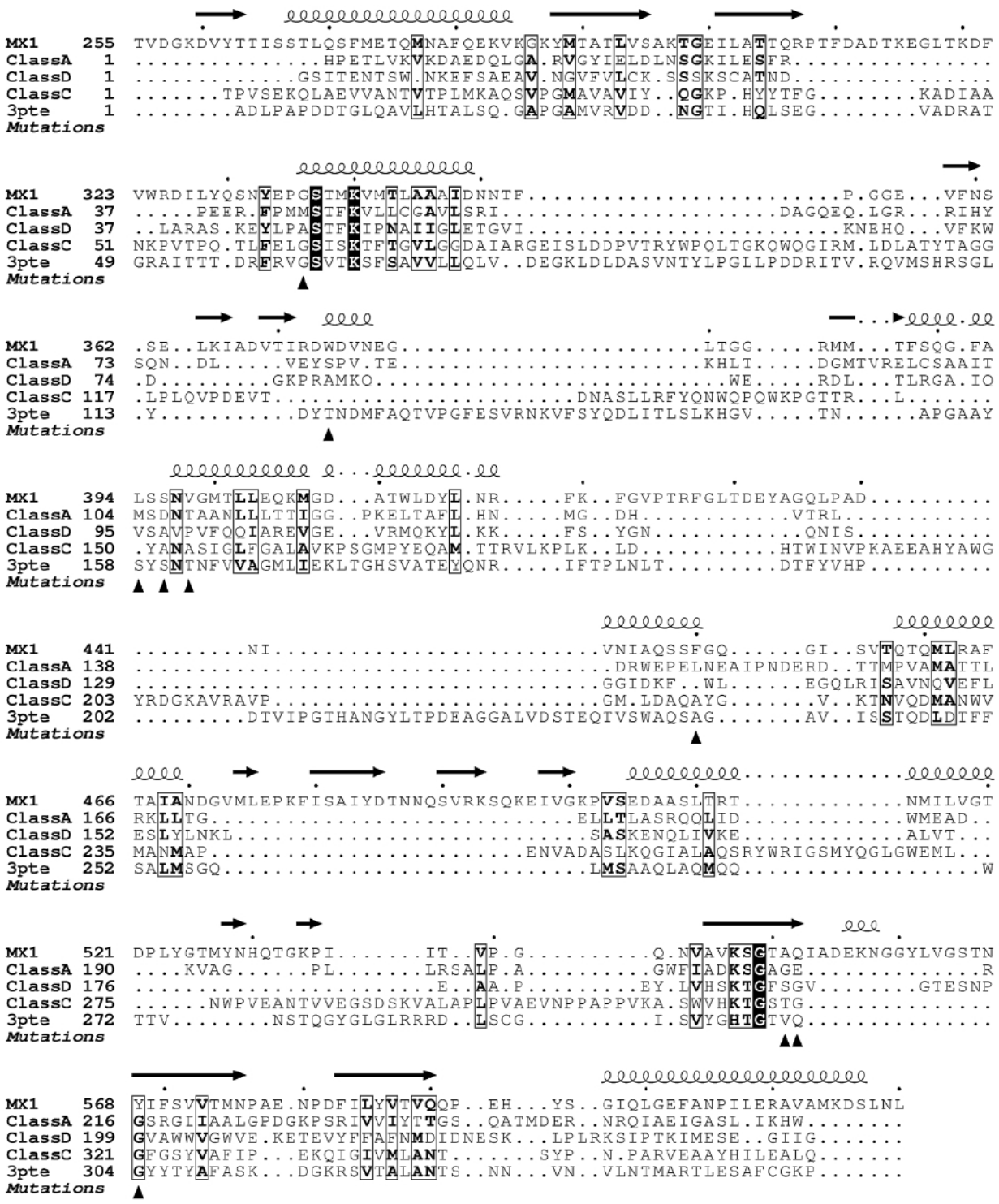

Figure 7: Sequence alignment of MX1 and 3pte as peptidases with 1btl, 1fof and 1gce as class A, class C and Class D β-lactamases respectively (From Peimbert and Segovia, 2003). Shaded letters indicate strictly conserved residues, homologous residues in boxes and the triangular shapes indicate residues mutated in C library. Secondary structural elements are shown (Peimbert and Segovia, 2003).

	Amino acid at position													
β-Lactamase	37	45	66	**70**	**73**	81	107	**130**	131	**132**	134	136	144	156
ABL consensus*	Glu	Gly	Phe	**Ser**	**Lys**	Leu	Pro	**Ser**	Asp	**Asn/ (Ser)**	Ala	Asn	Gly	Gly
M. tuberculosis										Gly				
N. lactamadurans	Gln													
P. vulgaris														Asn
L. enzymogenes													Asn	
Per-1/Per-2†	Val											Asp		
B. uniformis (cblA)	Leu											Asp		Ser
B. fragilis (cepA)	Ile		Tyr			Ala						Asp		
B. vulgatus (ctxA)‡	Val		Tyr			Cys							Asn	Pro
Sme-1/NmcA/IMI-1														

	Amino acid at position												
β-Lactamase	157	164	**166**	169	179	180	199	207	233	**234**	**235**	236	References
ABL consensus*	Asp	Arg	**Glu**	Leu	Asp	Thr	Leu	Leu	Asp	**Lys/ (Arg)**	**Thr/ (Ser)**	Gly	[58,140,158,165,176–178]
M. tuberculosis		Ala											[179]
N. lactamadurans													[158]
P. vulgaris													[158,159,180]
L. enzymogenes													[158]
Per-1/Per-2†	Ile/Val	Ala		Met	Asn	Trp			His				[151,161]
B. uniformis	Ile	Glu		Met	Asn	Trp	Phe		His				[160]
B. fragilis	Ile	His		Met	Asn	Trp	Phe	Ile	His				[160]
B. vulgatus (ctxA)‡	Arg	Tyr		Met	Asn	Tyr	Ile	Ile	His				[160,161]
Sme-1/NmcA/IMI-1								Tyr					[169,171]

Figure 8: Consensus in class A β-lactamases (From Matagne *et al.*, 1998). It shows the conserved residues in Class A β-lactamases. *Mycobacterium tuberculosis* β-lactamase shows Gly at position 132 instead of Asn. Ser is found in *Bacillus cereus* III, in three carbenicillin hydrolyzing enzymes. *P. mirabillis* GN79 shows Arg at position 234 instead of Lys.

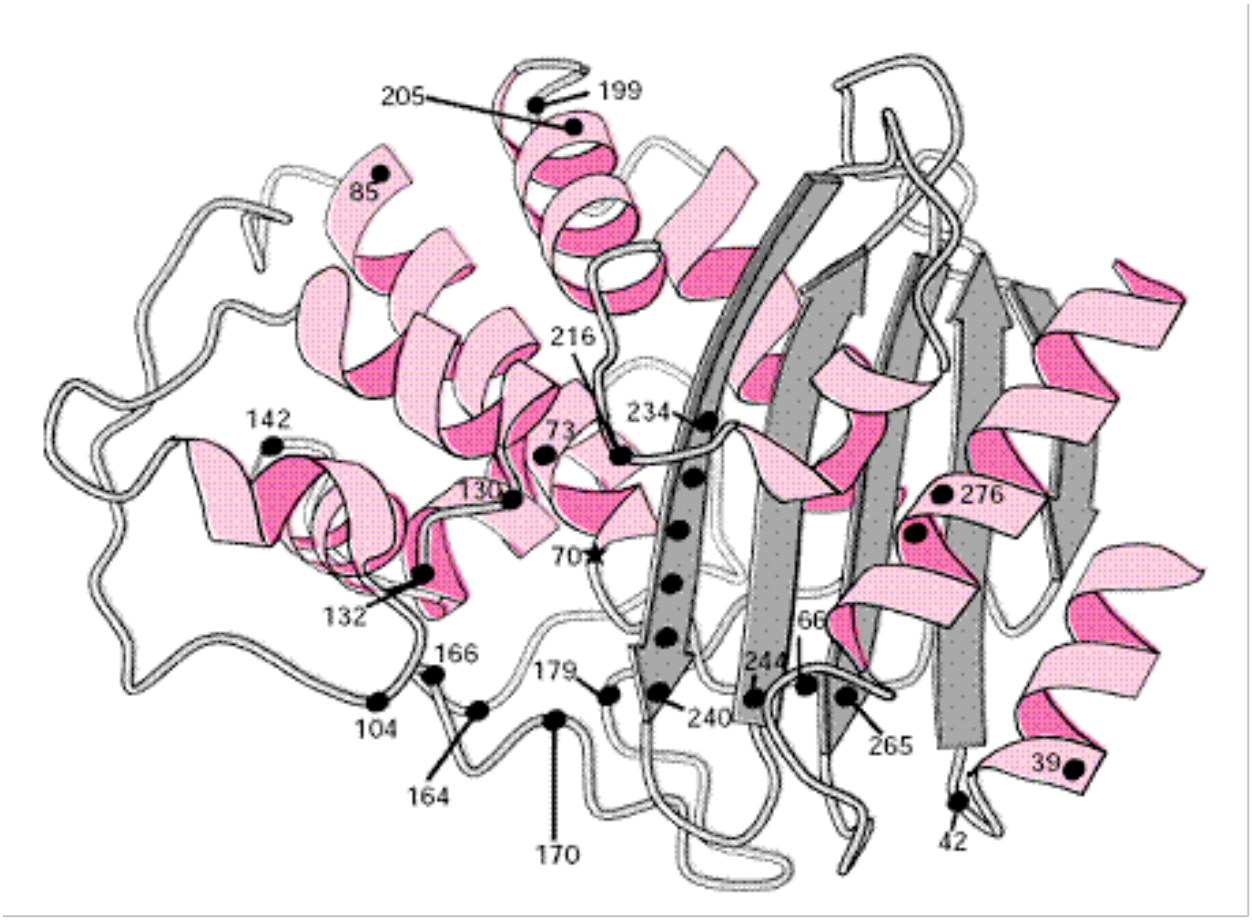

Figure 9: A class A TEM β-lactamase (From Metagne *et al*., 1998). The numbers indicated in the picture correspond to conserved positions in the PBPs and the class A β-lactamases.

1.2. The β-lactamase substrate and the mechanism of the enzyme catalyzed reaction

1.2.1 Nitrocefin as a substrate.

The natural substrates for β-lactamases are penicillins or β-lactams (Weston *et al*., 1998). The structural element common to all β-lactams is the four-membered lactam ring (Figure 1) that can either be alone or fused with another ring as in cephalosporins (Weston *et al.,* 1998) (Figure 12) . This lactam ring is found in nitrocefin, which is a cephalosporin.

Nitrocefin is hydrolyzed to produce absorbance at 492 nm and 494 nm as determined spectrophotometrically. After hydrolyzing nitrocefin, the product diffuses out of the active site producing a pale pink color.

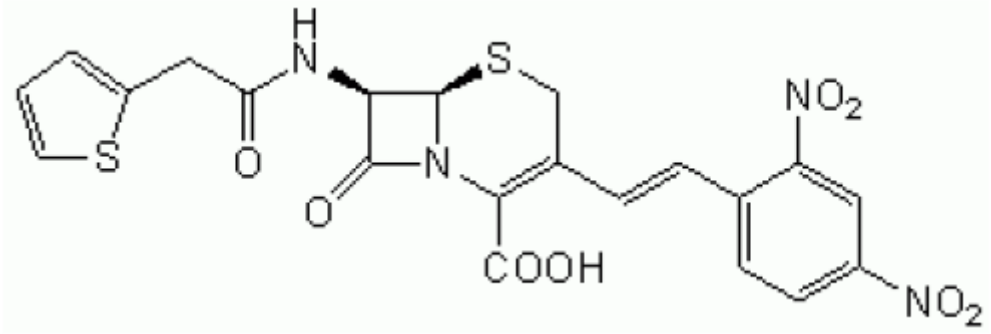

Figure 10. Nitrocefin structure (From Calbiochem Data Sheet).
3-(2,4-Dinitrostyryl)-(6R, 7R)-7-(2-thienylacetamido)-ceph-3-em-4-carboxylic Acid, E-isomer (EMDMillipor.com from EMD Group)

Nitrocefin belongs to the family of the cephalosporins. They contain a dihydrothiazine ring fused to the beta lactam ring. A general structure for cephalosporins is:

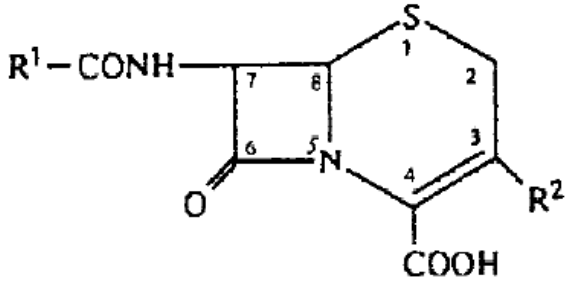

Figure 11. General structure for cephalosporins (From Essack, 2001). Cephalosporins are characterized by the β-lactam ring fused to a dihydrothiazine ring (Essack, 2001).

1.2.2. Hydrolysis of penicillin by β-lactamase

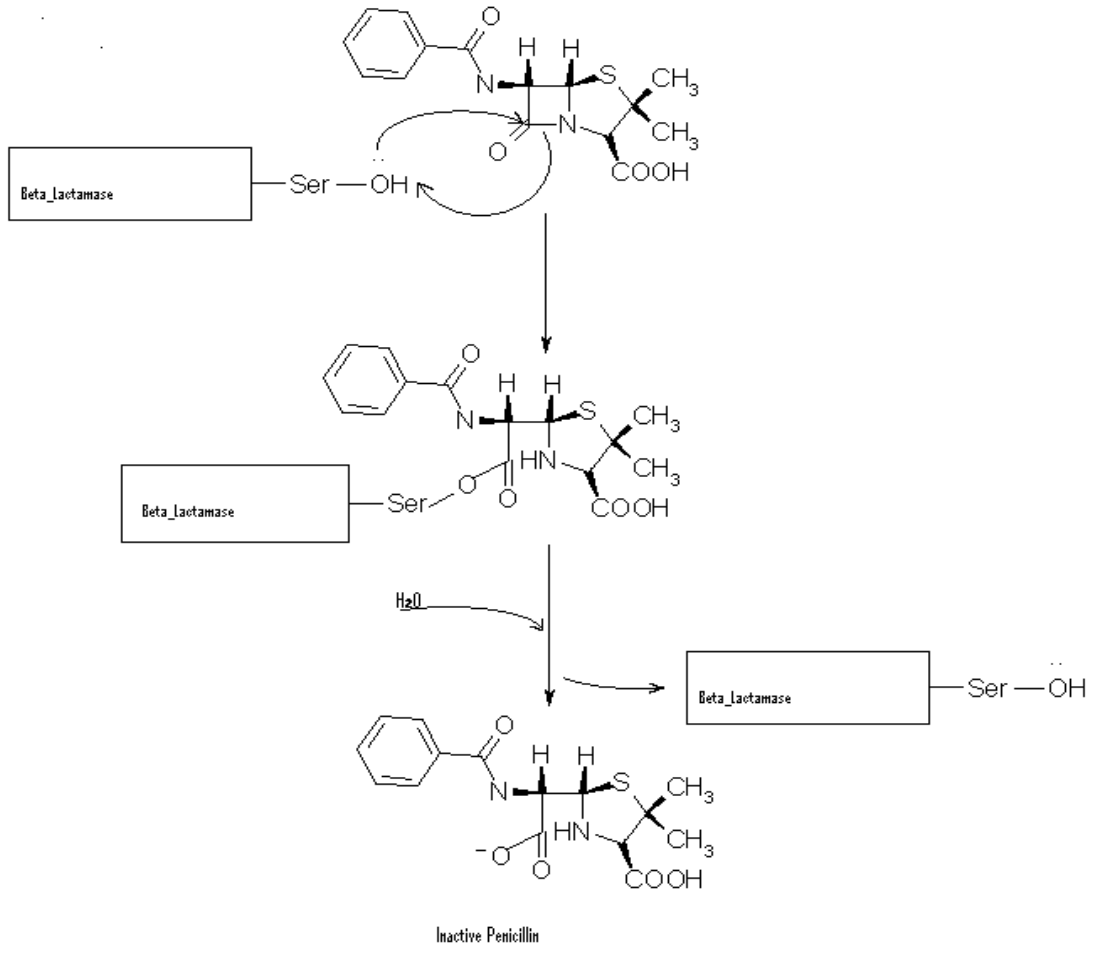

Figure 12: Scheme for hydrolysis of a penicillin by a serine β-lactamase (Nelson and Cox, 2008).

1.2.2.1. Acylation half reaction

An *ab initio* quantum mechanical/molecular mechanical study (QM/MM) calculations of class A β-lactamase acylation by Meroueh *et al*. (2005) determined that the long accepted acylation model in which Glu166 acts as a general base through a conserved water molecule is in competition with a process in which Lys73 is the base that abstracts the proton from Ser70 to activate it for catalysis. Molecular dynamics simulations then reveal that at the next step Ser130 and Lys73 conjugated acid are the source of protons. Ser130 protonates the nitrogen of the β-

lactam ring, Lys73 conjugated acid protonates Ser130, and Glu166 in the protonated form serves as the ultimate proton donor. This process drives the collapse of the beta lactam ring and the tetrahedral intermediate. According to Meroueh *et al.,* among 133 clinical variants of TEM-1 β-lactamases, no mutations are observed at Lys73 or Glu166.

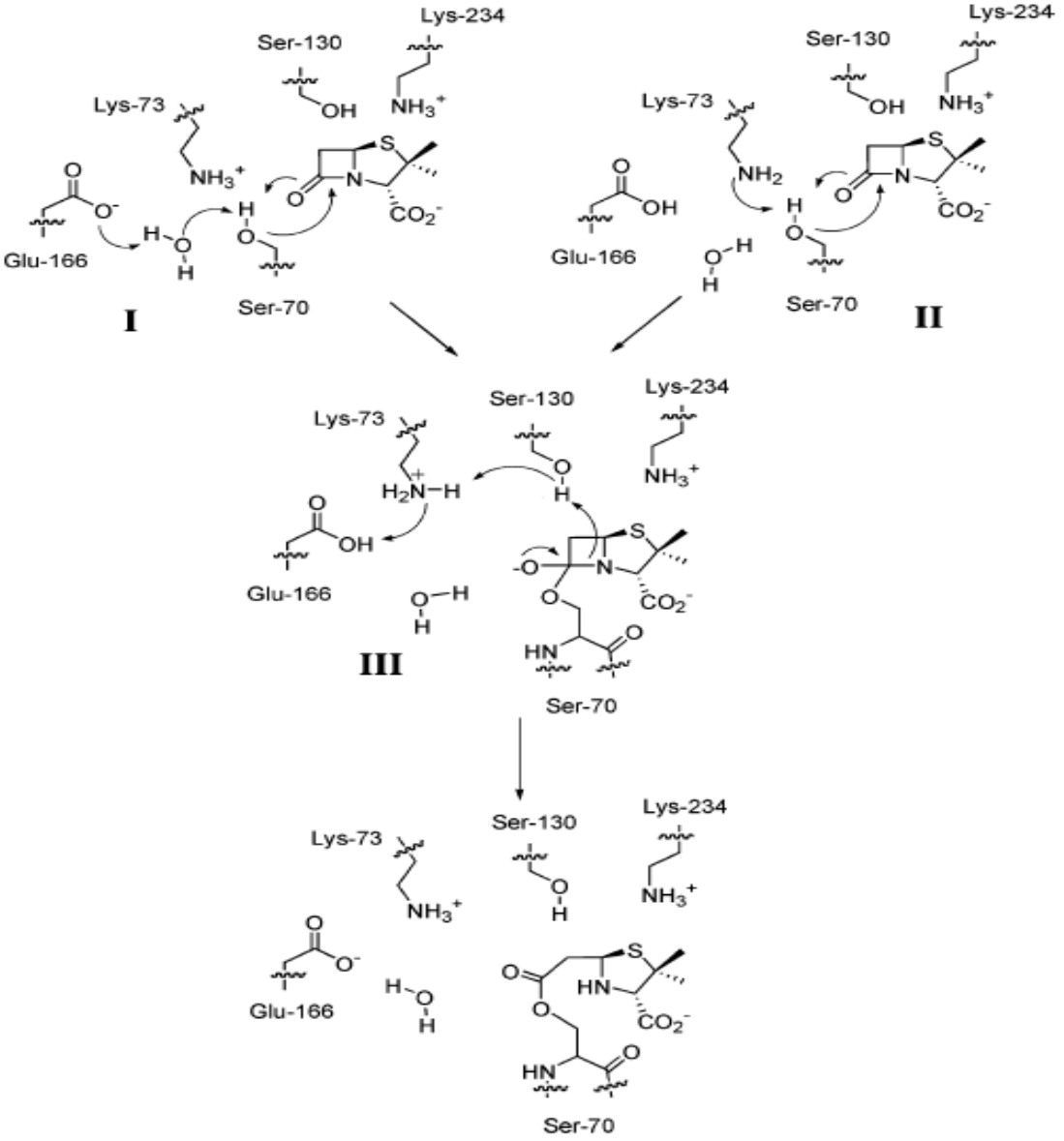

Figure 13: Acylation mechanism for class A β-lactamases (From Meroueh *et al.*, 2005).
In this study Meroueh *et al*., conclude that paths I and II compete for the promotion of Ser70 to the tetrahedral intermediate.

1.2.2.2. Deacylation half reaction

The deacylation of class A β-lactamases was studied by Hata *et al*. (2006). These workers did theoretical calculations in which they observed that Glu166 acts as a general base, Lys73 also participates in the reaction as a proton donor to Ser70, and Ser130 acts as a bridge to C3 carboxyl of the penicillin. The C3 carboxyl group assists the deacylation by deprotonating Lys73 through Ser130, thus making it a substrate assisted reaction. In the case of cephalosporins like nitrocefin the carboxyl group is on C4 and the distance they computed is too weak for a hydrogen bond (3.78 Å) and for a hydrogen abstraction from the hydroxyl group of Ser130. The more appropriate pathway is the one suggested in the substrate-independent deacylation mechanism by Class A β-lactamase (Figure 14) as proposed by the (Hata *et al*., 2006).

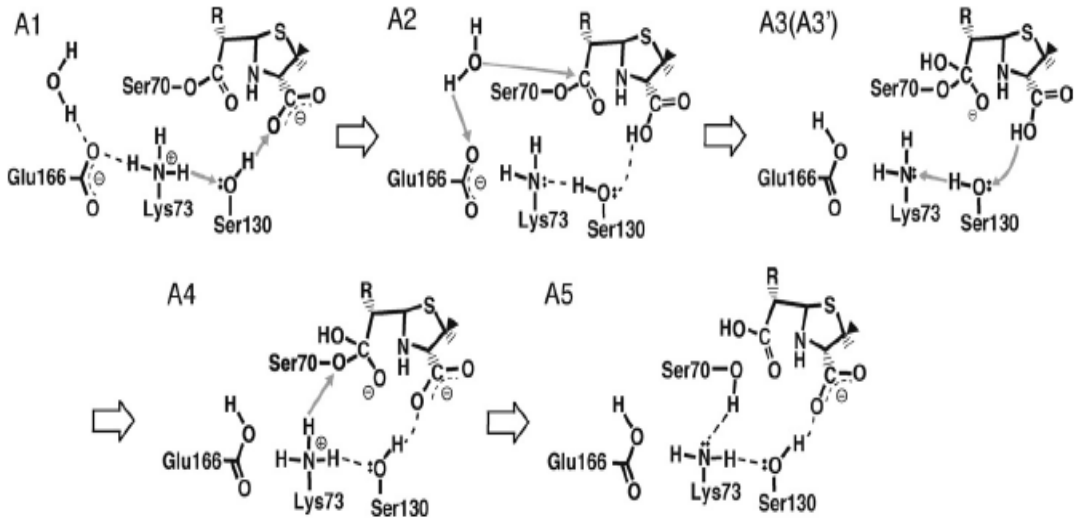

Figure 14: Deacylation mechanism for class A β-lactamases (From Hata *et al*. 2006). Glu166 as a general base catalyst, Lys73 is a co participant in the reaction, Ser130 forms a bridge between Lys73 and C3 carboxyl group of the substrate.

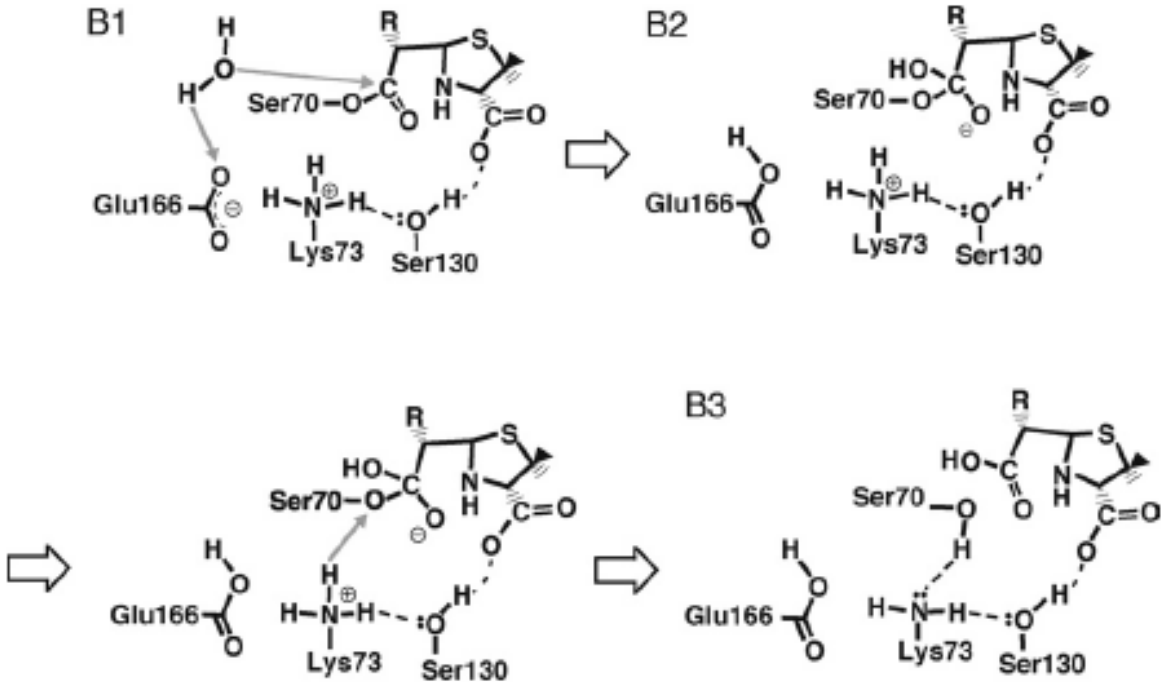

Figure 15: Substrate-independent deacylation mechanism for Class A β-Lactamases (From Hata *et al.*, 2006). Mechanism proposed by Fuji *et al*. Glu166 abstracts a proton from water and the hydroxyl group forms the tetrahedral intermediate with Ser70 and the substrate via nucleophilic attack. Ser130 maintains a weak hydrogen bond with the carboxyl group of the substrate while maintaining a hydrogen bond with Lys73 but keeping it protonated. Next, Lys73 donates a proton to Ser70 to collapse the tetrahedral intermediate.

Nitrocefin, therefore, has a lower deacylation rate than the penicillins, thereby making it more resistant to β-lactamases.

In the two schemes above no consideration was given to the role of the oxyanion hole formed by the two hydrogens of the side chain amino groups of A237 and Ser70 that is occupied by one of the oxygens in the tetrahedral intermediates (Meroueh *et al.,* 2005).

Another residue of interest is Lys234. According to Lamotte-Brasseur *et al*. (1999), who performed continuum electrostatic calculations, Lys234 may play a role in the stabilization of the tetrahedral complex because shows an increase in pKa value in the range of 11.1 to 12.0 in TEM-1 and *B. licheniformis* β-lactamases in the absence and presence of ligands such as

benzylpenicillin, cephalotin, benzylpenicillin methyl ester, cephalosporin lactone, benylpenicillin tetrathedral intermediate.

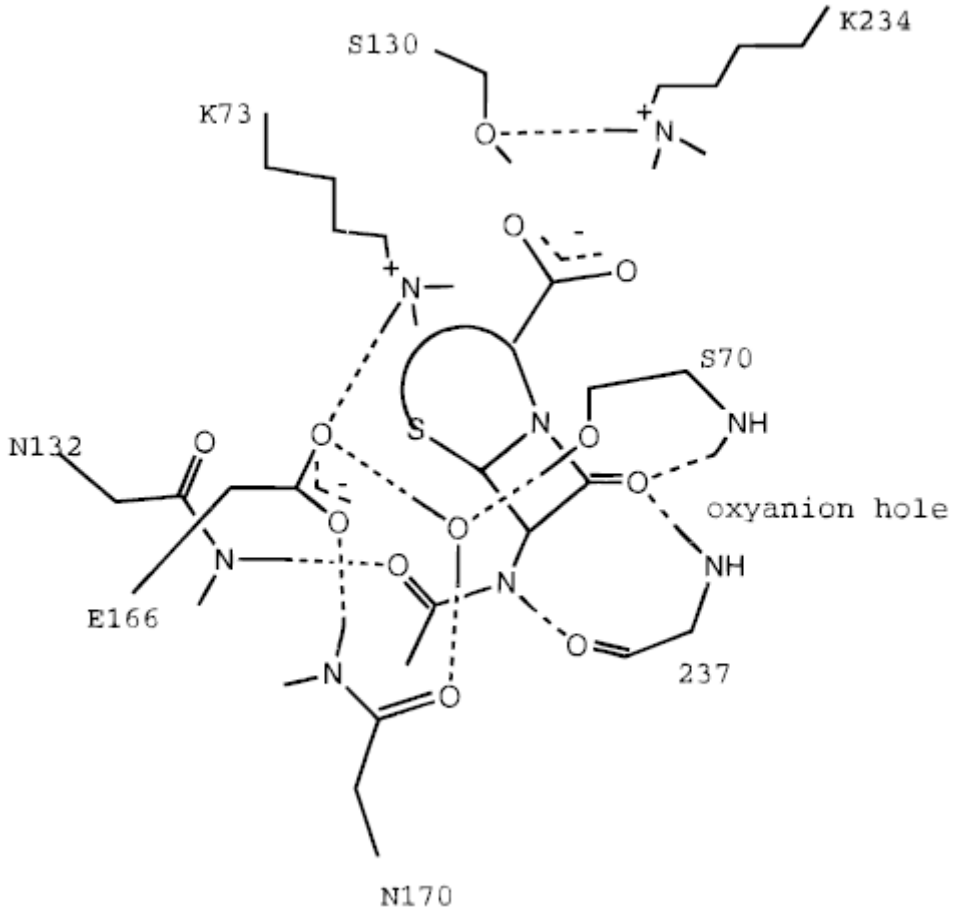

Figure 16: Scheme showing a class A β-lactamase active site and its substrate (Lamotte-Brasseur *et al*., 1999).

1.3. Boronic Acids as potential inhibitors of *Mycobacterium tuberculosis* and *Bacillus cereus* 569/H9 β-lactamases.

Boronic acids could be used as inhibitors of β-lactamases because Boron easily interconverts between sp^2 and sp^3 hybridization forms. In sp^3 hybrid a boronic acid mimics the transition state the of enzyme-β-lactam complex in the tetrahedral structures of the half acylation reaction in the active site (Hall, 2005) (Figure 25 and 26). Boronic acids show reversible competitive inhibition (DeSoyza, 1990) (Weston *et al*., 1998).

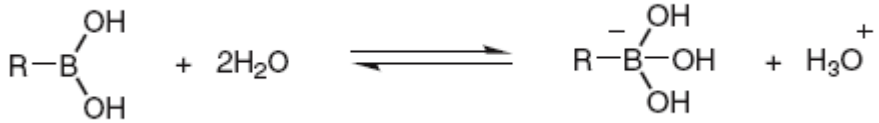

Figure 17: Ionic equilibrium of boronic acid in water (From Hall, 2005).

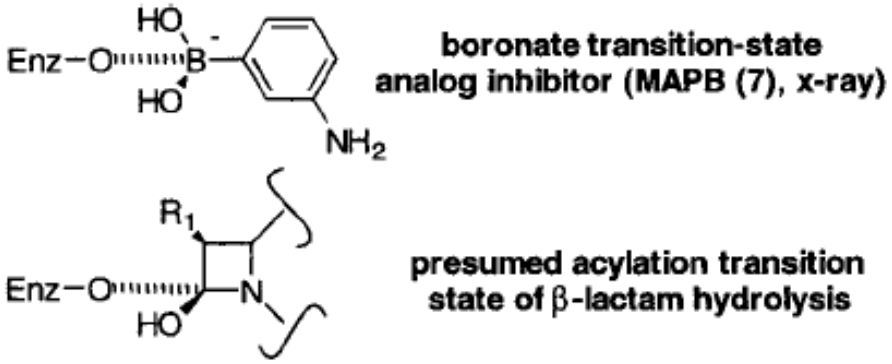

Figure 18. Boronic acids as transition state analogues (From Weston *et al.,* 1998). *m*-aminophenylboronic acid (MAPB) compared to a presumed transition-state structure during acylation (Weston *et al,.* 1998) (Steinberg, 1964) (Usher, 1998).

Boronic acids are also of interest for safety reasons:

Boronic acids have low toxicity compared to other organic compounds, they show no particular threat to the environment, small water soluble boronic acids are excreted unchanged by the kidney, large fat soluble boronic acids are moderately toxic, and they are not readily oxidized in

air or aqueous conditions since the coordination of water or hydroxide ions with boron protects them against any attack by oxygen (Hall, 2005). The first serine protease boron based inhibitor that found its way into the market was a dipeptidyl boronic acid inhibitor under the trademark Valcade in 2003 (Gonzales, 2012) which is currently used in the treatment of multiple myeloma (Hall, 2005).

2. Materials and Methods

2.1. Kinetic Studies.

To determine the inhibitory efficacy against β-lactamase a thermodynamic constant is used: the thermodynamic inhibitor dissociation constant (Ki) (www.bio.cmu.edu) (Eisenberg, 1979) (Philipp, 1971).

starting with the classical equation for competitive inhibition: (University of Virginia website)

$Vi = Vmax [S] / (Km (1+ [I] / Ki) + [S])$ where Vi is velocity of the inhibited reaction.

$Vu = Vmax [S] / (Km + [S])$ where Vu is the velocity of the uninhibited reaction.

when Km >> [S] these simplify to

$Vi = Vmax [S] / (Km (1+ [I] / Ki))$

$Vu = Vmax [S] / Km$

dividing Vu by Vi, we have

$Vu / Vi = (Vmax [S] / Km) / (Vmax [S] / (Km (1 + [I] / Ki))$

or

$Vu / Vi = (1 + [I] / Ki)$

$Vu / Vi - 1 = [I] / Ki$

we arrive at:

$Ki = [I] / (Vu / Vi - 1)$ Equation (1)

Where:

[I]: Molar inhibitor concentration.

Vu: Initial velocity of the uninhibited reaction which is the slope of the curve in the first 10 minutes of the reaction.

Vi: Initial velocity of the inhibited reaction which is the slope of the curve in the first 10 minutes of the inhibited reaction.

When de reaction was run to completion the formula used was:

$$Ki = [I] / (ku / ki - 1) \qquad \text{Equation (2)}$$

ku: Rate constant of the uninhibited reaction equal to the slope of the line formed by the points calculated from ln(A – Max A) (Clement, 2006)

ki: Rate constant of the inhibited reaction equal to the slope of the line formed by the points calculated ln(A – Max A) (Clement, 2006)

A: Absorbance.

ln: natural logarithm.

2.1.1. Kinetic Studies of Boronic Acids against BlaC with Nitrocefin as Substrate.

2.1.1.1. Preparation of Boronic acids.

Stock solutions of Boronic acids from various vendors were prepared by dissolving approximately 10.0 mg of Boronic acid in 100 mL of Dimethylsulfoxyde (DMSO) 99.8% CAS 67-68-5 from EMD and 900 μL of pH 7.00 buffer of potassium dihydrogen phosphate / dipotassium hydrogen phosphate at ionic strength of 0.1 M. for a total of 1000 μL. In the case whereby the boronic acid salted out when the phosphate buffer was added, then the stock solution was prepared in DMSO (99%).

2.1.1.2. Preparation of Nitrocefin as substrate.

Stock Nitrocefin was prepared per instructions from the manufacturer at a concentration of 1 mM in pH 7.00 phosphate buffer ionic strength 0.1 M and kept refrigerated for later use. Nitrocefin was diluted to 0.5 mM before the assay.

2.1.1.3. Preparation of enzyme.

1 mL aliquots of *Mycobacterium tuberculosis* BlaC enzyme at 6.36 μM were received as a gift from Dr. Janet Gonzales from this lab. Subsequently, 1-mL aliquots of 300 μM concentration were prepared by diluting 47.2 μL of BlaC enzyme in 952.8 μL of phosphate buffer at pH 7.0, for a total of 1000 μL.

2.1.1.4. Preparation of buffer.

Phosphate buffers were prepared at ionic strength of I = 0.1 M as prescribed by the Biochemistry Handbook (Long, 1961).

2.1.1.5. Spectrophotometry

A Synergy multi-detection microplate reader (Biotek), was attached to a Dell personal computer for kinetic experiments. Data was collected using Gen5 Microplate Data collection and analysis software and saved as Excel files.

The wavelength used in this experiment was 494 nm as previously determined by a difference spectrum analysis of hydrolyzed and unhydrolyzed Nitrocefin. The experiments were set to run for 10 minutes and set the data collection at a minimum interval determined by the microplate reader varying from 8 to 12 seconds depending on the number of wells utilized for the experiment. The kinetic experimental results were subsequently analyzed by linear regression analysis and the Ki was determined according to equation (1) above.

2.1.1.6. Experiment set up

Cocktails were prepared in the microplate for a final concentration for BlaC enzyme of 24.0 nM; nitrocefin, 40 μM and the inhibitors at the indicated concentration millimolar concentrations. DMSO (10% v/v) solvent was added to the uninhibited reaction in equal amount as of the boronic acid solution as in the inhibited reaction.

The amounts where: enzyme, 20.0 μL; DMSO, 20 μL or boronic acid, 20 μL and buffer, 190 μL and nitrocefin 20 μL for a total well volume of 250 μL.

The order of application to the well was buffer, DMSO or inhibitor, nitrocefin and finally the enzyme.

2.1.2. Boronic Acids as Inhibitors of β-lactamase from *Bacillus cereus* 569/H9 I.

2.1.2.1. Preparation of enzyme.

A vial of *Bacillus cereus* 569/H9 (Calbiochem) containing 779.56 units of β-lactamase I and 75.28 β-lactamase II was dissolved in 2.0 mL of potassium dihydrogen phosphate/ potassium hydrogen phosphate buffer at pH 7.0 and I = 0.1 M and subsequently diluted to make 100 aliquots of 3.886 μM enzyme as stock solution. The concentration of the enzyme in the stock solution was determined as follows: The ExPASy ProtParam tool was utilized to get the extinction coefficient of the enzyme 28085 for the molecular weight of 31, 557.2 the closest to the reported value by Calbiochem of 31500 M.W. meaning we have a match.

Scanning the an aliquot of the vial from Calbiochem, it was determined that β-lactamase I had a concentration of 170 μM total.

2.1.2.2. Spectrophotometry.

A UV/VIS Spectrophotometer model Lambda 2 from Perkin-Elmer Corporation., equipped with Perkin Elmer WinLab PECSS software was utilized for these experiments. A quartz cuvette of 2.0 mL capacity was utilized for the reaction mixture. Temperature in the reaction mixture was maintained at 25 ˚C with the help of a water bath system equipped with a VWR heater (VWR Scientific, San Francisco, CA). Data points were taken every 10 seconds and the visible light lamp set at 494 nm.

2.1.2.3. Experiment set up.

Cocktails were prepared in a 2 mL quartz cuvette for a final concentration for TEM-1 enzyme 1.62 μM; Nitrocefin, 16.2 μM (68% of Km). Km reported in the literature was 24 μM (Villacorta, 1991). The inhibitors were added in various concentrations depending on the inhibitor, buffer final concentration was kept at 0.1 molar. The volumes added to the cuvette were: enzyme, 430.0 μL; 37.6 μL DMSO or boronic acid, 500 μL buffer and 32.4 μL nitrocefin for a total cuvette volume of 1000 μL.

The order of application to the well was buffer, DMSO or inhibitor, nitrocefin and finally the enzyme. The absorbance at 494 nm was taken and a progress curve of product formation was recorded. When the plateau of the absorbance curve was reached (around 60 minutes or more) the experiment was stopped. The data was transferred to an Excel worksheet where the formula Ln(At-A∞) was applied. A linear regression analysis was performed on the data. The absolute value of the slope was taken as reaction rate, ku for uninhibited and ki for the inhibited reaction. Then K_i was found with the formula:

$K_i = [I]/((ku/ki)-1)$.

2.1.2.4. Disabling β-Lactamase II (metallo-enzyme) from *Bacillus cereus* 569/H9.

Ethylenediaminetetraacetic Acid (EDTA) was used at concentration of 1 mM to completely inhibit β-Lactamase II present in the vial (Calbiochem). In kinetic experiments EDTA concentration was maintained 5 fold to 10 fold greater than that of β-lactamase II.

2.2. Modeling *in silico* the inhibitor-enzyme complex in the inhibition of β-lactamases by boronic acids.

2.2.1. Selection of the *Mycobacterium tuberculosis* (BlaC) β-lactamase x-ray structure for modeling studies.

The first β-lactamase used was provided by Dr. Douglas S. Kernodle, M. D., Vanderbilt University School of Medicine, Division of Infectious Disease, Nashville, TN. USA, as a gift to Dr. Janet Gonzalez of this lab in a host for the recombinant protein *E. coli* Top10 (Invitrogen). This host contained the plasmid pTrcHisB (Invitrogen) expressing the gene *BlaC* in cosmid Y-49 a class A β-lactamase, from an attenuated *Mycobacterium tuberculosis* strain Rv37a (Voladri *et al.,* 1998). Dr. González, provided me with the purified enzyme that I needed for my project. Dr. Douglas S. Kernodle provided Janet with the amino acid sequence:

MRNRGFGRRELLVAMAMLVSVTGCARHASGARPASTTLPAGADL
ADRFAELERRYDARLGVYVPATGTTAAIEYRADERFAFCSTFKAPLVAAVLHQNPLTH
LDKLITYTSDDIRSISPVAQQHVQTGMTIGQLCDAAIRYSDGTAANLLLADLGGPGGG
TAAFTGYLRSLGDTVSRLDAEEPELNRDPPGDERDTTTPHAIALVLQQLVLGNALPPD
KRALLTDWMARNTTGAKRIRAGFPADWKVIDKTGTGDYGRANDIAVVWSPTGVPYVV
A VMSDRAGGGYDAEPREALLAEAATCVAGVLA
GenBank accession number Z73966.

BLAST search was conducted using the National Center for Biotechnology Information (NCBI) database (Figure 18).

NCBI BLAST search showed that the sequence is part of the β-lactamase super family (Figure 19) and then gave me an option to select among structures available in its data banks that are 100% identical to the sequence provided. 3CG5 was because it has a 100% identity and it contained an inhibitor (clavulanate) in the active site. According to Dr. Blanchard (Tremblay *et al.,* 2008) the source for this crystal structure was the *blaC* gene amplified from genomic *Mycobacterium tuberculosis* H37Rv which is identical to that of Rv37a per Dr. Kernodle (Voladri *et al*., 1998). According to Dr. Blanchard BlaC was expressed as an N-terminally

truncated form that missed the first 40 amino acids and this is why Ser42 in 3CG5 correspond to Ser70 in the class A β-lactamases.

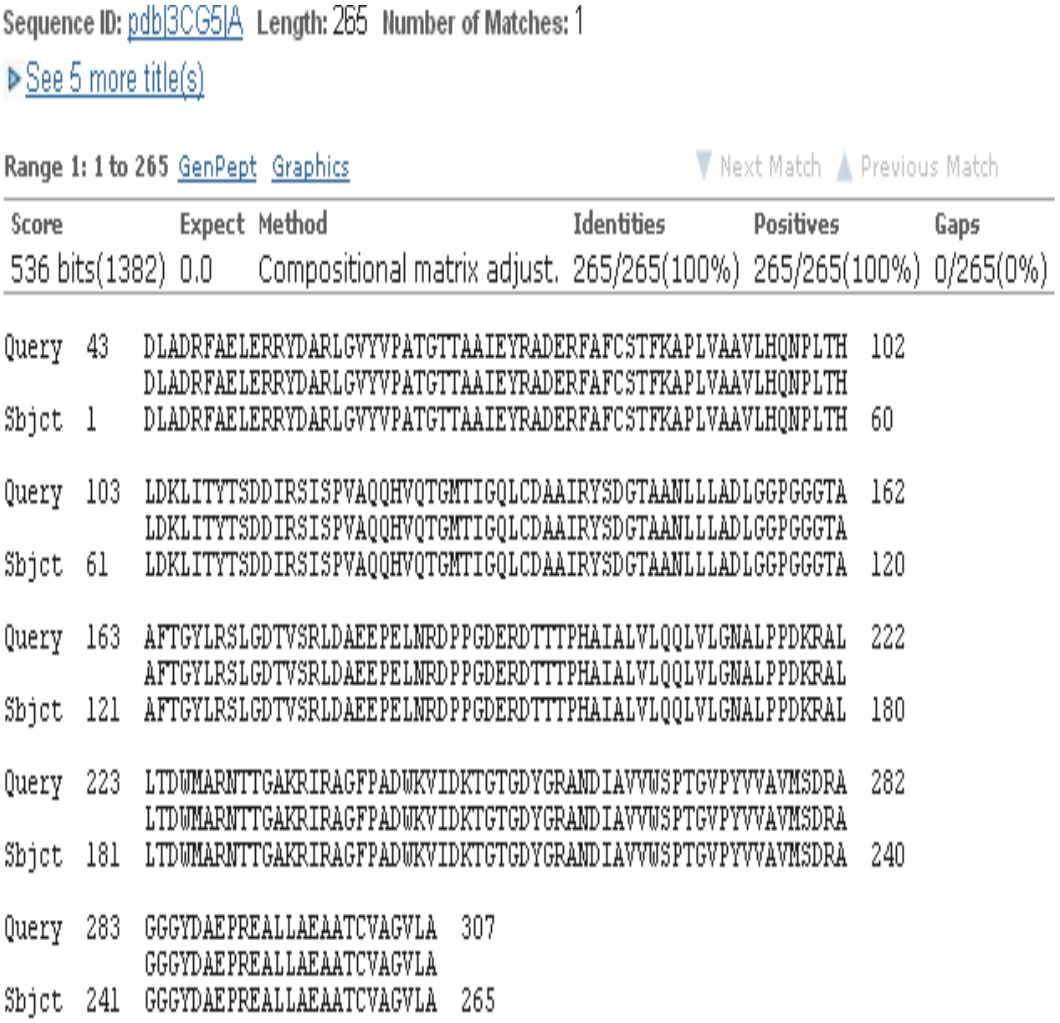

Figure 19: 3CG5 and the sequence provided by Dr. Kernodle. Note 100 % homology.

2.2.2. Selection of the *Bacillus cereus* 569/H9 β-lactamase x-ray structure for modeling studies.

β-lactamase *Bacillus cereus* was searched in the protein data bank of NCBI and one of the sequences, *Bacillus cereus* a non-metallo β-lactamase was the sequence in GenBank accession number ACV20891.1 a TEM enzyme per comments by the authors in NCBI. I searched in NCBI protein structures for a TEM enzyme. NCBI accession number 1ERO is a TEM-1 enzyme, it contains a boronic acid in its active site reason why it was selected. A Clustal sequence alignment between ACV2089.1 and 1ERO reveal two substitutions. V84I and A184V:

ACV20891.1 Ile84 corresponds to Val84 in 1ERO and Val184 in ACV20891.1 corresponds to Ala184 in 1ERO. These variants of TEM-1 are found in TEM-116 (Hu *et al.,* 2007, Lahey clinic website). Only the TEM-1 structure was located at NCBI.

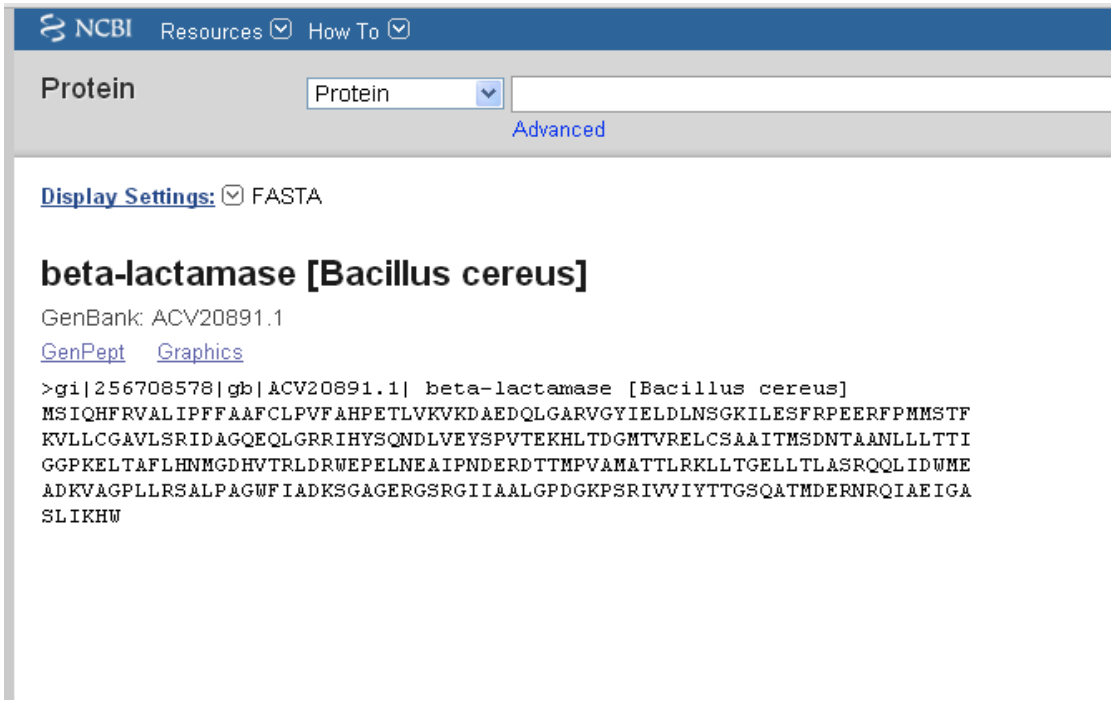

Figure 20: NCBI search for "β-lactamase *Bacillus cereus*". Search results in GenBank: Accession number ACV2089.1 and FASTA sequence.

2.2.3 Docking Procedure

2.2.3.1. Preparation of the enzyme

A pdb file was downloaded from NCBI (for example 3CG5) with *Sculpt* from MDL. With *NotePad* from Microsoft the water molecules were deleted. *Swiss-PdbViewer* was used for adding all the protons to the enzyme except the one in Ser42 (70) γO that was deleted. The *Sculpt* format is maintain by opening the pdb file and saving it with *Sculpt*. E*asyConvert* (EC) from *AutoDock Vina* was used for converting the pdb to pdbqt file which is a pdb formated for *AutoDock Vina*.

2.2.3.2. Preparation of the boronic acids structures for docking.

Drawings were made of boronic acids with *Draw* 2.5 from MDL. Carbon was utilized instead of boron for purposes of docking. 3D optimization and hydrogens were obtained using *ACD*/*Chem Check Freeware* from Advance Chemistry Development then saved as a ".mol" file.

The ".mol" file was converted to a ".pdb" file using *Open Babel* from OpenBabelGUI by Chris Morley (www.openbabel.org). Finally the ".pdb" file was converted to a ".pdbqt" file using EC as in preparation of the enzyme above.

2.2.3.3 Conducting the *in silico* experiment.

The enzyme ".pdbqt" and the boronic acid ".pdbqt" were dragged to *AutoDock Vina* utility (Pcvt). The program returned nine possible docking outcomes or less, each with a ΔG. *AutoDock Vina* suggests the best docking result per lowest ΔG . Coordinates were for the active site known, gamma serine 42 in the case of 3CG5 or serine 70 in the case of 1ERO was set as the coordinates in a grid size of 10 Angstroms. If the coordinates were not entered the inhibitor could go somewhere else other than the active site. The coordinates for Ser42(70) γO in 3CG5 were:

-11.982, -10.876, 6.645 and for 1ERO 38.287, 37.117, 30.517. The above parameters were found in the pdb file.

After docking, the original protonated pdb file of the enzyme was merged with the dokcing pdb file for the small molecule given by *AutoDock Vina* using *Swiss-PdbViewer***.** Sculpt was used to identify and map the active site by throwing a surface in a 10.0 Å sphere around the inhibitor. *Discovery Studio visualizer* was for determining the important interactions such as hydrogen bonding and pi stacking.

2.2.3.4 Computation of Ki from ΔG (affinity constant) from *AutoDock Vina***.**

ΔG = - RTlnK, where K = association constant (Eisenberg, 1979).

$K = e^{-(\Delta G/RT)}$ Where K is an association constant. Then Ki would be 1/K and the formula is

$Ki = (1/ e^{-(\Delta G/RT)})x10^6$ in order to express the value in the micromolar units (University of Oulu website).

3. Results

3.1. Kinetic results

3.1.1. Selection of kinetic wavelength.

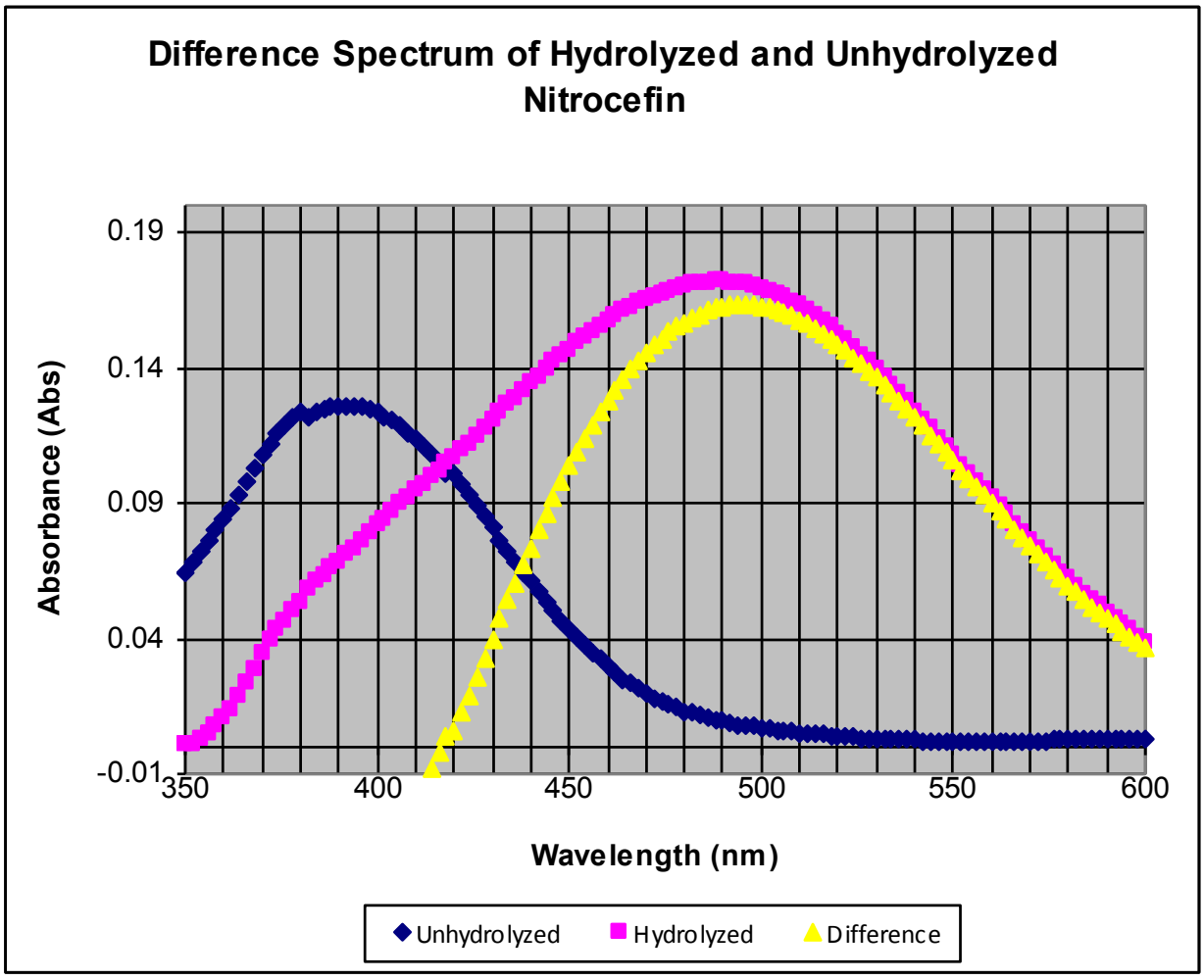

Figure 21: Difference Spectrum of Nitrocefin unhydrolyzed and hydrolyzed. Maximum difference is at 494 nM . Enzyme used was BlaC. Nitrocefin was purchased in Calbiochem

3.1.2. Effect of EDTA on β-lactamase from *Bacillus cereus* 569/H9.

In the graph in (Figure 28) it can be observed that EDTA inhibits the mixture of enzymes β-lactamase I and β-lactamase II (Calbiochem). That the inhibition does not increase by a great margin as the concentration of EDTA is increased, and that there is a reduction of hydrolysis that can be visually assessed to be approximately 10 % which is the content of β-lactamase II (the metallo-enzyme) in the vial. The total units in the vial is 854.84 units; β-lactamase I units in the vial are 779.56 (91 % of total) and the β-lactamase II units in the vial are 75.28 units (9 % of total). A characteristic of metallo-enzymes that sets them apart from the other classes of β-lactamases is their sensitivity toward EDTA (Chakraborty *et al.*, 2010)

In figure 29 we can see that the effect of EDTA is constant as one of the enzymes is disabled and does not affect the other enzyme.

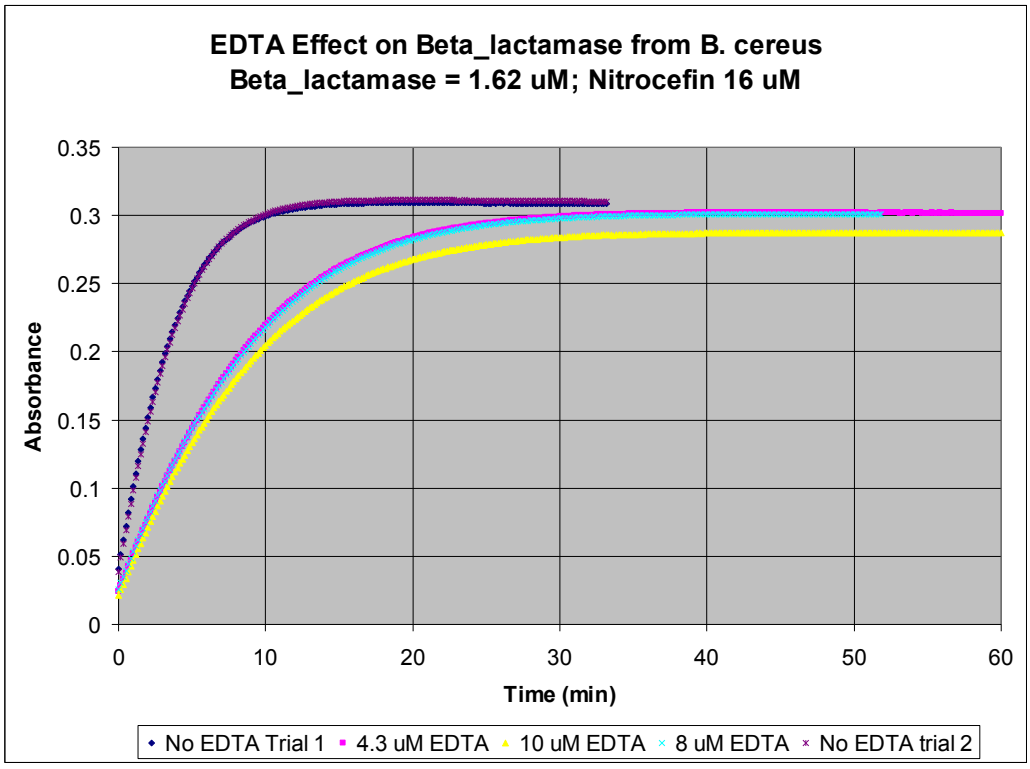

Figure 22: EDTA effect on the activity of β-lactamase from *Bacillus cereus* 569/H9.

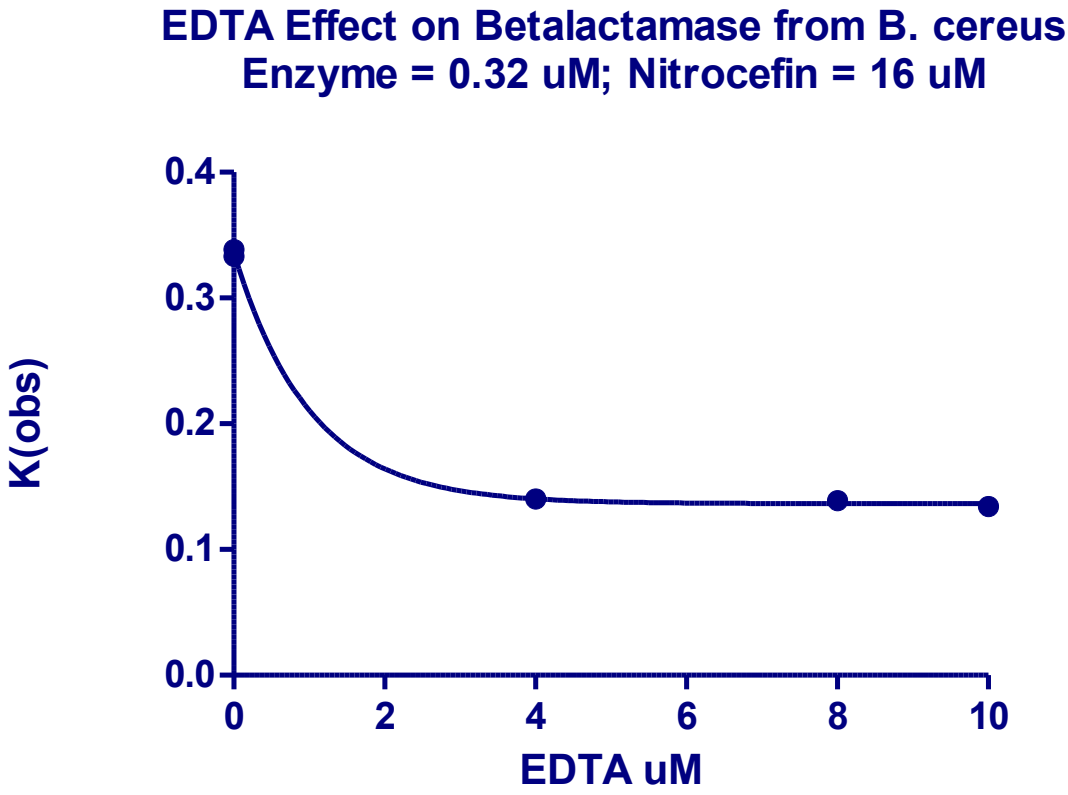

Figure 23: EDTA effect on the activity of β-lactamase from *Bacillus cereus* 569/H9 (Calbiochem). Vial contains serine β-Lactamase I 779.56 units/vial; Metallo β-Lactamase II 75.28 units/vial. EDTA inhibits the metallo-enzyme but not the serine β-Lactamase.
K(observed) was computed and plotted in GraphPad Prism 5.03 from GraphPad Software, Inc.

3.1.3 Kinetic run results

3.1.3.1. Kinetics results for BlaC.

Table 1: Results for boronic acids as inhibitors of BlaC.

Boronic Acid	Ki (μM)	Vina's ΔG **	Vina's Ki (μM)	
3,4,5-Trifluorophenylboronic acid	176	-5.9	47	
3-Nitrophenylboronic acid	214	-6.3	24	
2,3,4,5-Tetrafluorophenylboronic acid	229	-6.0	40	
3,5-Bis(trifluoromethyl)benzeneboronic acid	302	-3.4	3207	*
2,3,5-Trifluorophenylboronic acid	477	-5.7	66	
2-Carboxythiophene-5-boronic acid	493	-5.6	78	
5-Trifluoromethyl-1,3-phenyldiboronic acid	644	-4.4	592	
3-Chloro-4-fluorobenzeneboronic acid	658	-5.6	78	*
3-carboxy-5-nitrophenylboronic acid	845	-4.5	500	
3-Carboxy-4,5-difluorophenylboronic acid	1469	-6.1	34	*
4-Bromophenylboronic acid	1919	-5.3	130	*
Diphenylborinic anhydride	2043	-6.2	28	
2,3,4,6-Tetrafluorophenylboronic acid	2184	-5.4	109	*
4-Chlorobenzeneboronic acid	2581	-5.3	130	*
2-Phenyl-1-ethynylboronic acid pinacol ester	5277	-5.4	109	*
2,4,6-Trifluorophenylboronic acid	5999	-5.5	92	*
Phenylboronic acid	6364	-5.6	78	*

Table 2: Non-boronic compounds as inhibitors of BlaC.

	Kinetics Ki (μM)	Vina's ΔG	Vina's Ki (μM)	
4,4'-DDT	48	-6	40	
Quinine Hydrochloride	2452	10.5	>10000	*

* Preliminary data, more tests needed for marked compounds.

** All ΔG reported in this dissertation are in kcal/mol.

3.1.3.2 Kinetic results for β-lactamase I from *Bacillus cereus* 569/H9 TEM-116

Table 3: Boronic acids as inhibitors of β-Lactamase I from *Bacillus cereus* 569/H9 TEM-116 (kinetics) and TEM-1 (*in silico*).

Compound name	Ki (μM)	Vina's ΔG	Vina's Ki (μM)
2-Carboxythiophene-5-boronic acid	1.1	-5.3	130
3-Carboxyphenylboronic acid	19.4	-6.2	28
2-Carboxythiopehene-4-boronic acid	46.5	-5.9	47
3-Carboxy-4-fluorophenylboronic acid	47.1	-5.6	78
3-carboxy-5-nitrophenylboronic acid	65.8	-3.9	1378
3-Amino-5-carboxylphehylboronic acid	136.9	-5.1	182
3-Nitrophenylboronic acid	247.3	-6.1	34
2,3,5-Trifluorophenylboronic acid	394.6	-5.4	109
2,3,4,5,6-Pentafluorobenzeneboronic acid	461.5	-4.5	500
2,3,4,6-Tetrafluorophenylboronic acid	573.6	-5.4	109
2-Phenyl-1-ethynylboronic acid pinacol ester	848.0	0.1	$>10^3$
3-Pyridineboronic acid	1063.0	-4.9	255
2,3,4,5-Tetrafluorophenylboronic acid	1121.0	-4.8	301
3-Chloro-4-fluorobenzeneboronic acid	1163.0	-4.9	255
3-carboxytiophene-2-boronic acid	1337.0	-5.6	78
2,4,6-Trifluorophenylboronic acid	1663.0	-5	215
Phenylboronic acid	2998.0	-4.9	255
3,4,5-Trifluorophenylboronic acid	7228.0	-5.2	153

3.2. Sequence alignments and computer modeling results

3.2.2. Finding differences and homology between one peptidase and the two enzymes available in the present research.

```
CLUSTAL O(1.2.0) multiple sequence alignment


2BCF:A      MADADVQPAGSVPI-----PDGPAQTWIVADLDSGQVLAGRDQNVAHPPASTIKVLLALV
3CG5:A      --------DLADRFAELERRYDARLGVYVP-ATGTTAAIEYRADERFAFCSTFKAPLVAA
1ERO:A      ------HPETLVKVKDAEDQLGARVGYIELDLNSGKILESFRPEERFPMMSTFKVLLCGA
                         .                    .        :  .   **:*. *   .

2BCF:A      ALDELDLNSTVVAD-----VADTQAECNCVGVKPGRSYTVRQLLDGLLLVSGNDAANTLA
3CG5:A      VLHQN--PLTHLDKLITYTSDDIRSISPVAQQHVQTGMTIGQLCDAAIRYSDGTAANLLL
1ERO:A      VLSRVDAGQEQLGRRIHYSQNDLVEYSPVTEKHLTDGMTVRELCSAAITMSDNTAANLLL
            .* .       :         *    .  .  :   . *: :* .. :  *   *** *

2BCF:A      HMLGGQDVTVAKMNAKAATLGATSTHAT--TPSGL-DGPGGSGAS-TAHDLVVIFRAAMA
3CG5:A      ADLGGPGGGTAAFTGYLRSLGDTVSRLDAEEPELNRDPPGDERDTTTPHAIALVLQQLVL
1ERO:A      TTIGGPK----ELTAFLHNMGDHVTRLDRWEPELNEAIPNDERDTTMPAAMATTLRKLLT
              :**       :..   .:*   ::     *.     *  .  :     :.  ::  :

2BCF:A      NPVFAQIIAEPSAMFPSDDGEQLIVN-------QDELLQRYPGA--IGGKTGYTNAARKT
3CG5:A      G-----------NALPPDKRALLTDWMARNTTGAKRIRAGFPADWKVIDKTGTGDYGRAN
1ERO:A      G-----------ELLTLASRQQLIDWMEADKVAGPLLRSALPAGWFIADKSGAGERGSRG
                        :   .   *            :    *.   :  *:*  : .

2BCF:A      FVG-AAARGGRRLVIAMMYGLVKEGGPTYWDQAATLFDWGFALNPQASVGSLGSHHHHHH
3CG5:A      DIAVVWSPTGVPYVVAVMSDRAGGG-YDAEPREALLAEAATCV-----AGVLA-------
1ERO:A      IIA-ALGPDGKPSRIVVIYTTGSQ--ATMDERNRQIAEIGASL-----IKHW--------
             :. . .  *    :.::            :   : : . .:
```

Figure 24: Multiple Sequence Alignment of a PBP (2BCF), BlaC (3CG5) and TEM-1 (1ERO). Asterisks: Conserved residues in all three enzymes (Clustal Omega).

Figure 25: Clustal sequence alignment of 3CG5 and 1ERO transcribed to *Excel*.

Table 4: Consensus, motifs (or elements), BlaC (3CG5), TEM-1 (1ERO) compared.

Element / Motif (charge)	Amino acid	3CG5 position	Consensus *	1ERO position
I (+1)				
SxxK	SER	42	70	70
	THR	43	71	71
	PHE	44	72	72
	LYS	45	73	73
II (-1)	SER	100	130	130
SDN or	ASP	101	131	131 ASN
SDG	GLY	102	132	132
III (+1)				
KTG	LYS	208	234	234 SER
	THR	209	235	235
	GLY	210	236	236
IV (-2)	GLU	140	166	166
(In Omega loop)	PRO	141	167	167
ExELN	GLU	142	168	168
	LEU	143	169	169
	ASN	144	170	170

* Consensus (Metagne *et al.*, 1998).

In Table 4 is presented further results of the alignment of the two β-lactamases in this research and the consensus reported by Metagne *et al.*, (1998). The electrical charges found in the motifs are stated per Verma *et al.,* (2013). Keeping in mind the net electrostatic charges of the elements that comprise the active site pocket may assist us in selecting specific groups for substituents in the aromatic ring of the inhibitor. The 4th element is imbedded in the Ω-loop that comprises sixteen residues in the form xRxExxLNxxxxxxxx (Verna *et al,*. 2013).

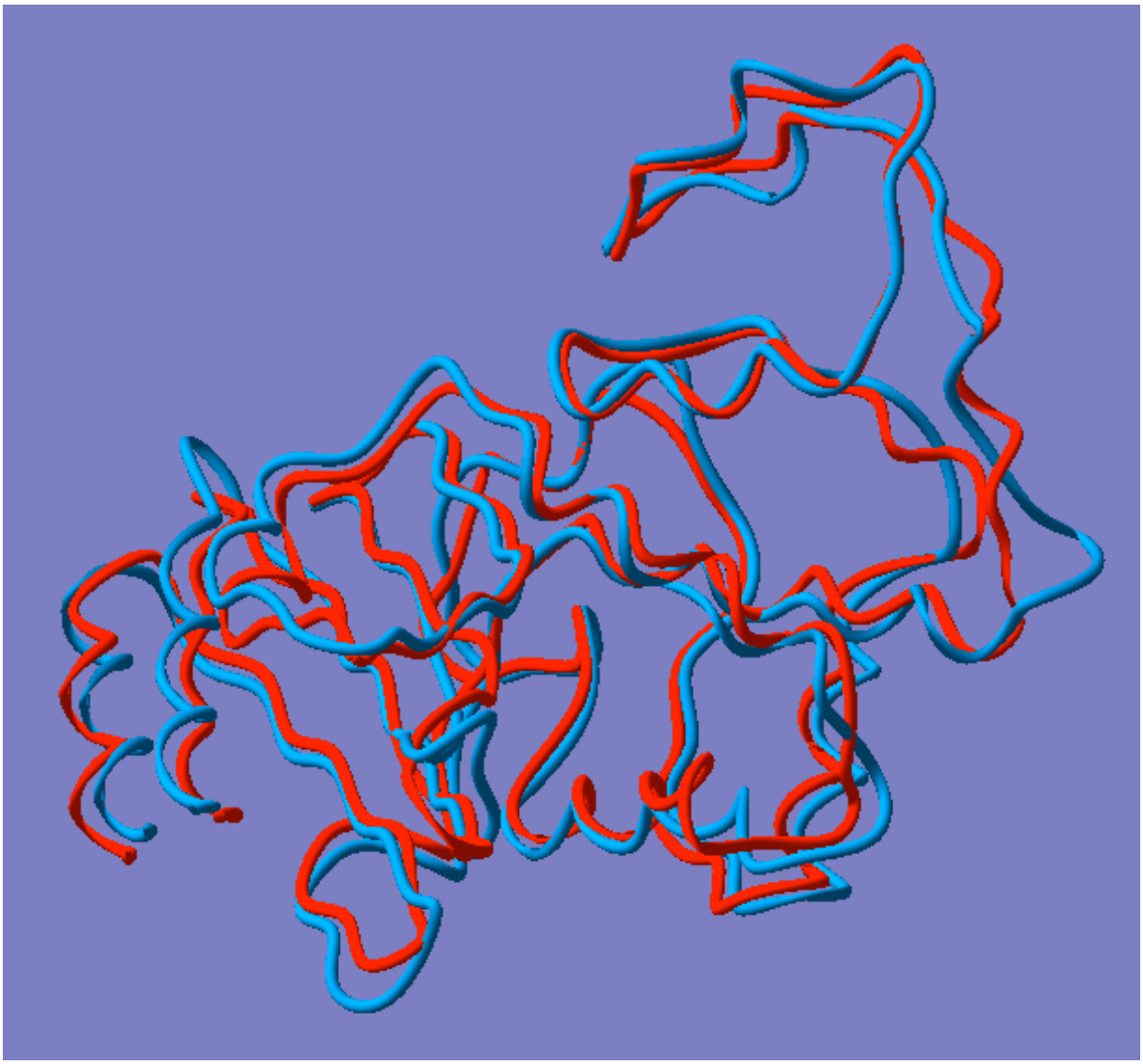

Figure 26: 3CG5 (red) superposition on 1ERO (blue) in *Sculpt*. Model made in *Sculpt* as a result of a sequence alignment submitted to SDS CD-EMC server from University La Sapienza of Rome (http://schubert.bio.uniromal.it/CEMC/)

In figure 35 one can see a near perfect alignment of the backbones of BlaC (3CG5) and TEM-1 (1ERO) can be observed. They were submitted for alignment to the server at University La Sapienza (Rome) through their website.

3.2.4. Modeling of inhibitors in the active site of BlaC and TEM-1 β-lactamases.

3,4,5-Trifluorophenylboronic acid in the active site of BlaC (3CG5) and TEM-1 (1ERO).

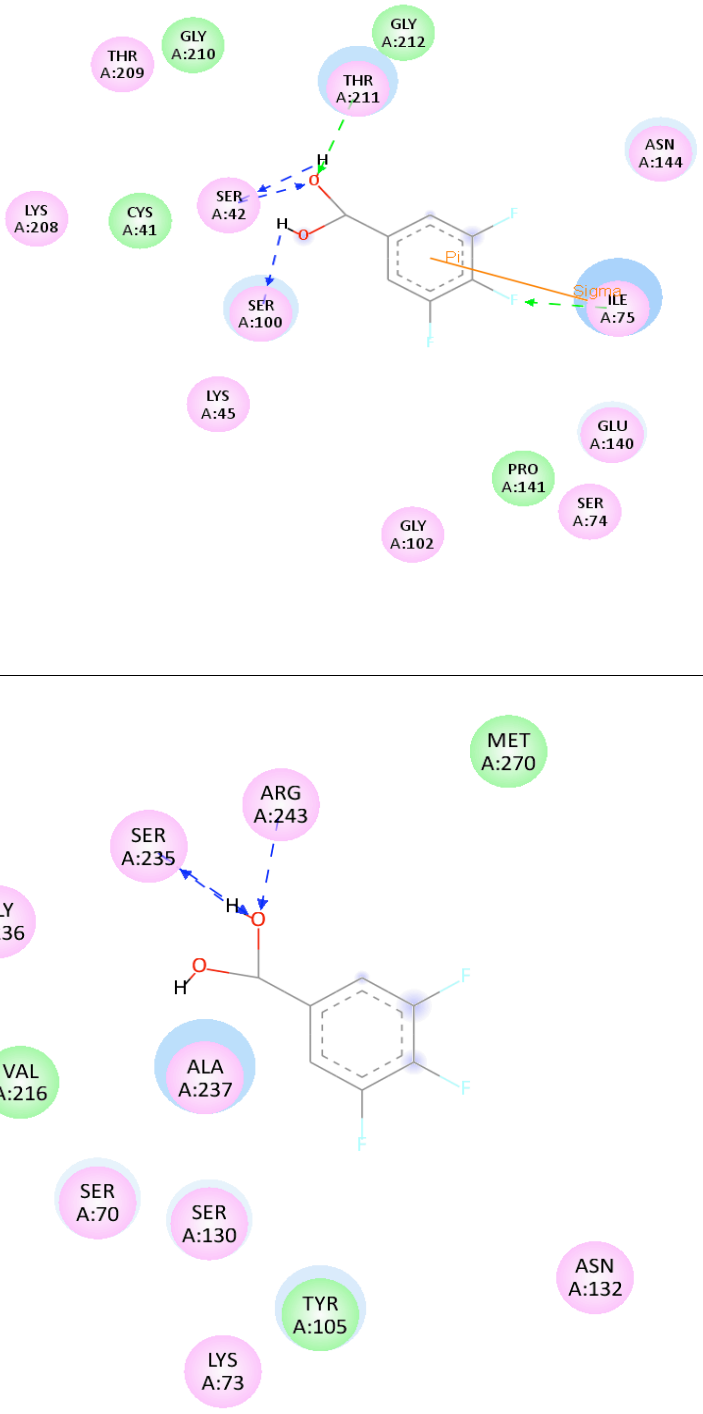

Figure 27: 3,4,5-Trifluorophenylboronic acid in the active site of BlaC (3CG5) (top) and TEM-1 (1ERO) (bottom) (See appendix E for color code).

Table 5: 3,4,5-Trifluorophenylboronic acid in BlaC (3CG5) and TEM-1 (1ERO). Important interactions.

3,4,5-Trifluorophenylboronic acid			
		BlaC	**TEM-1**
3CG5(1ERO)			
		Å	**Å**
Ser42(70)	Side chain Oxygen to Boron	3.65	5.09
Ile75 Tyr(105)	Hydrogen bond to ligand's Fluorine C(4) of ring	2.42	-
Ile75 Tyr(105	Pi stacking - distance to C(3)	2.71	-
Ser100(130)	Hydrogen bond to ligand's boronate hydroxyl	1.90	-
Ala217 Arg(243)	Hydrogen bond to ligand's boronate hydroxyl	-	2.12
Thr209 Ser(235)	Hydrogen bond to ligand's boronate hydroxyl	-	2.35
Thr209 Ser(235)	Hydrogen bond to ligand's boronate hydroxyl	-	2.44
Thr211 Ala(237)	Hydrogen bond to ligand's boronate hydroxyl	2.10	-

3,4,5-Trifluorophenylboronic acid in the active site of BlaC (3CG5).

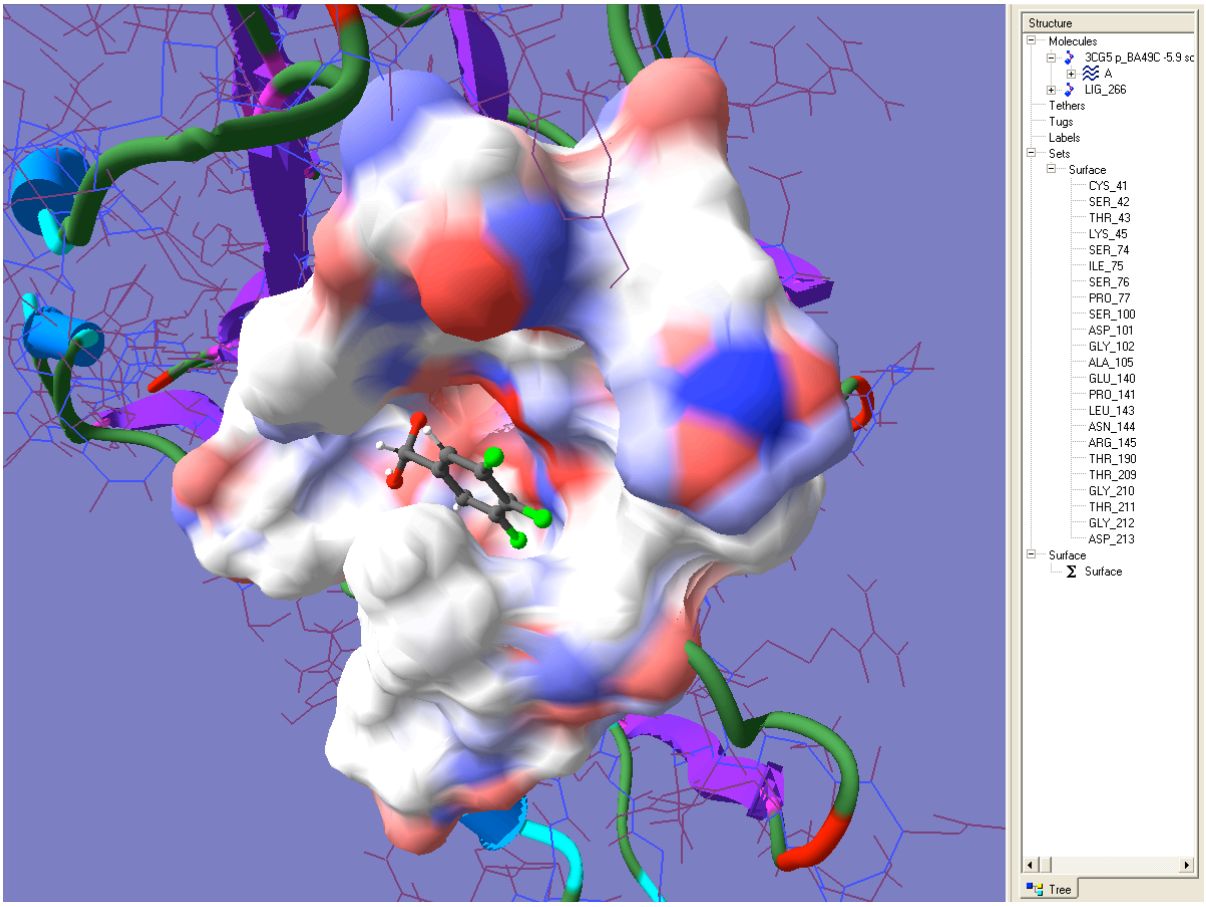

Figure 28: 3,4,5-Trifluorophenylboronic acid in BlaC active site of BlaC. Surface on within a 10.0 Å sphere of the inhibitor. All amino acids that are within 10 Å from the inhibitor show on a list on the side.

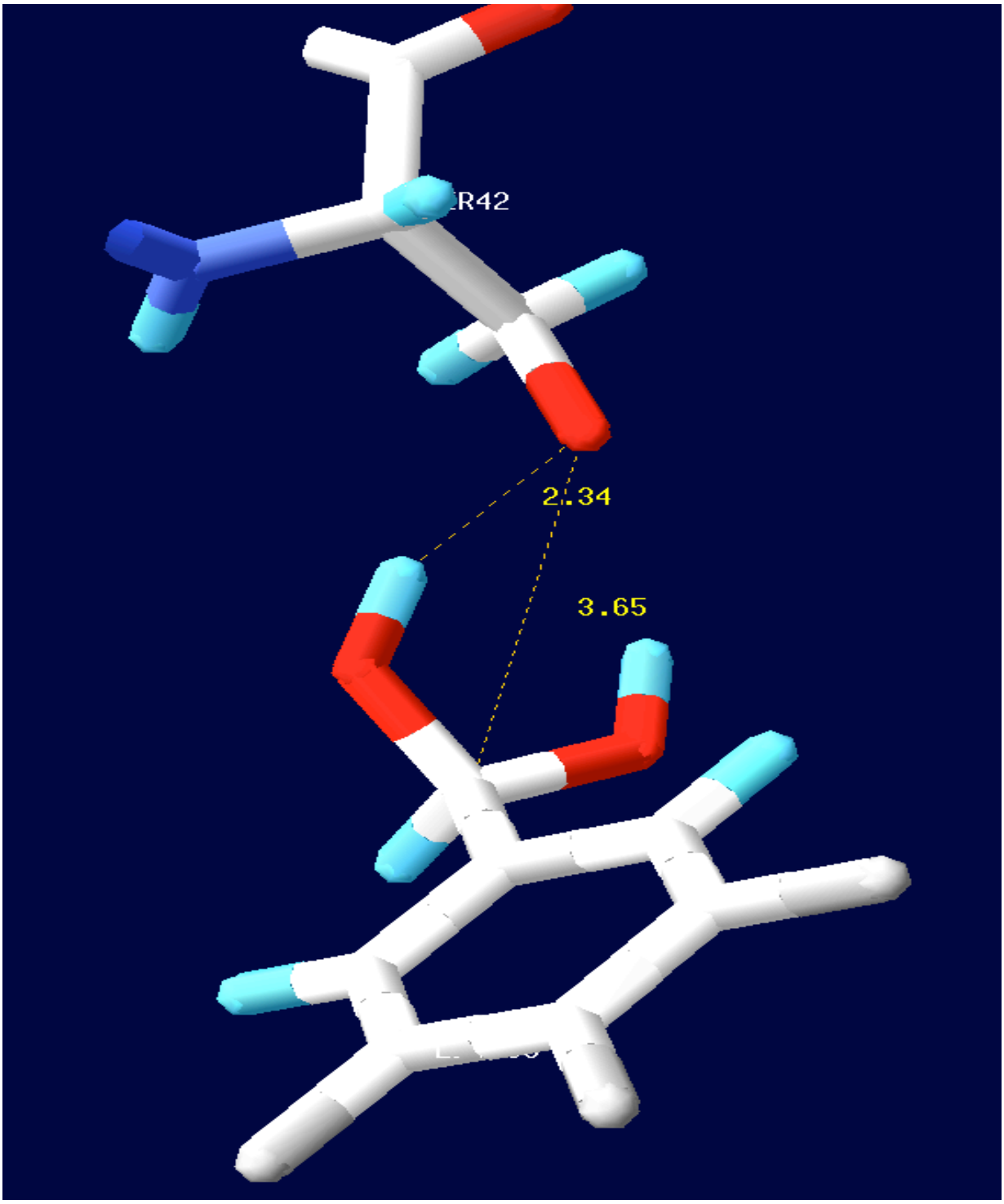

Figure 29: 3,4,5-Trifluorophenylboronic acid in the active site of BlaC (3CG5). Distances between Ser42(70) and the inhibitor.

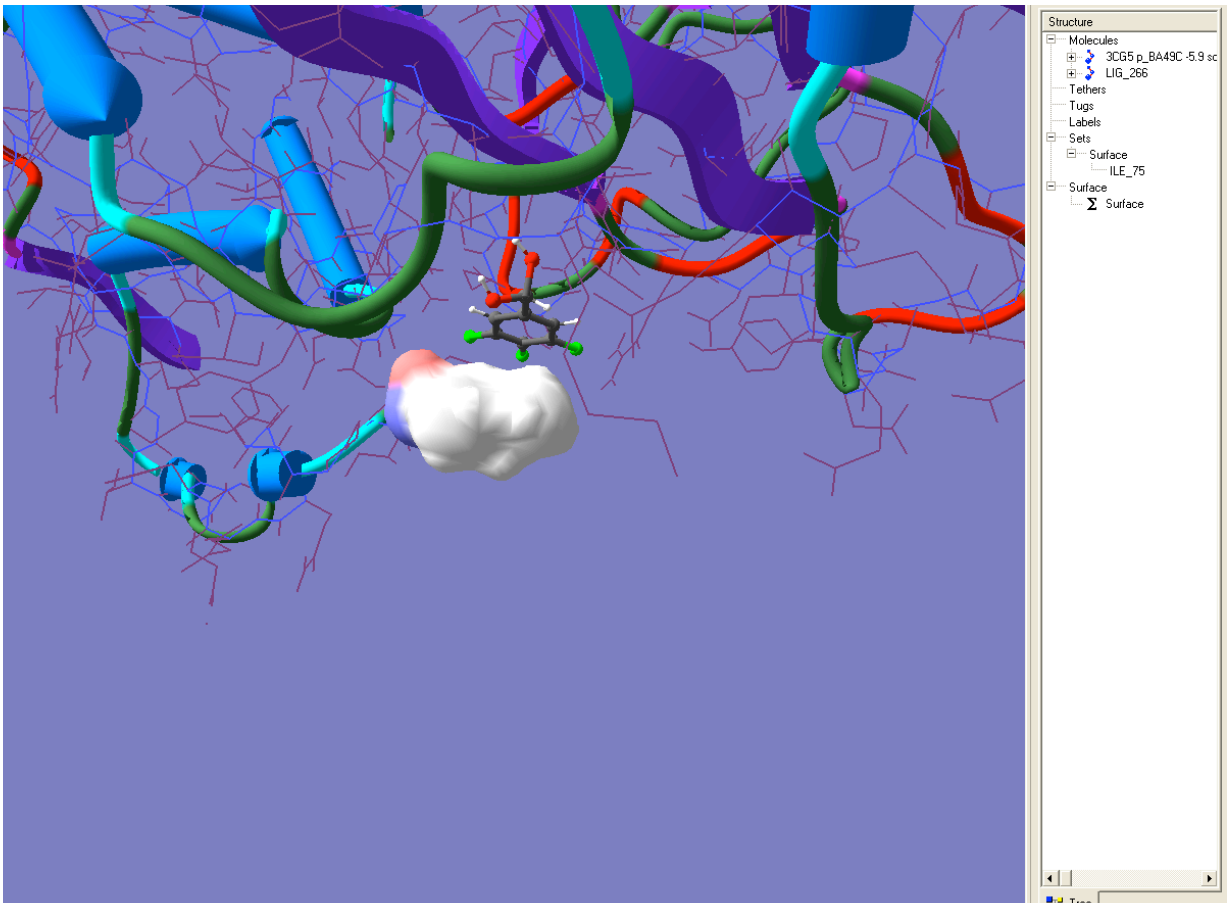

Figure 30: 3,4,5-Trifluorophenylboronic acid (ball and sticks) in the active site of BlaC (3CG5). Surface on within 5 Å of the inhibitor. Ile75 is the only amino acid in this sphere.

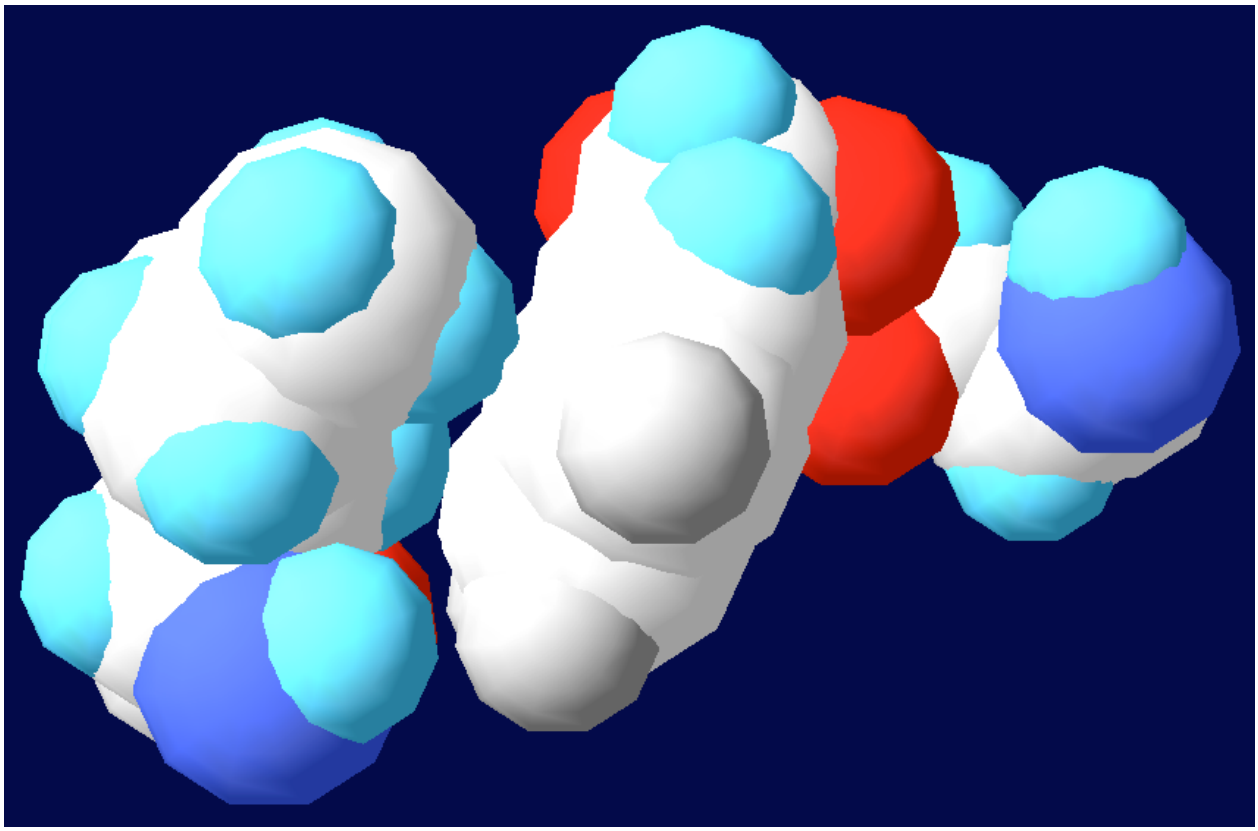

Figure 31: 3,4,5-Trifluorophenylboronic acid in the active site of BlaC (3CG5). Ile75 is located on the left, ligand in the middle and Ser42 on the right.

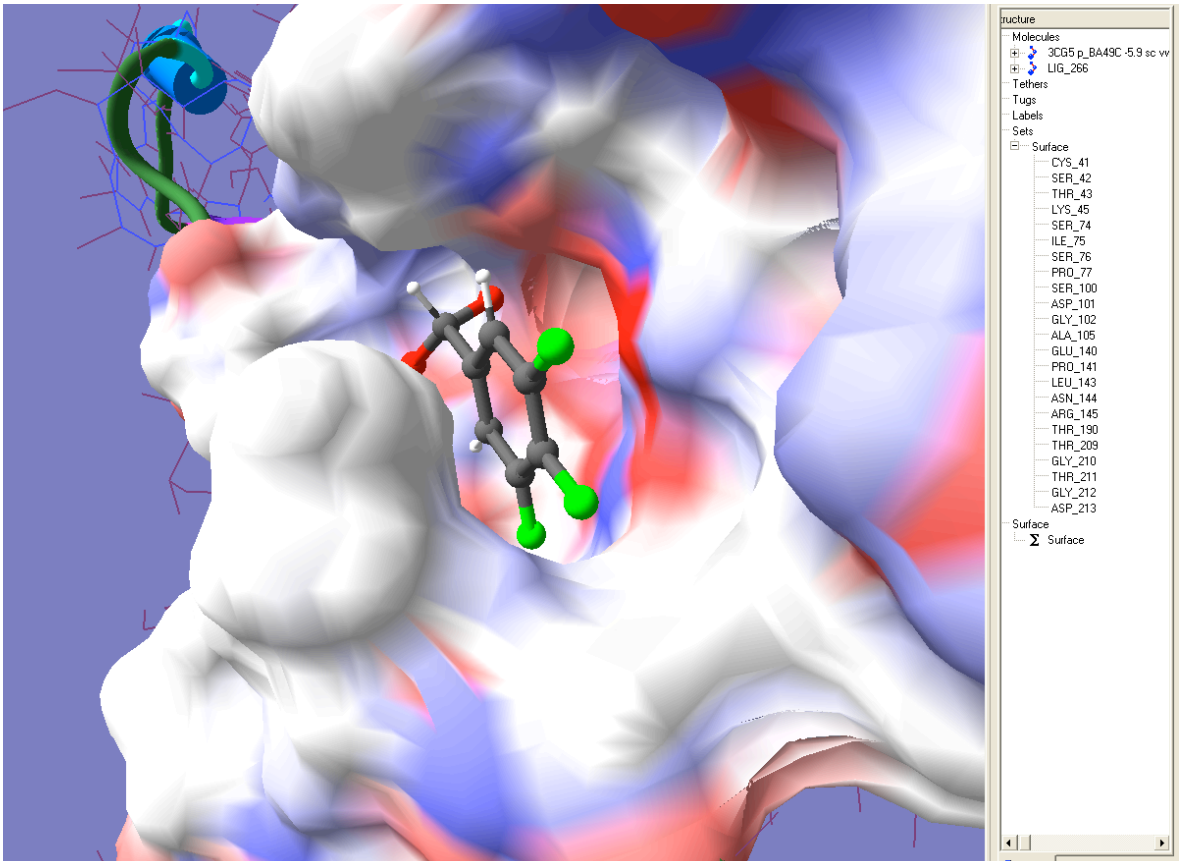

Figure 32: 3,4,5-trifluorophenylboronic acid in the active site of BlaC (3CG5). Ile75 shows as the protuberance on the left of the benzene ring of the inhibitor.

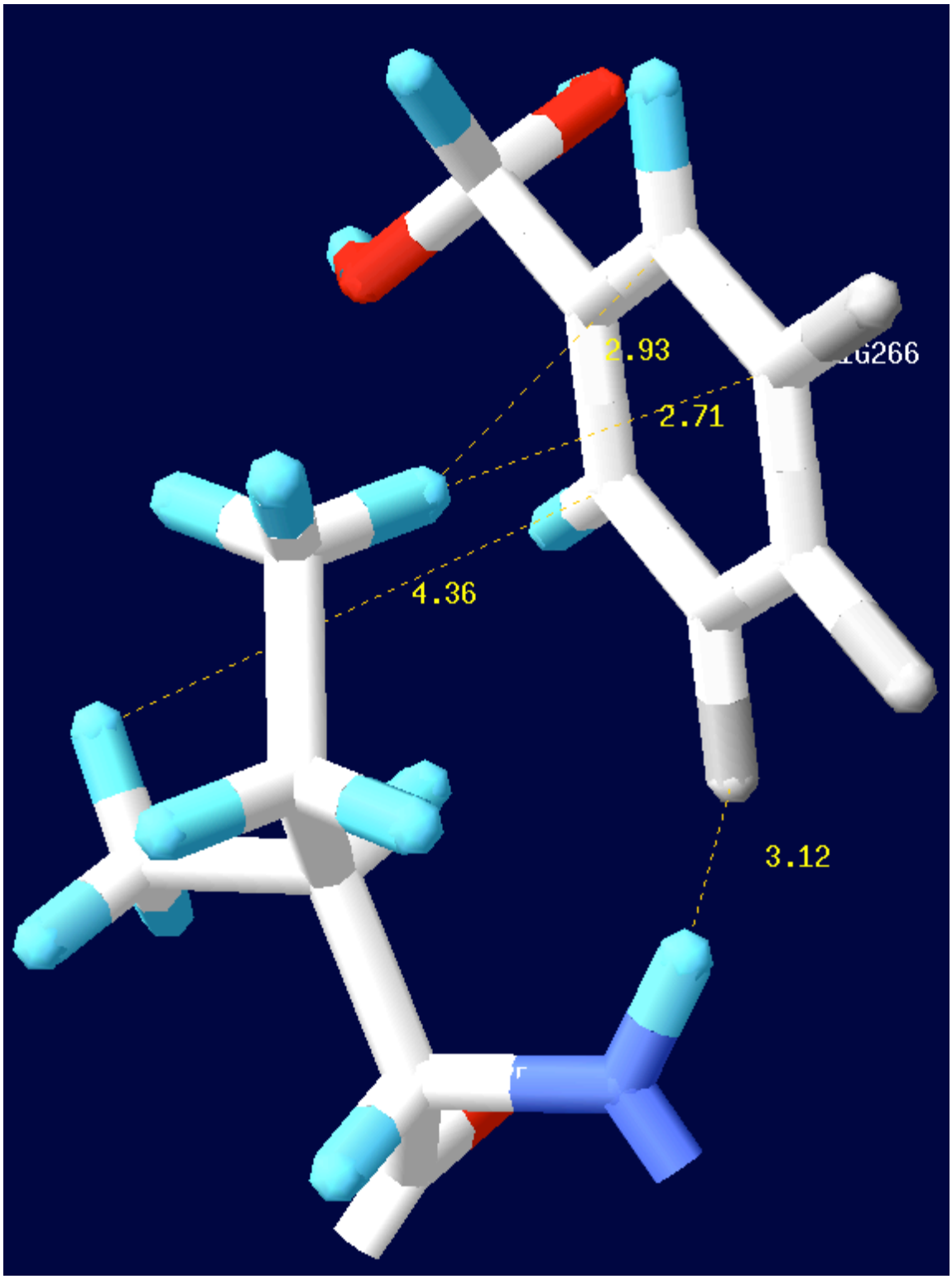

Figure 33: 3,4,5-Trifluorophenylboronic acid in the active site of BlaC (3CG5). Distances between Ile75 and the inhibitor.

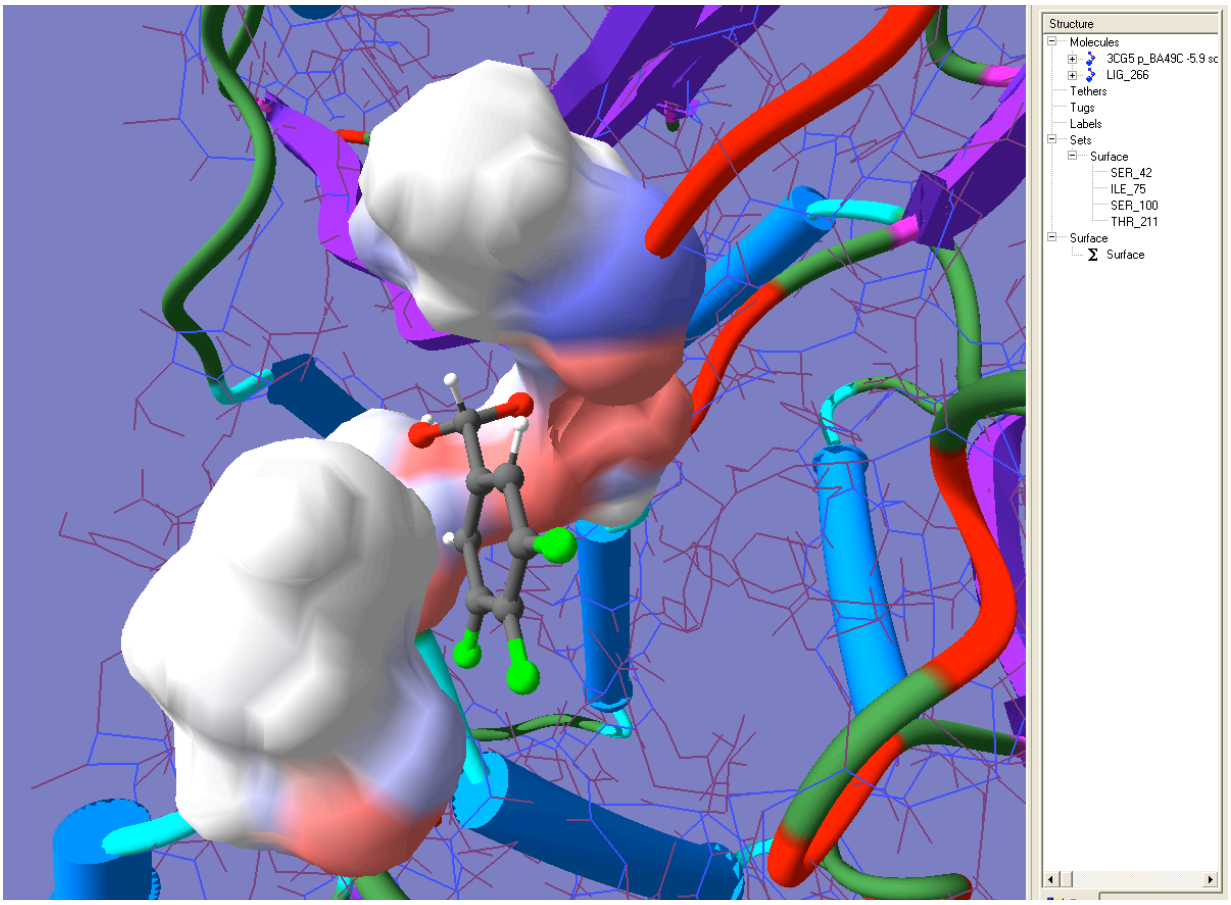

Figure 34: 3,4,5-trifluorophenylboronic acid in the active site of BlaC (3CG5). Surface on within 6 Å of the inhibitor. Ser42(70), Ser100(130) and Thr211 (Ala237) are the surface in the 6 Å sphere.

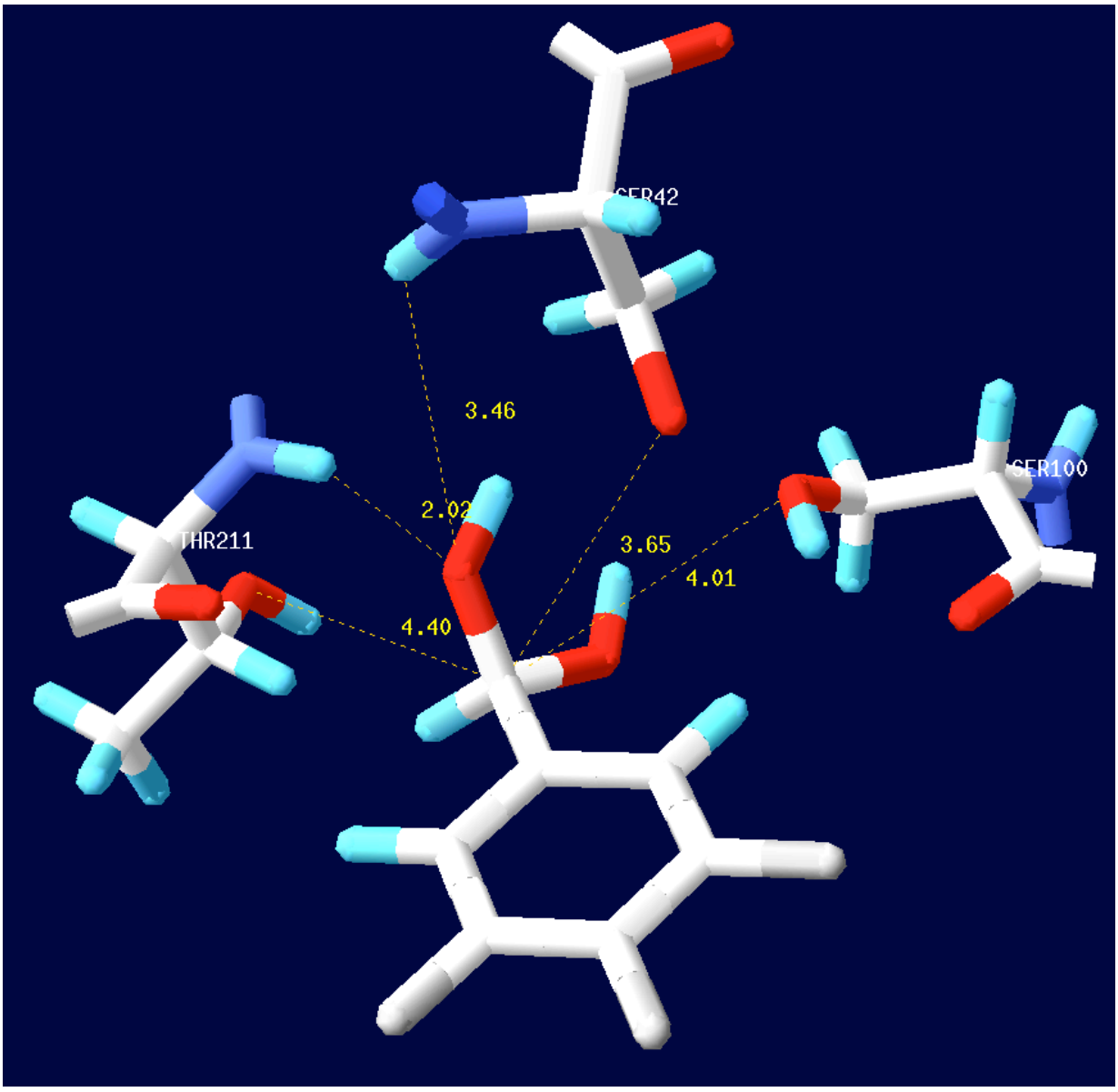

Figure 35: 3,4,5-trifluorophenylboronic acid in the active site of BlaC (3CG5). Distances between Ser100(130), Ser42(70), and Thr211 (Ala237) and the inhibitor.

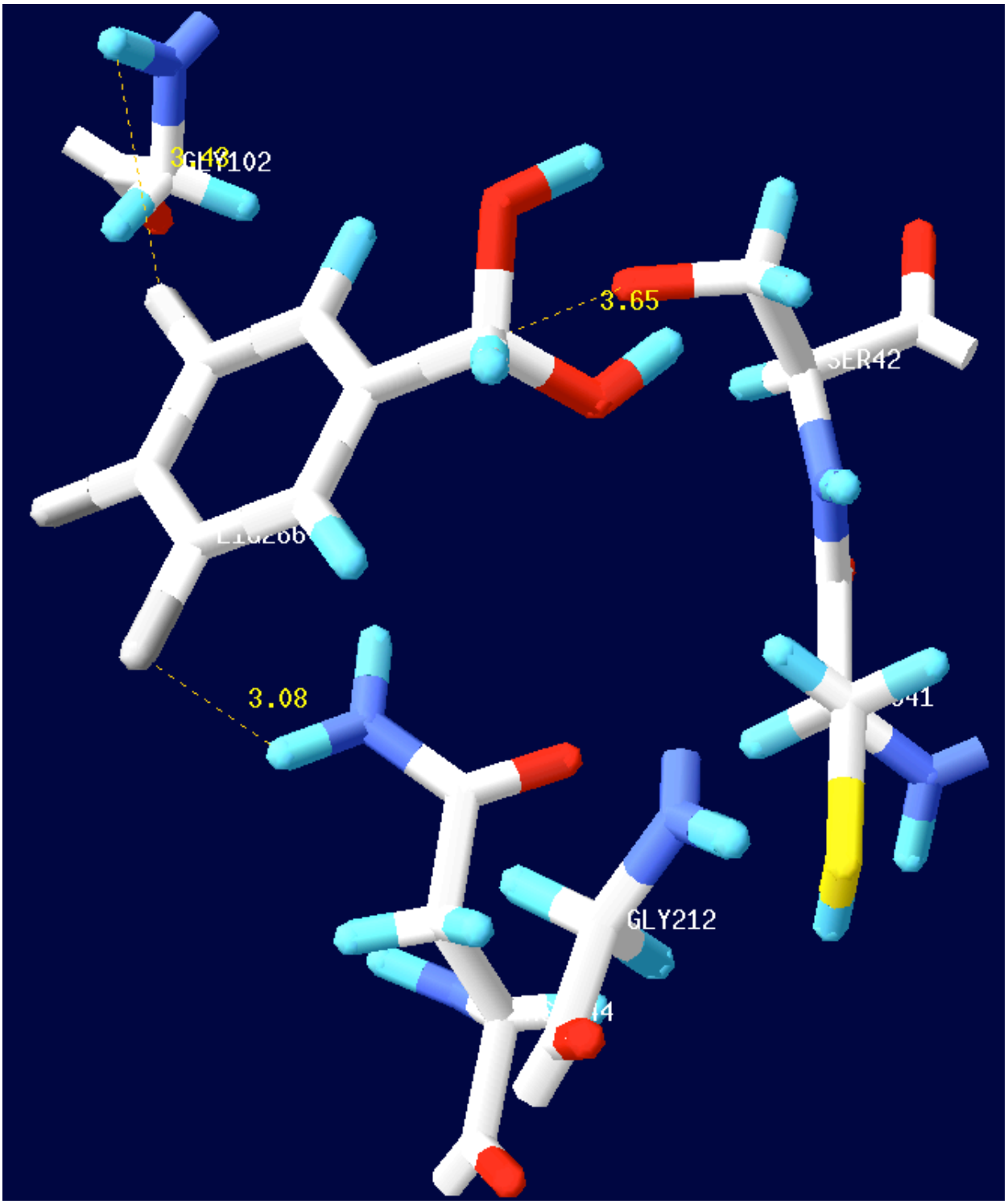

Figure 36: 3,4,5-trifluorophenylboronic acid in the active site of BlaC (3CG5). Included Ser42(70) for reference. Hydrogen bond possible between Gly102(132) N terminus Hydrogen and F(5) of ligand 3.43 Å and another hydrogen bond possible between Asn144(170) γNH and F(3) of ligand 3.08 Å. 7 Å sphere around the inhibitor.

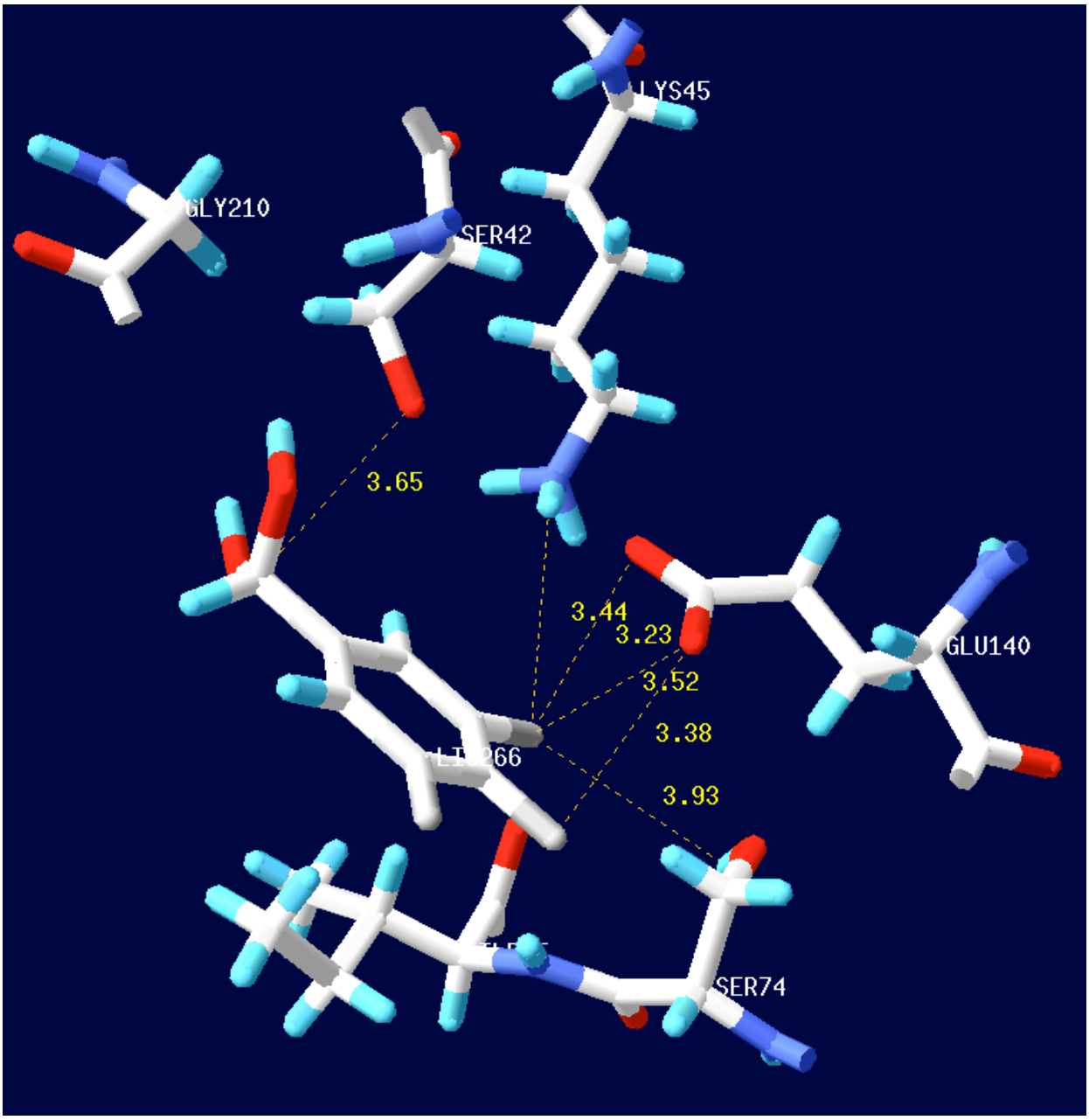

Figure 37: 3,4,5-trifluorophenylboronic acid in the active site of BlaC (3CG5). Amino acids in the 8 Å sphere around the inhibitor. Lys45, Ser74, Glu140 and Gly210. The relevant possible interactions are Hydrogen bonds between δ Hs and F(3) measuring 3.23 Å and 3.52 Å of Glu140 and 3.38 Å to the F(4). Also Lys45 ε H and F(3). Ser74 β H to F(3) 3.93 Å

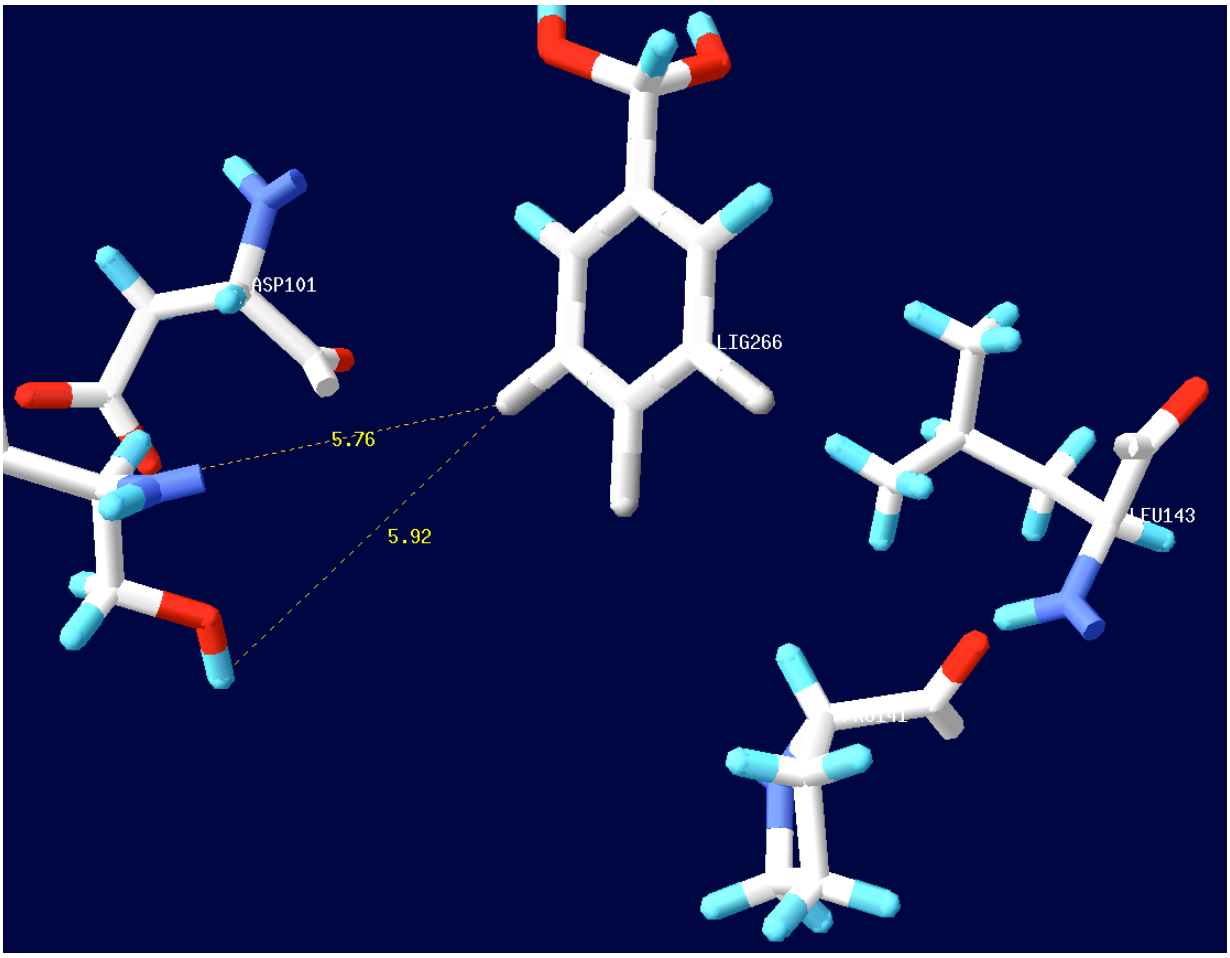

Figure 38: 3,4,5-trifluorophenylboronic acid in the active site of BlaC (3CG5). Amino acids in the 9 Å sphere around the inhibitor. No relevant distance noted. Ser76 N-terminus H with F(5) 5.74 Å and β H with F(5) 5.92 Å

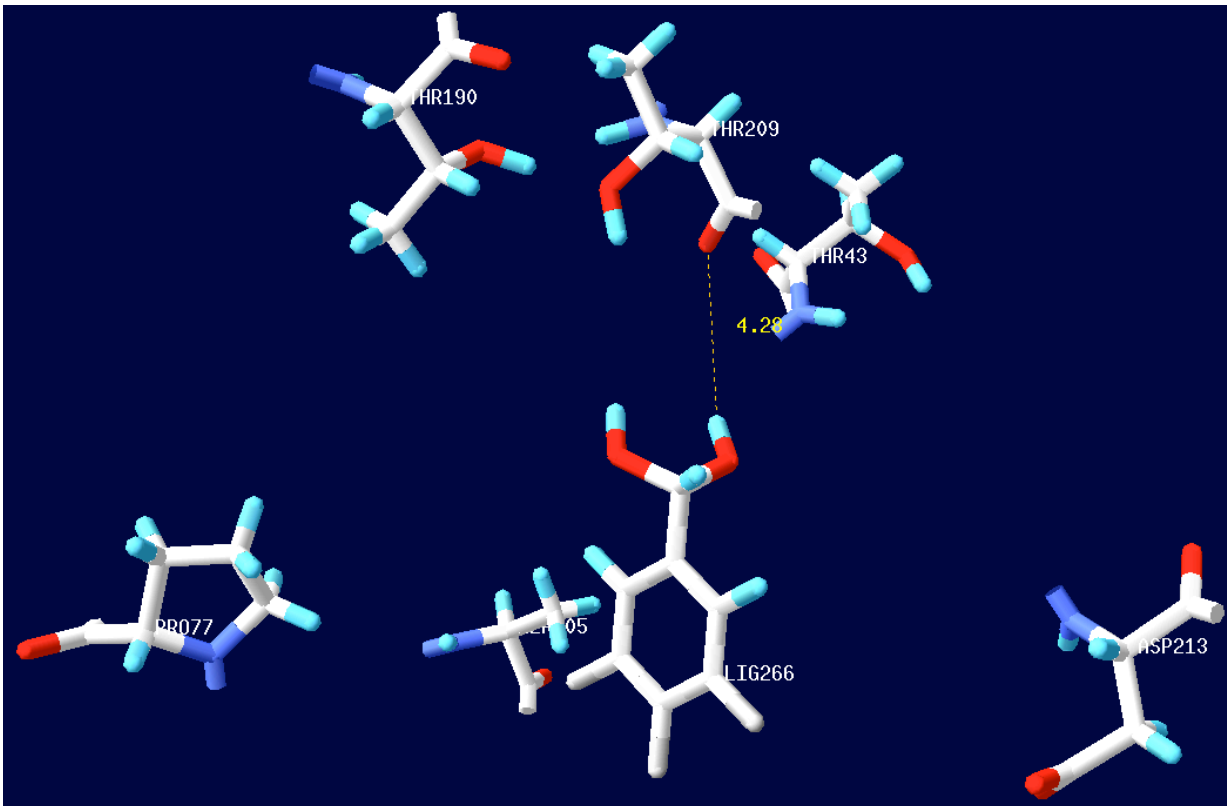

Figure 39: 3,4,5-trifluorophenylboronic acid in the active site of BlaC (3CG5). Amino acids in the 10 Å sphere around the inhibitor.

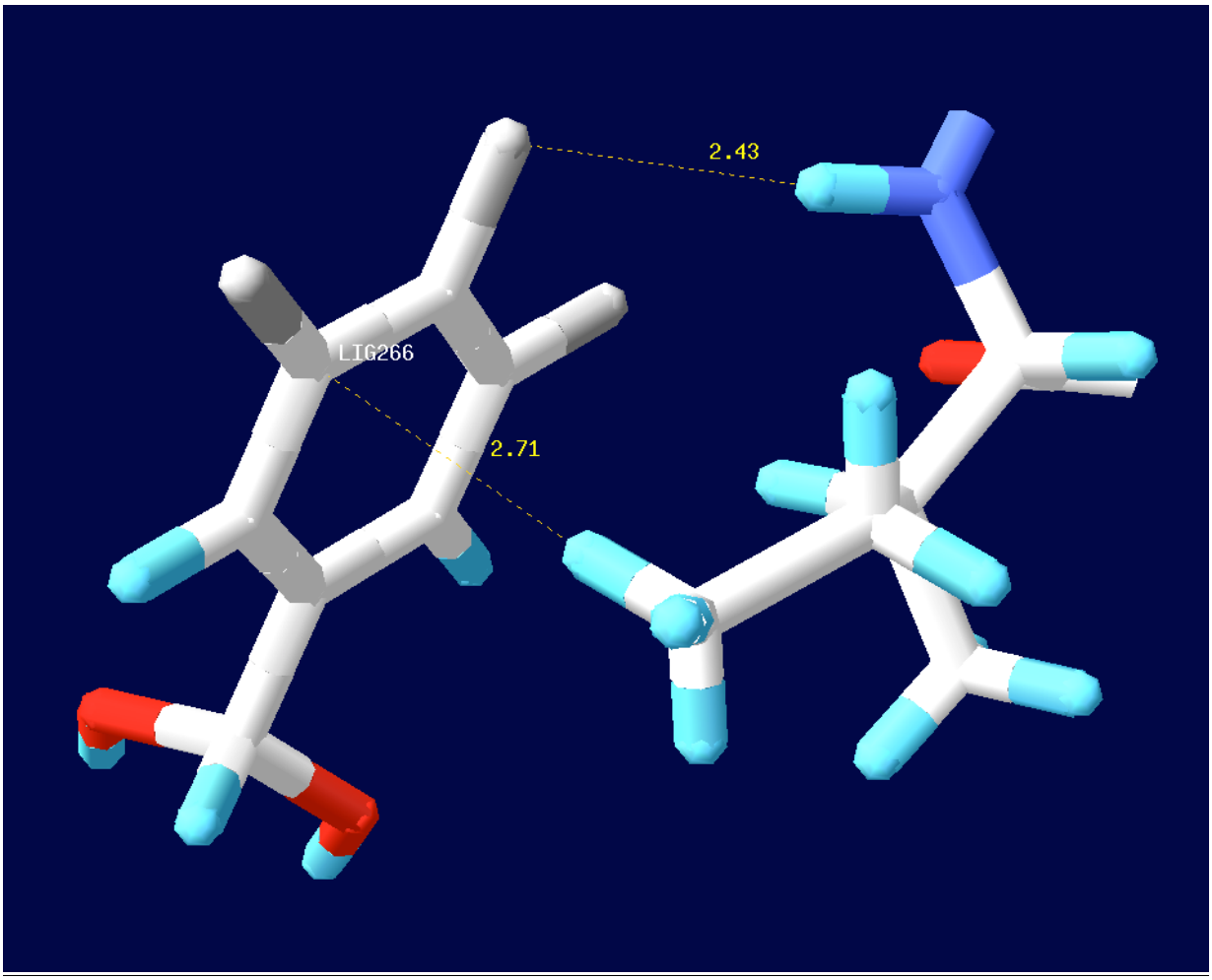

Figure 40: 3,4,5-Trifluorophenylboronic acid in the active site of BlaC (3CG5). Ile75 distance to the ring 2.71 Å and 2.43 Å from αNH(H) to F(4) in the inhibitor.

3,4,5-Trifluorophenylboronic acid in the active site of TEM-1 (1ERO).

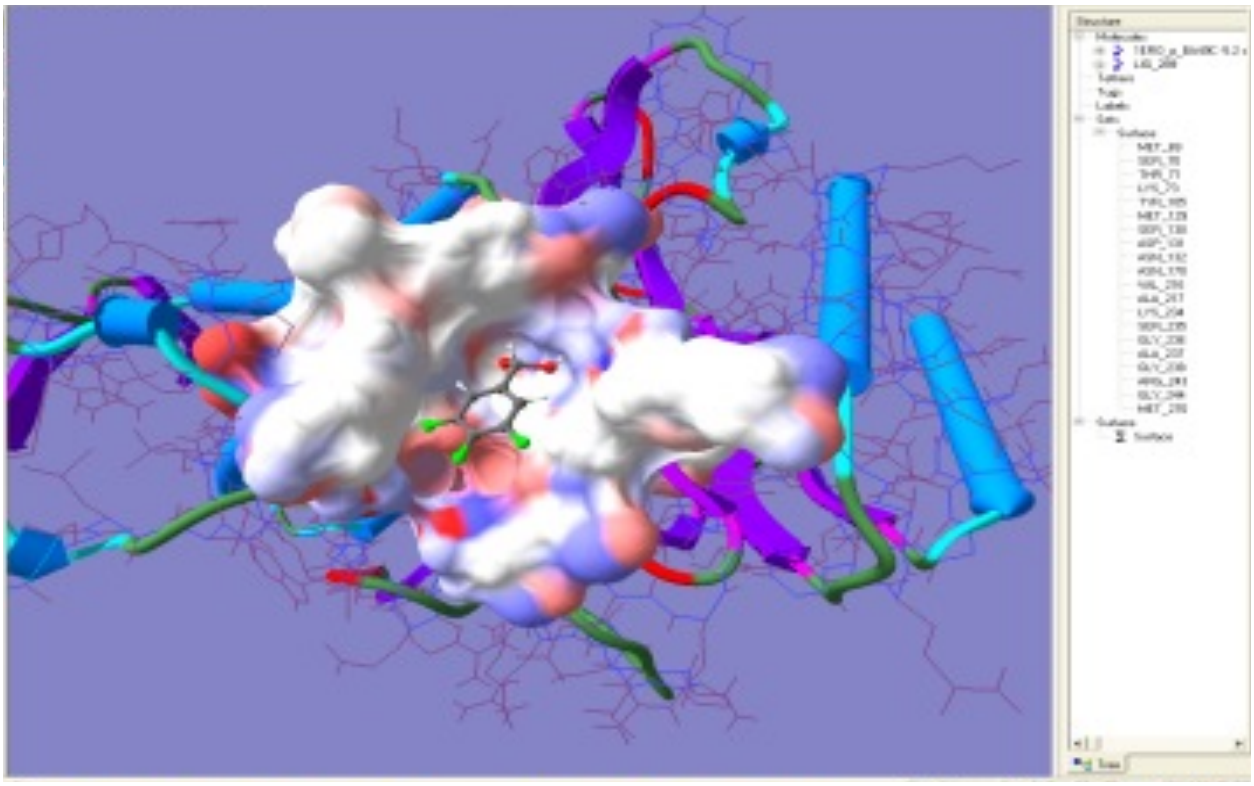

Figure 41: 3,4,5-Trifluorophenylboronic acid in the active site of TEM-1 (1ERO). Surface on within 10.0 Å of the inhibitor. List of amino acids in the 10.0 Å sphere from the inhibitor shown in the window at the right.

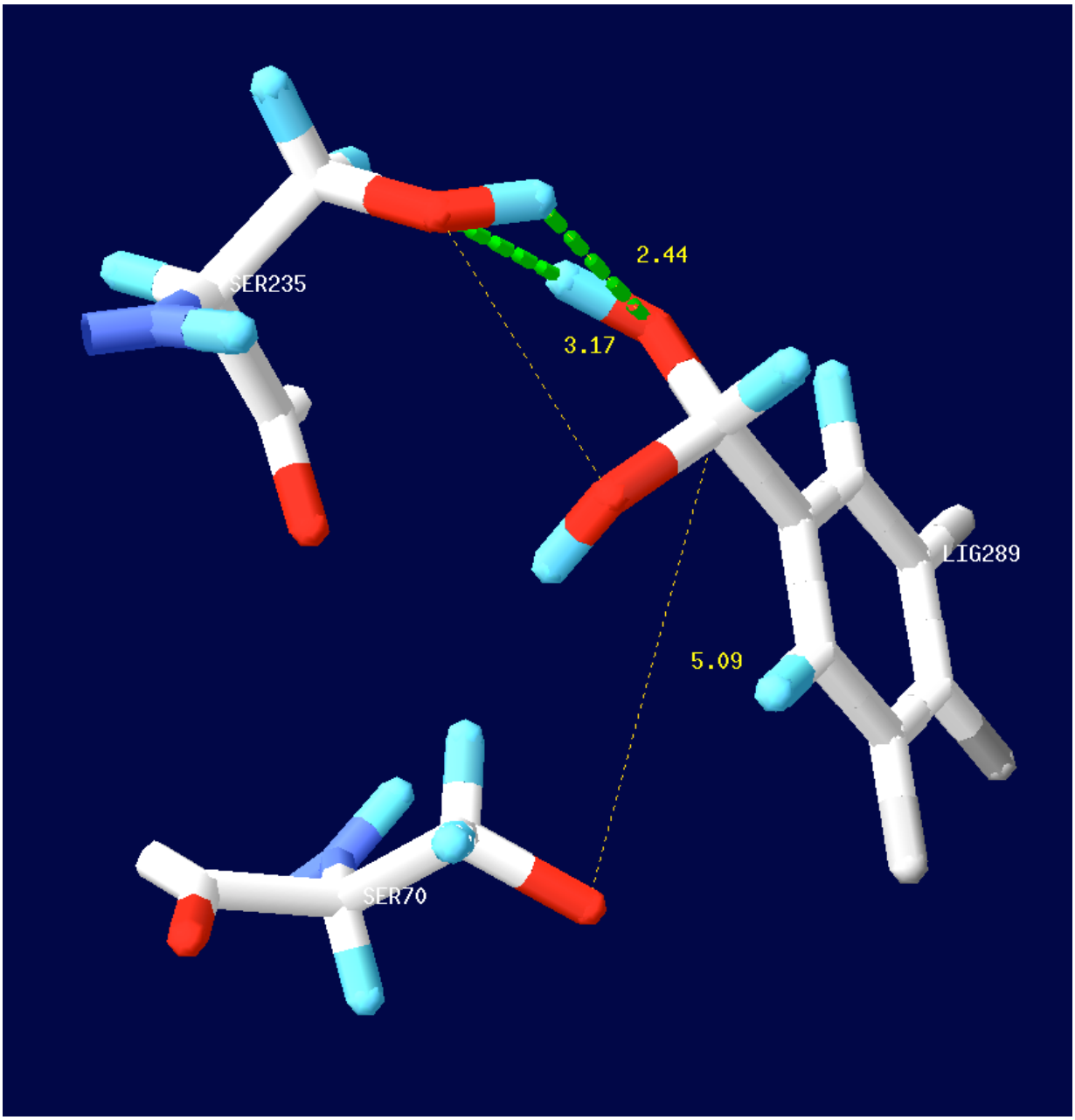

Figure 42: 3,4,5-Trifluorophenylboronic acid in the active site of TEM-1 (1ERO). Distances between Ser70 and Ser235 and the inhibitor.

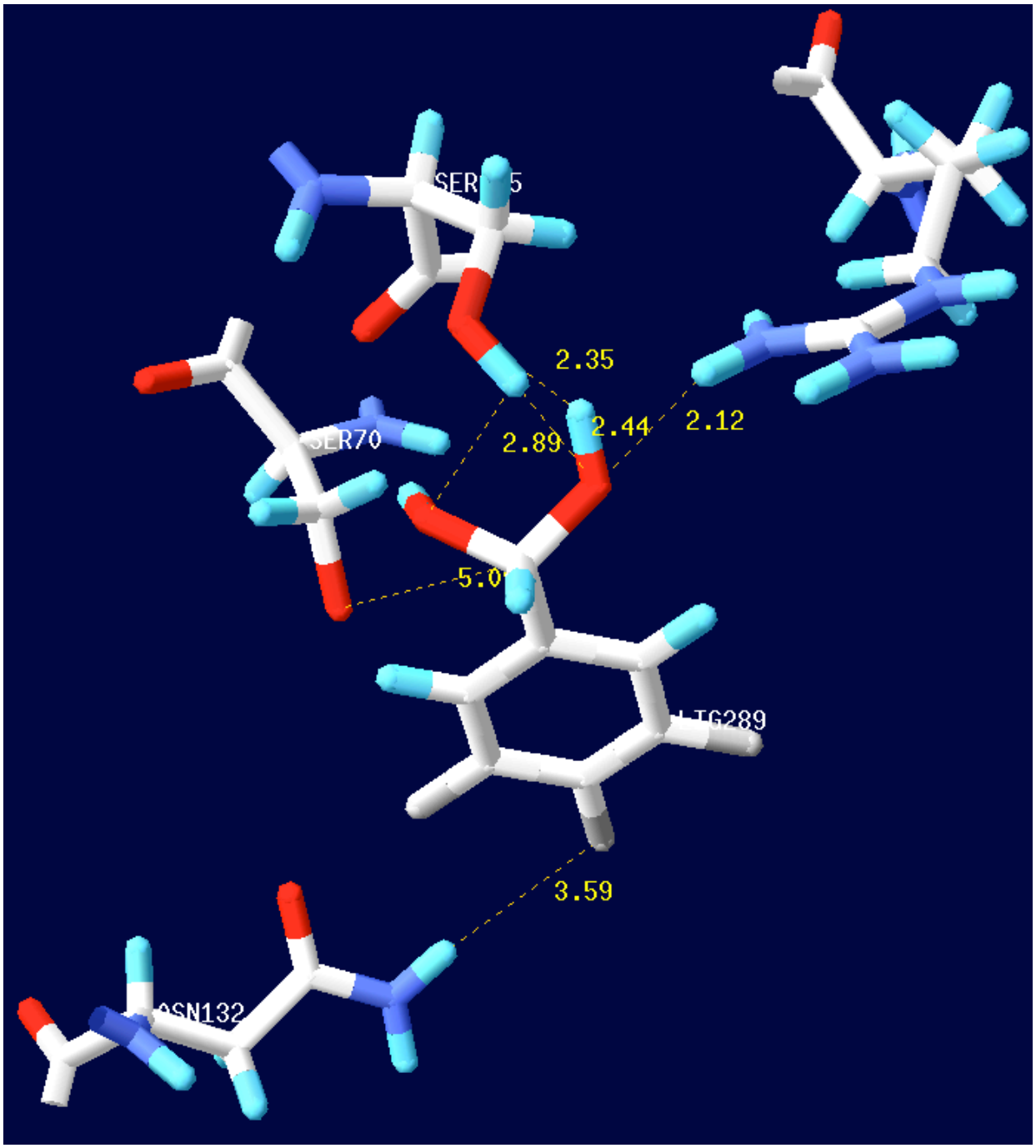

Figure 43: 3,4,5-Trifluorophenylboronic acid in the active site of TEM-1 (1ERO). Distances between Asn132 and Arg243 with the inhibitor. Ser70 and Ser235 are shown for reference.

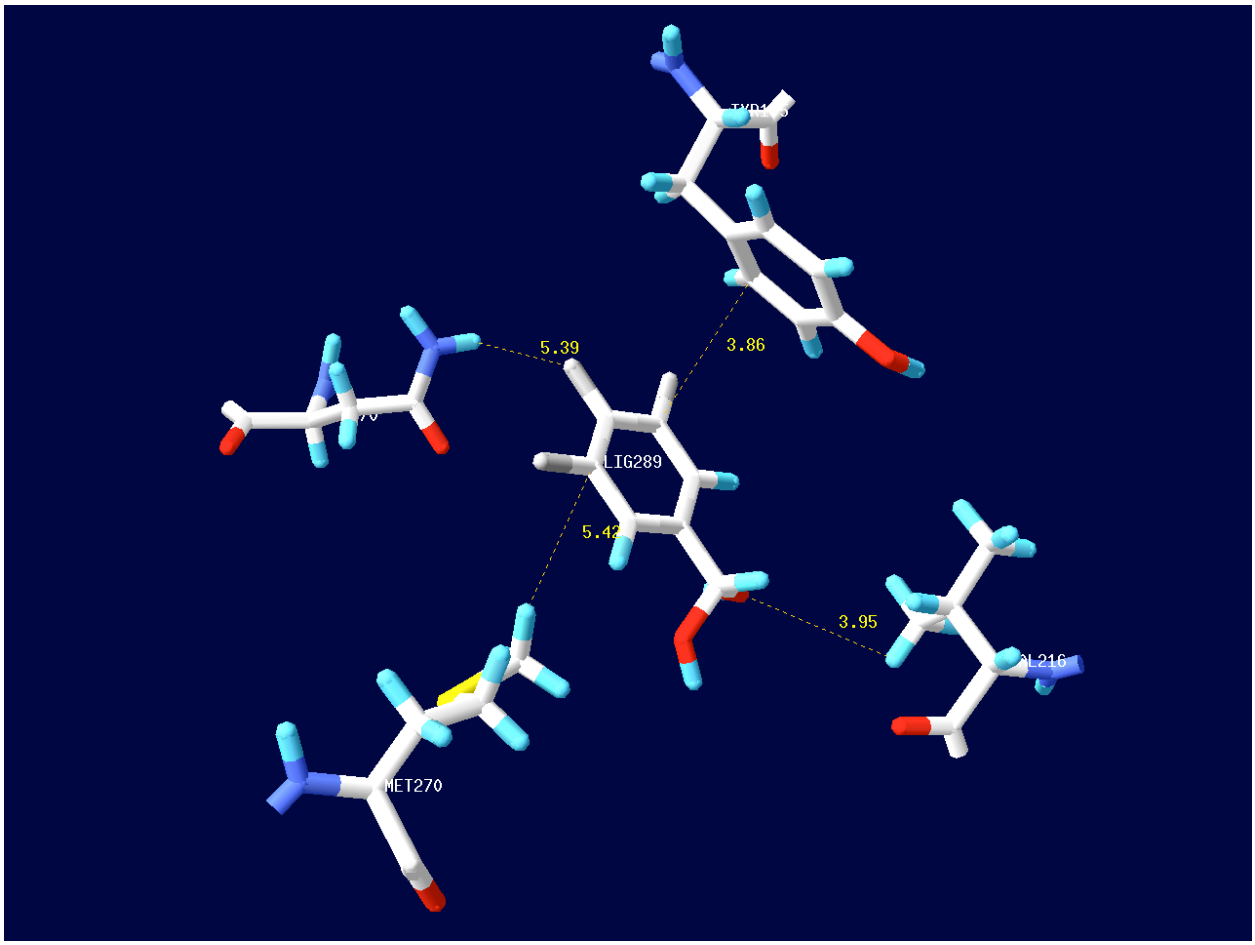

Figure 44: 3,4,5-Trifluorophenylboronic acid in the active site of TEM-1 (1ERO). Distances between Tyr105, Asn170, Val216, Met270 and the inhibitor.

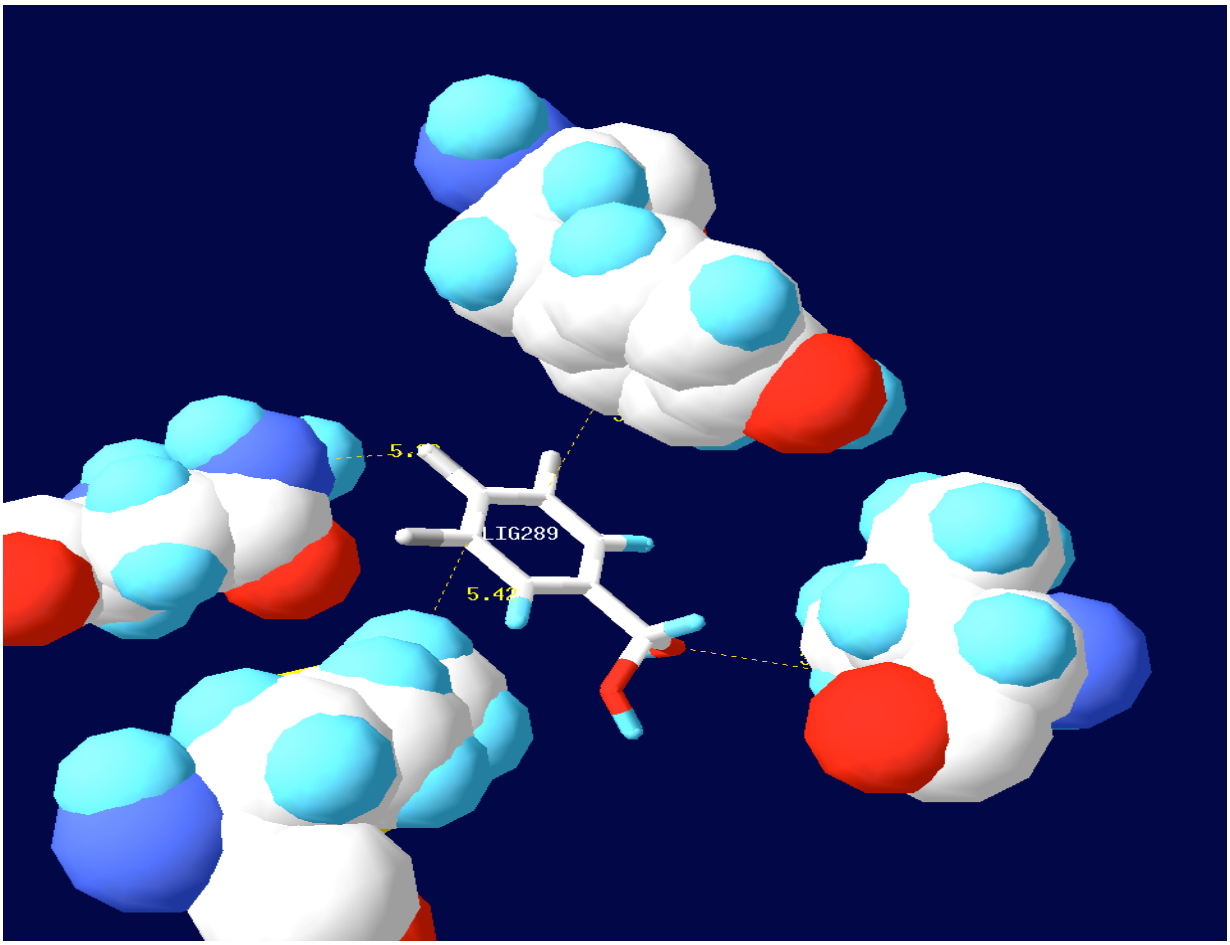

Figure 45: 3,4,5-Trifluorophenylboronic acid in the active site of TEM-1 (1ERO). Space filling model of Tyr105, Asn170, Val216, Met270 and the inhibitor in the active site.

3-Nitrophenylboronic acid in the active site of BlaC (3CG5) and TEM-1 (1ERO).

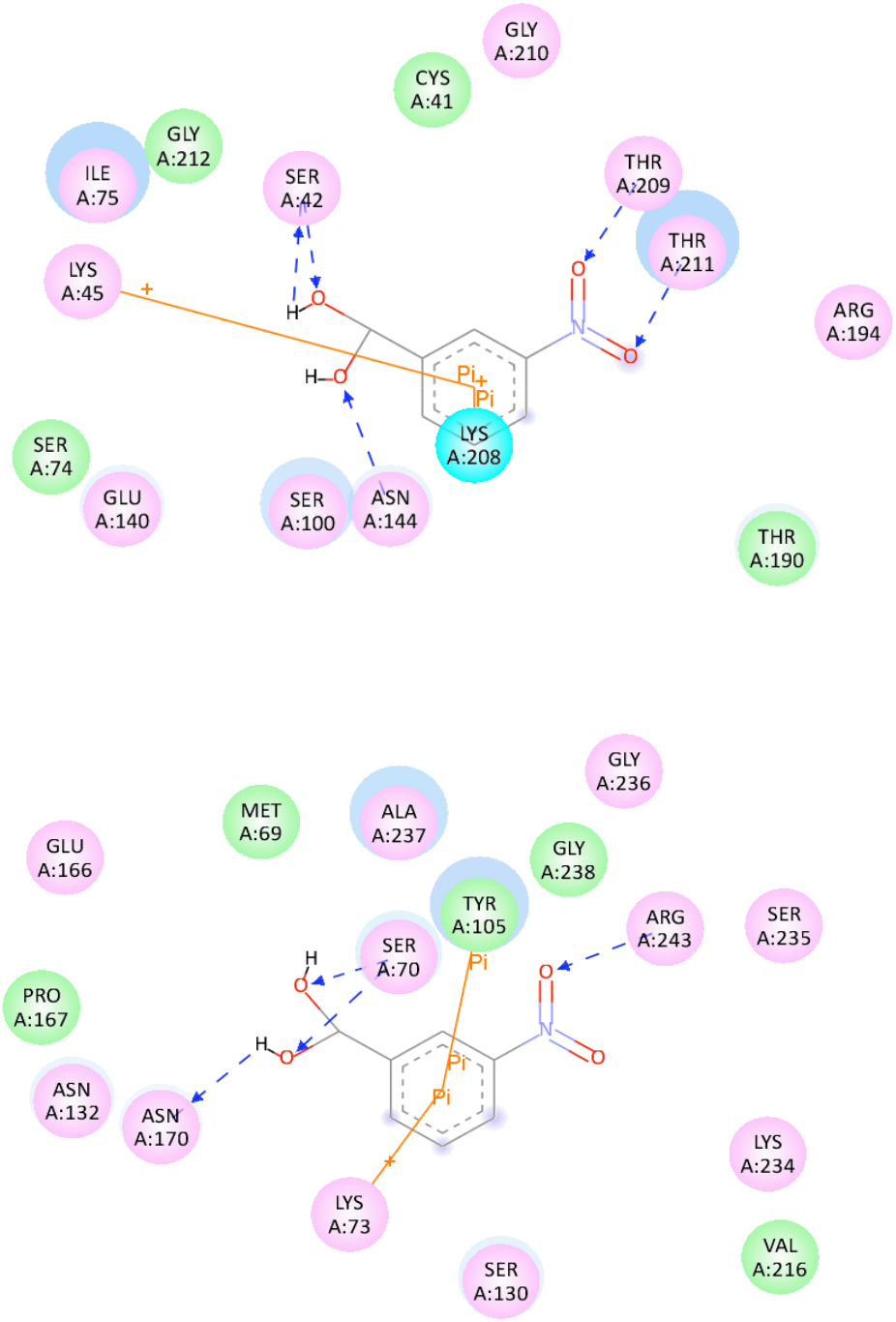

Figure 46: 3-Nitrophenylboronic acid in the active site of BlaC (3CG5) (top) and TEM-1 (1ERO) (bottom).

Table 6: 3-Nitrophenylboronic acid in BlaC (3CG5) and TEM-1 (1ERO) active sites. Important distances.

3-Nitrophenylboronic acid			**BlaC**	**TEM-1**
3CG5(1ERO)	**BlaC**	**TEM-1**	**Å**	**Å**
Ser42(70)	Side chain Oxygen to Boron		3.64	3.29
Lys45(73)	NH(H) to C(1) Pi		4.19	
Ile75 Tyr(105)	NH(H) to C(2) Pi	C(3) to C(4)	3.14	3.50
Asn144(170)	N(H) to OH(O) H-b	αN(H) to OH(O)	2.46	1.82
Lys208(234)	N(H) to C(3)		4.91	
Thr209 Ser(235)	OH(H) to NO(O) H-b		2.07	
Thr211 Ala(237)	OH(H) to NO(O) H-b		2.11	
Ala217 Arg(243)	NH(H) to NO(O) H-b			2.43

See page 82 (Table 8) for abbreviations.

3-Nitrophenylboronic acid in the active site of BlaC (3CG5).

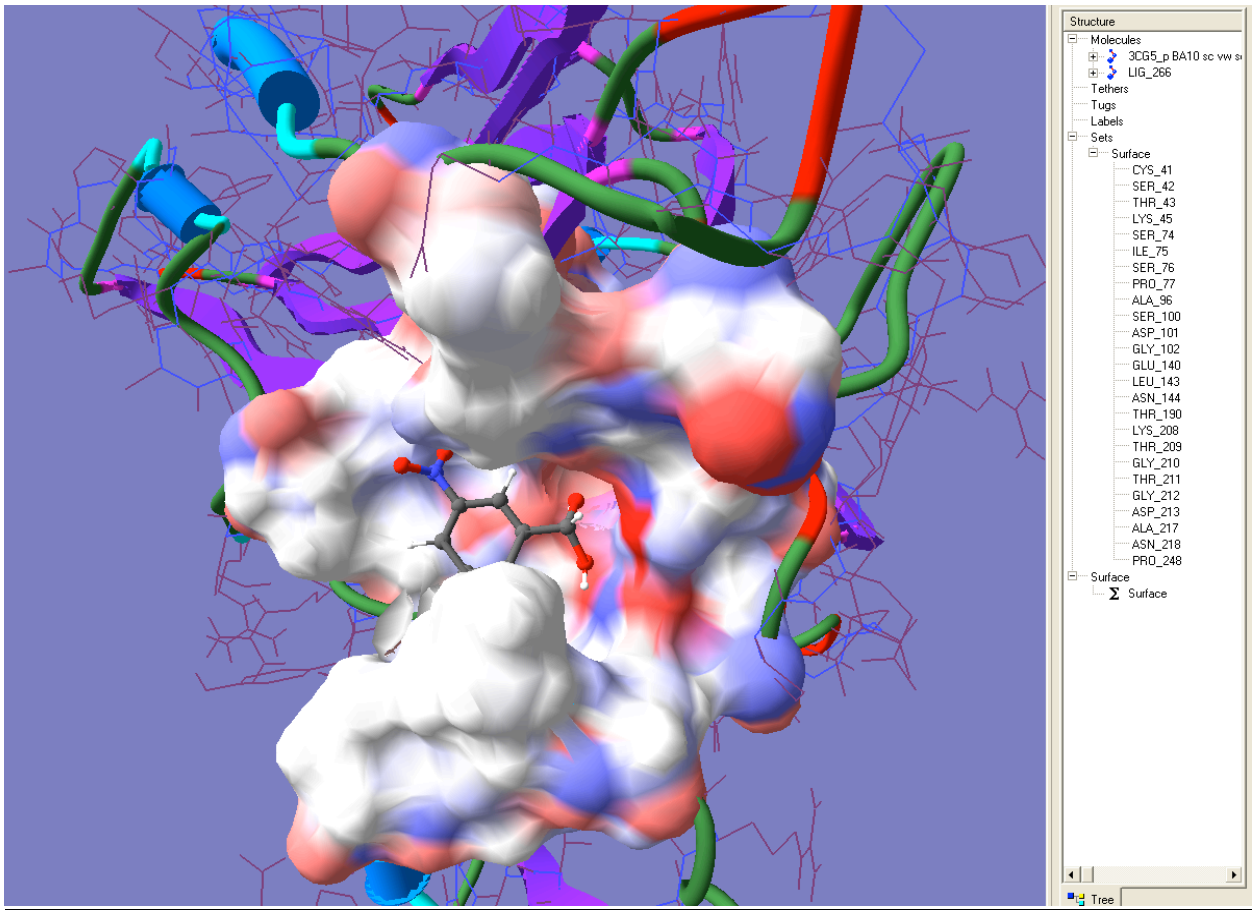

Figure 47: 3-Nitrophenylboronic acid in the active site of BlaC (3CG5). Surface on within 10.0 Å of the inhibitor. A list of amino acids in the 10.0 Å sphere from the inhibitor is shown in the window at the right.

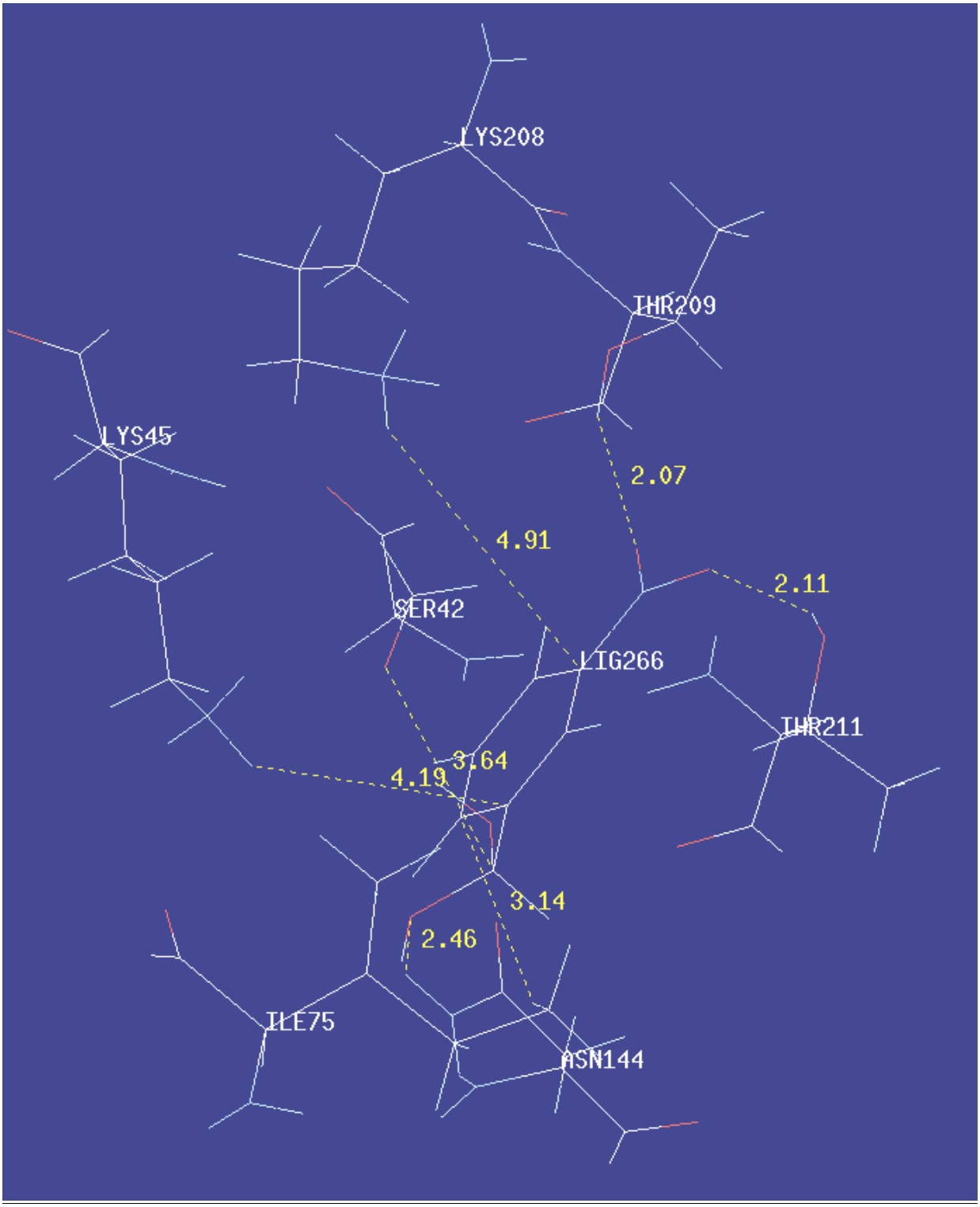

Figure 48: 3-Nitrophenylboronic acid in the active site of BlaC.

TEM-1 and 3-Nitrophenylboronic acid

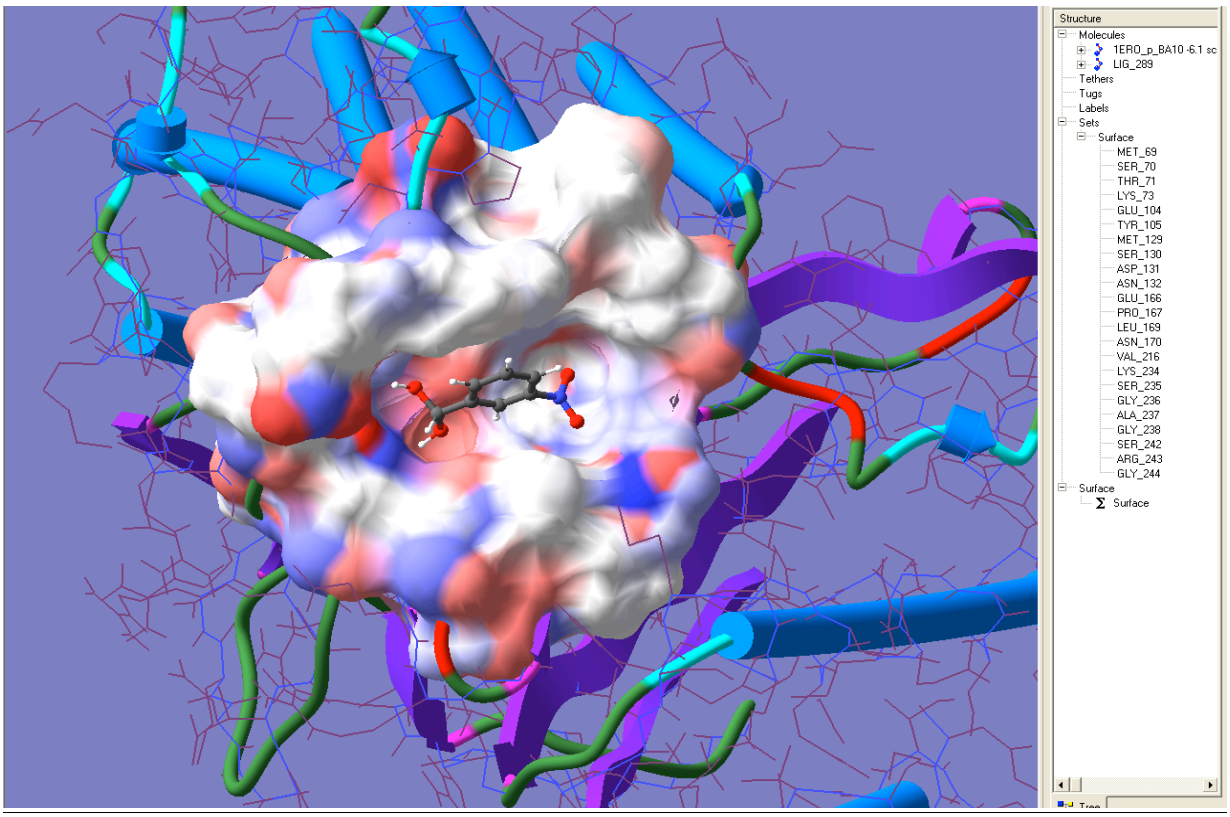

Figure 49: 3-Nitrophenylboronic acid in the active site of TEM-1 (1ERO). Surface on within 10.0 Å of the inhibitor. A list of amino acids in the 10.0 Å sphere from the inhibitor is shown in the window at the right.

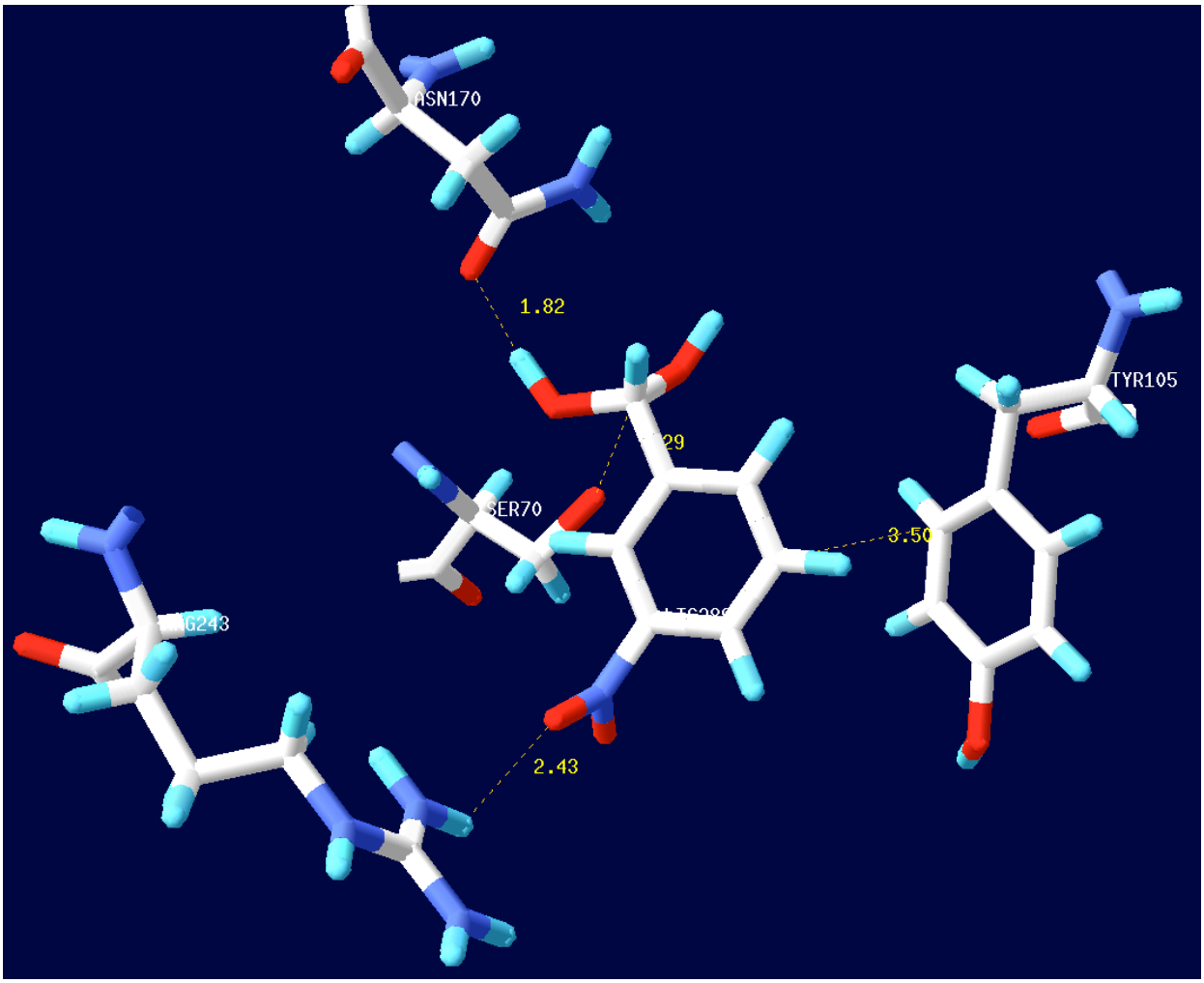

Figure 50: 3-Nitrophenylboronic acid in the active site of TEM-1. Distances of Ser70, Tyr105, Asn170, and Arg243 to the inhibitor.

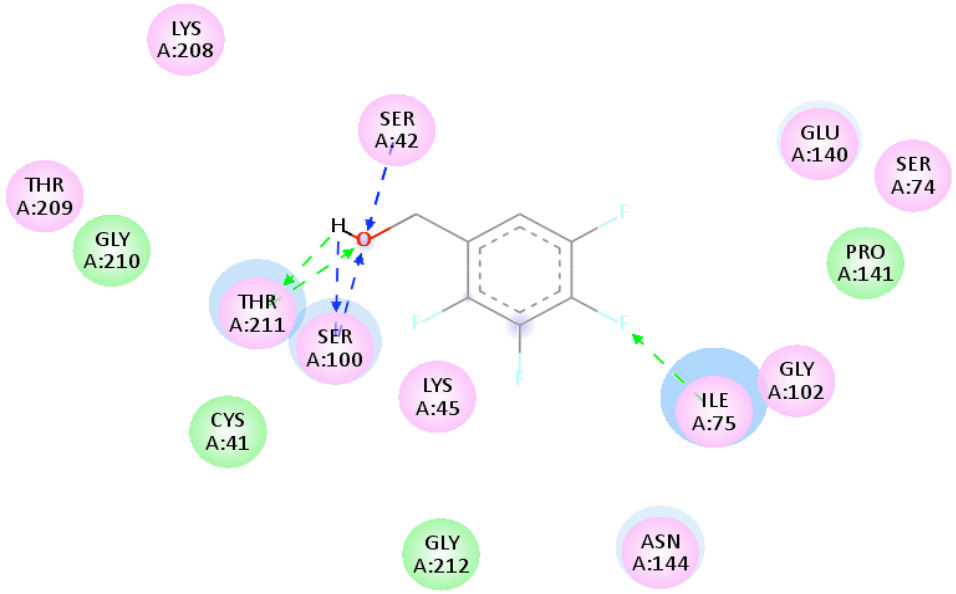

Figure 51: 2,3,4,5-Tetrafluorophenylboronic acid in the active site of BlaC (3CG5).

Table 7: 2,3,4,5-Tetrafluorophenylboronic acid in the active site of BlaC (3CG5).

2,3,4,5-Tetrafluorophenylboronic acid

3CG5		*Sculpt* Sphere (A)	Element	H-b per *Discovery Studio*	Distance	Ser42	Inhibitor	H-b criteria <4.0
Ser	100	6	2	y	1.90	OH(O)	OH(H)	yes
Thr	211	6	-	y	2.10	αNH(H)	OH(O)	yes
Thr	211	6	-	y	2.39	αCO(O)	OH(H)	yes
Ser	100	6	2	y	2.40	OH(H)	OH(O)	yes
Ile	75	5	-	y	2.42	αNH(H)	C'4F	yes
Ser	42	6	1	y	2.92	O	OH(H)	yes
Asn	144	7	4		3.02	NH(H)	C'3F	yes
Gly	102	7	2		3.36	αNH(H)	C'3F	yes
Ser	42	6	1		3.48	αNH(H)	OH(O)	yes
Ile	75	5	-		2.66	βH	C'3	-
Gly	210	8	3		2.94	αH	OH(H)	-
Lys	45	8	1		3.29	NH(H)	C'2	-
Ser	42	6	1		3.46	O	B	-
Pro	141	9	4		3.71	βH	C'3F	-
Ser	76	9	-		5.29	αH	C'3F	-
Asp	101	9	2		5.74	αCO(O)	C'2H	-
Leu	143	9	4		6.02	δH	C'3	-

See page 82 (Table 8) for abbreviations.

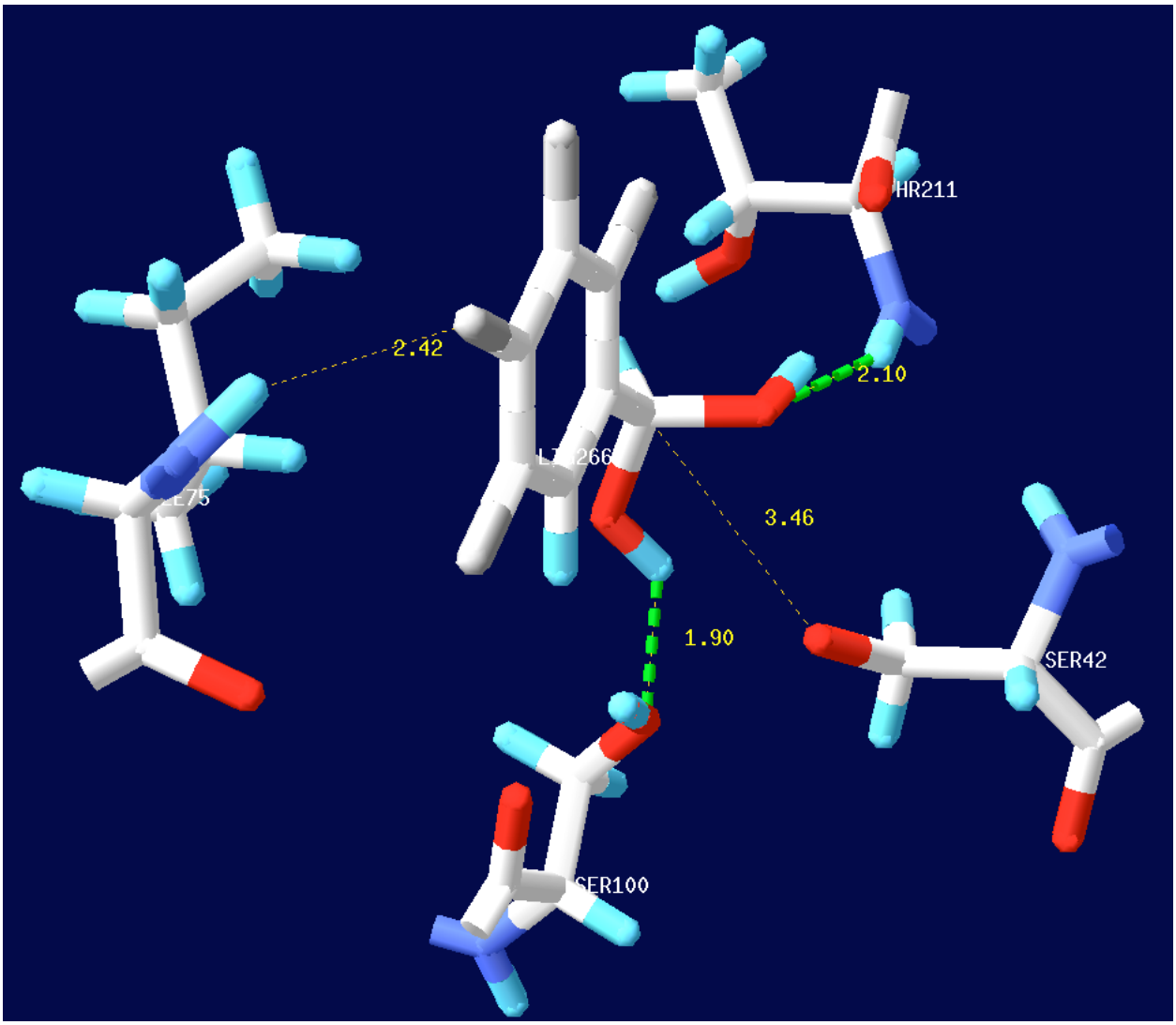

Figure 52: 2,3,4,5-Tetrafluorophenylboronic acid and the active site of BlaC. Distances between Ser42, Ile75, Ser100, Thr211 and the inhibitor. Dotted lines in green are hydrogen bonds calculated by *Swiss-PdbViewer*.

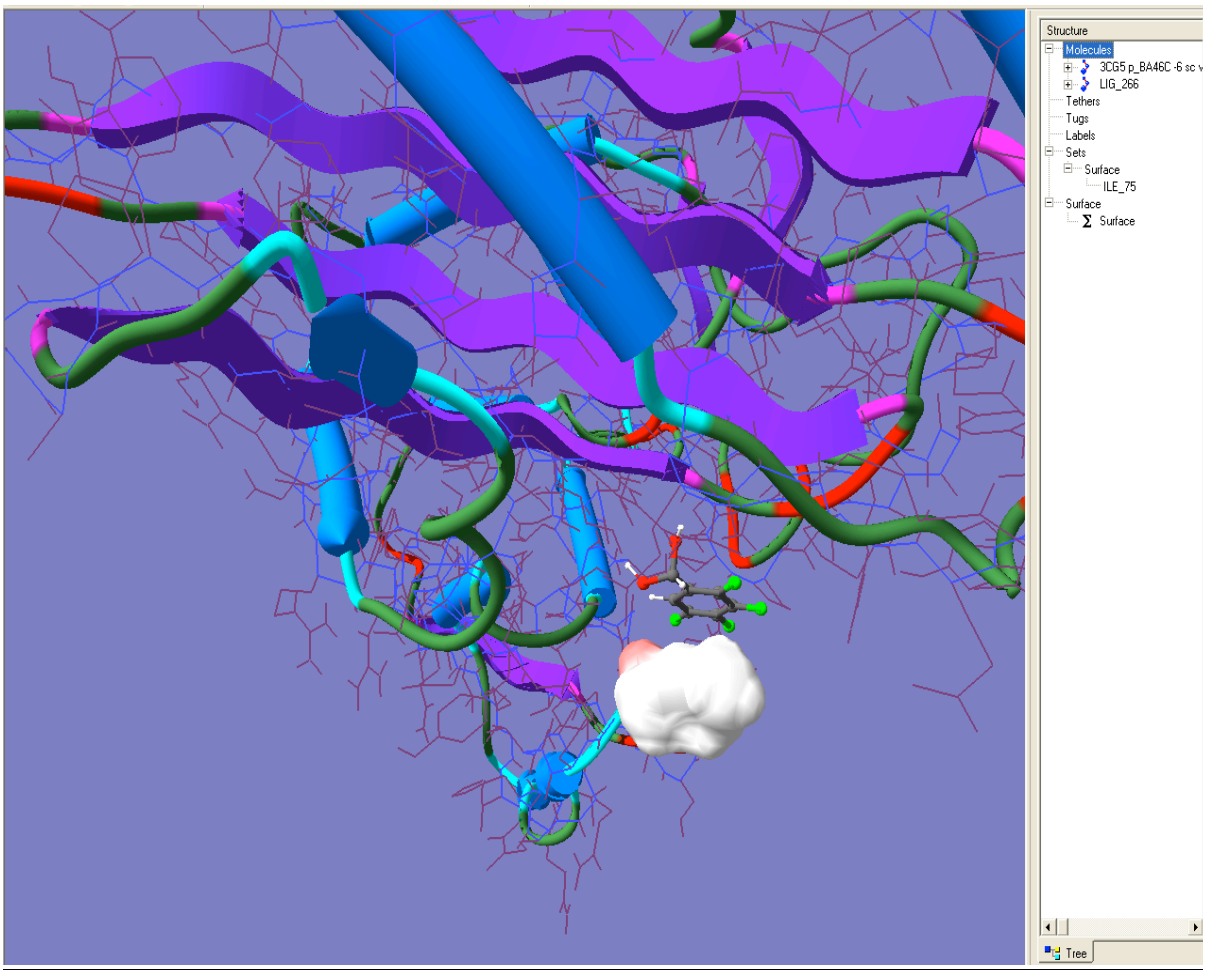

Figure 53: 2,3,4,5-Tetrafluorophenylboronic acid and the active site of BlaC. Ile75(105) shows in the first sphere around the ligand that is 5 Å from the ligand. (*Sculpt*)

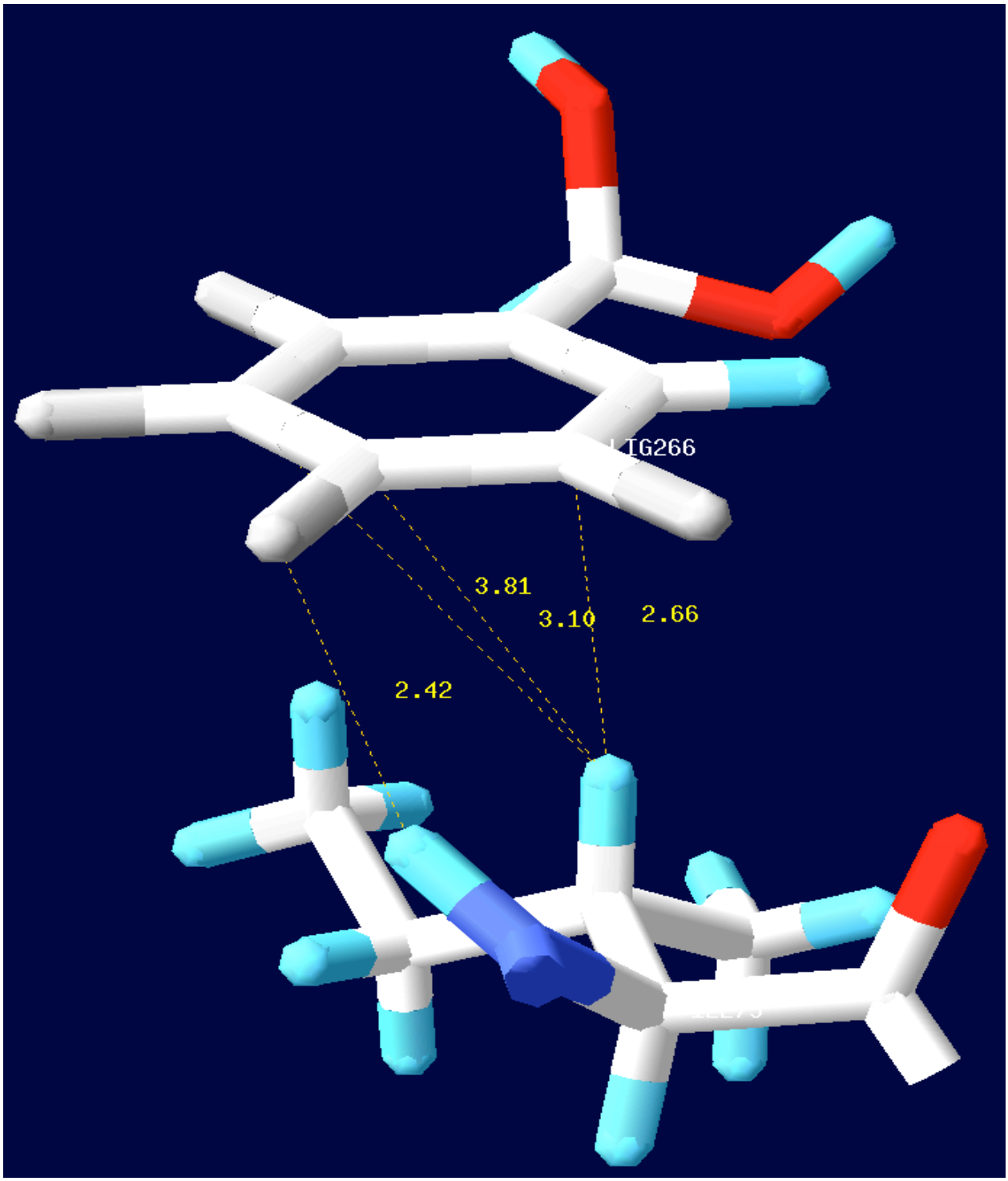

Figure 54: 2,3,4,5-Tetrafluorophenylboronic acid and the active site of BlaC. Ile75(105) shows in the first sphere around the ligand that is 5 Å from the ligand. *(Swiss-PdbViewer)*

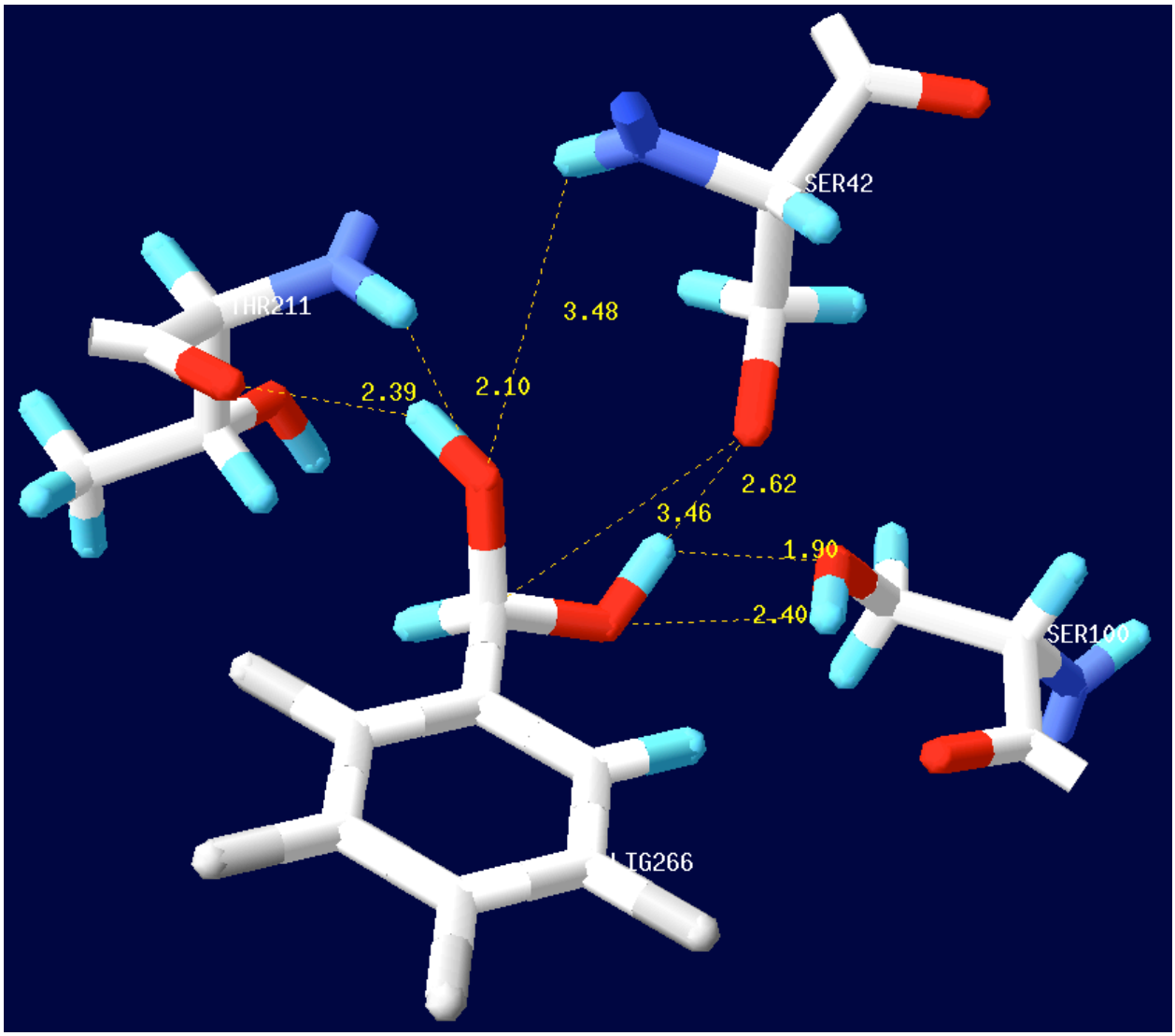

Figure 55: 2,3,4,5-Tetrafluorophenylboronic acid and the active site of BlaC. Distances between residues that show in *Sculpt* at 6 Å sphere around the inhibitor.

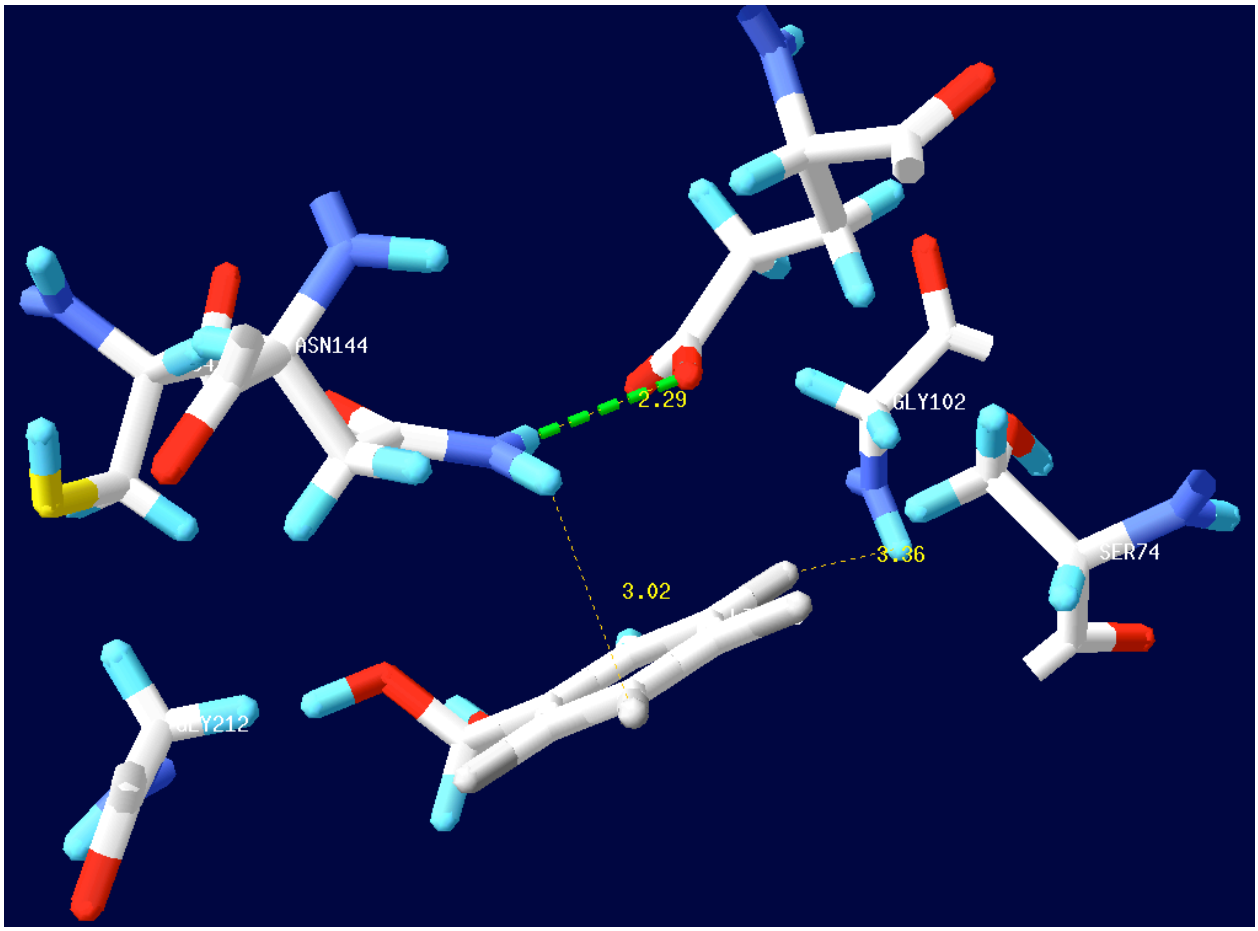

Figure 56: 2,3,4,5-Tetrafluorophenylboronic acid and the active site of BlaC. Distances between residues that show in *Sculpt* at 7 Å from the ligand.

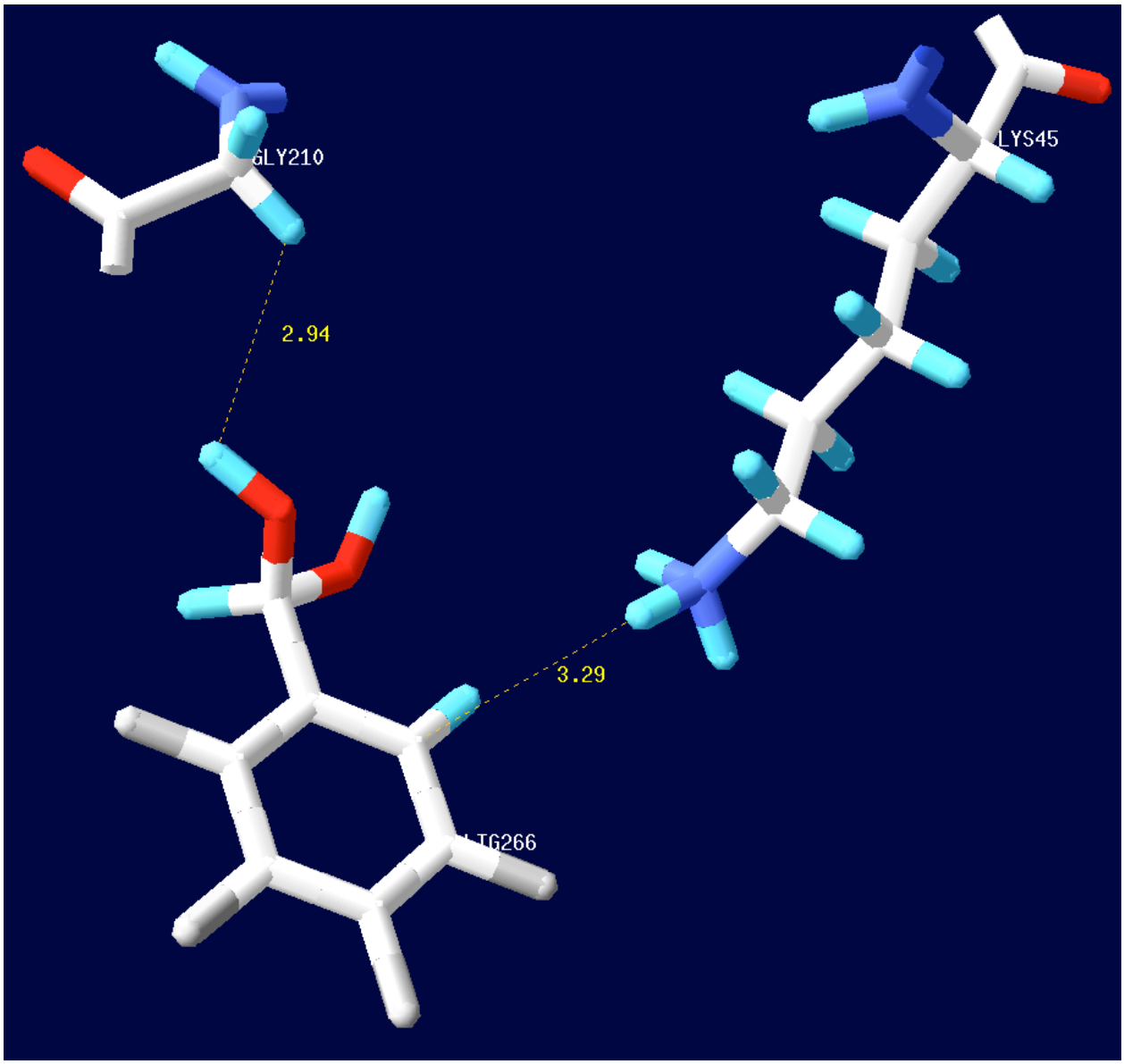

Figure 57: 2,3,4,5-Tetrafluorophenylboronic acid and the active site of BlaC. Distances between residues that show in *Sculpt* at the 8 Å sphere around the inhibitor.

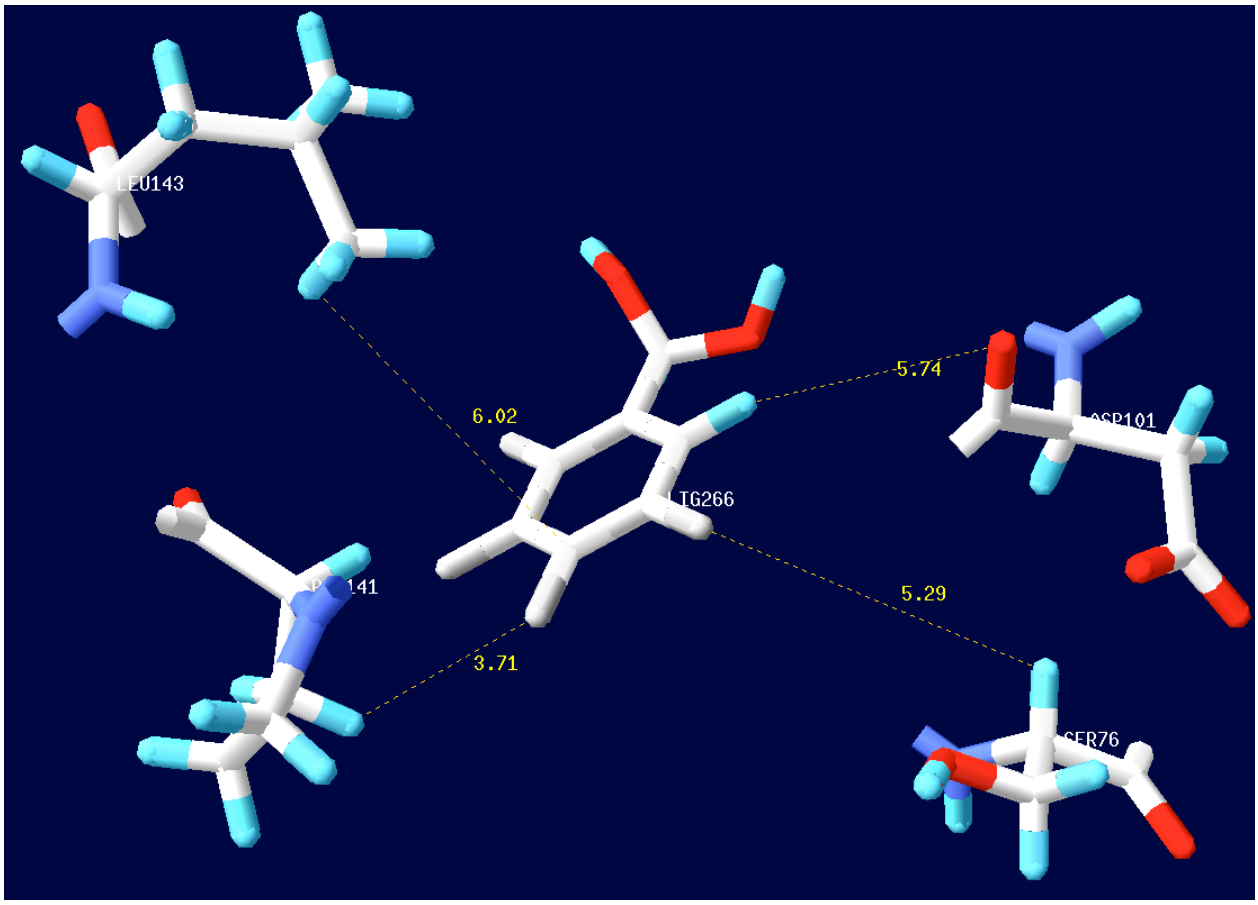

Figure 58: 2,3,4,5-Tetrafluorophenylboronic acid and the active site of BlaC. Distances between residues that show at the 9 Å sphere around the inhibitor in *Sculpt*.

3,5-Bis(trifluoromethyl)phenylboronic acid in BlaC (3CG5).

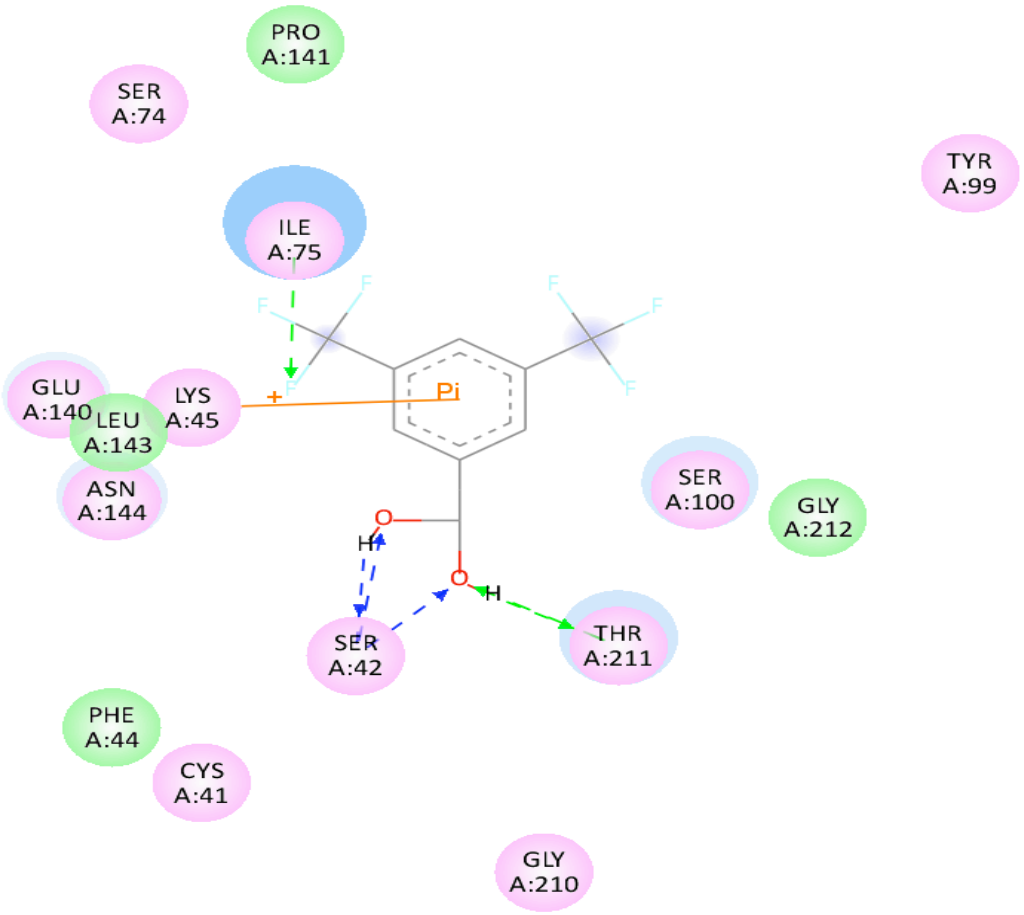

Figure 59: 3,5-Bis(trifluoromethyl)phenylboronic acid in the active site of BlaC (3CG5).

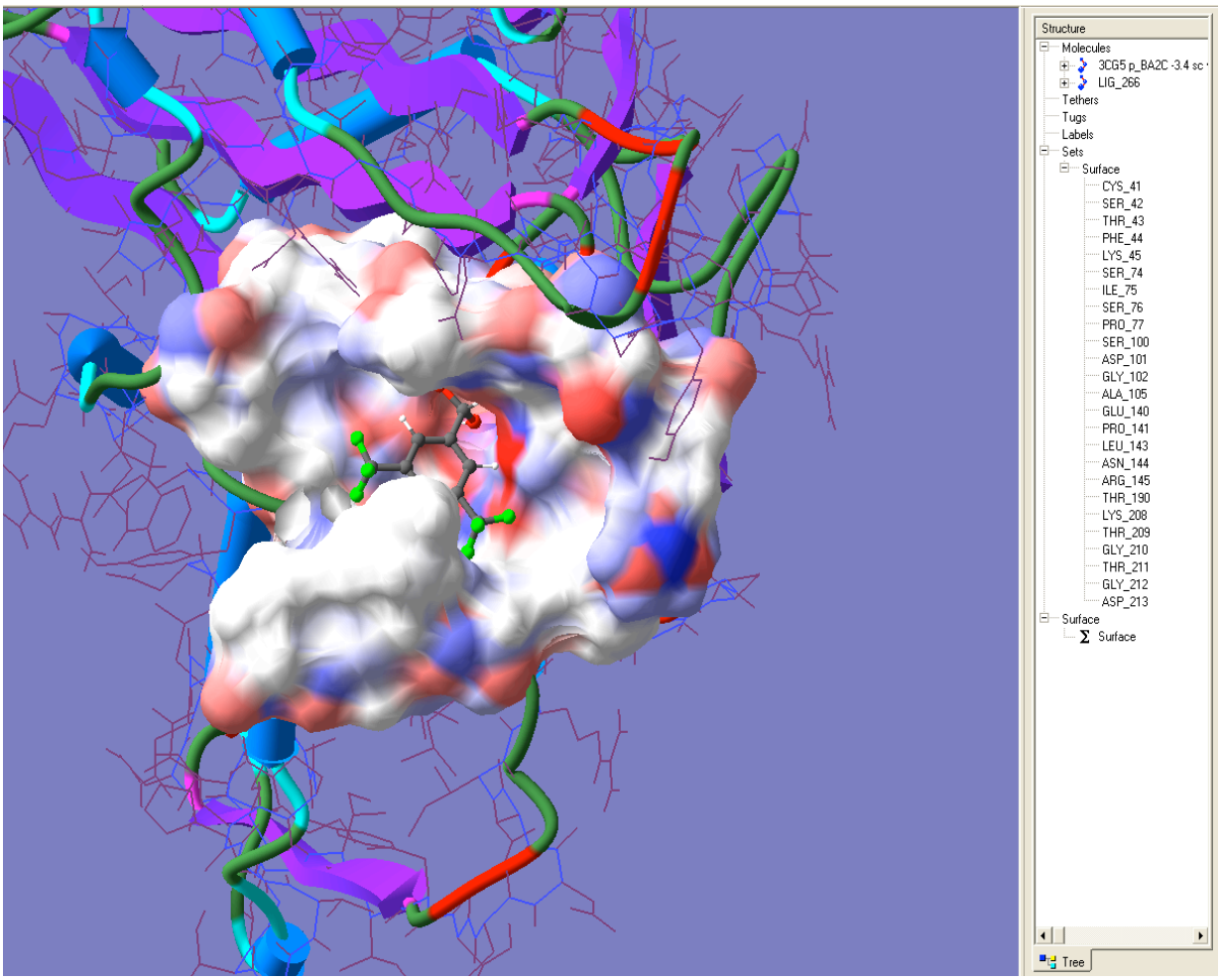

Table 60: 3,5-Bis(trifluoromethyl)phenylboronic acid in BlaC (3CG5). Surface on within 10.0 Å of the inhibitor. A list of amino acids in the 10.0 Å sphere from the inhibitor is shown in the window at the right.

Table 8: 3,5-Bis(trifluoromethyl)phenylboronic acid in BlaC.

3CG5	Residue Number	*Sculpt* Sphere (Å) *	Element **	H-b per *Visualizer* §	Distance (Å)	Enzyme	Inhibitor	H-b
Ile	75	5			1.35	αNH(H)	mF	yes
Thr	211	6		y	1.67	αNH(H)	OH(H)	yes
Ile	75	5		y	1.71	αNH(H)	mF	yes
Ser	42	6	1	y	1.96	γO	OH(H)	yes
Gly	210	7	3		2.83	αCO(O)	OH(H)	yes
Ser	100	6	2		3.16	γO(H)	mF	yes
Asn	144	6	4		1.77	δN	C'2H	-
Ser	74	8			2.00	βH	mF	-
Cys	41	7			2.37	βH	OH(O)	-
Glu	140	7	4		2.94	δO	C'2H	-
Ser	42	6	1		3.03	γO	B	-
Gly	212	7			3.48	αH	mH	-
Lys	45	8	1		3.86	εNH(H)	C'1	-
Pro	141	9	4		4.13	βH	mF	-
Thr	209	9	3		4.24	βOH(H)	mF	-
Pro	77	10			4.28			
Asp	101	9	2		4.68			
Leu	143	8	4		4.97			
Gly	102	7	2		5.05			
Ser	76	9			5.32			
Lys	208	10	3		5.58			
Thr	43	10	1		5.64			
Ala	105	10			5.64			
Arg	145	10			5.70			
Asp	213	10			6.73			

mF: Methyl fluoride.
C'2: Carbon 2, starting from the junction with the rest of the molecule, in the ring.
βH: Hydrogen in the β carbon.
εNH(H): The hydrogen in the epsilon amino group takes part in this bond.
αNH(H): The hydrogen in the backbone amino group takes part in this bond.
αCO(O): The oxygen of the carboxyl end of the residue takes part in this bond.
OH(H): The hydrogen of one of the hydroxyl groups in the boronic acid takes part in the bond.
OH(O): The oxygen of one of the hydroxyl groups in the boronic acid takes part in the bond.
B: Boron.
H-b: Hydrogen bond.
*: *Sculpt* Sphere in Å: When surface on is activated in Sculpt at the indicated number, the residue in the line appears as part of the surface.
**: This amino acid belongs to the element indicated, in accord with table 4.
§: "y" indicates that per *Discovery Studio Visualizer* this link shows as a hydrogen bond.

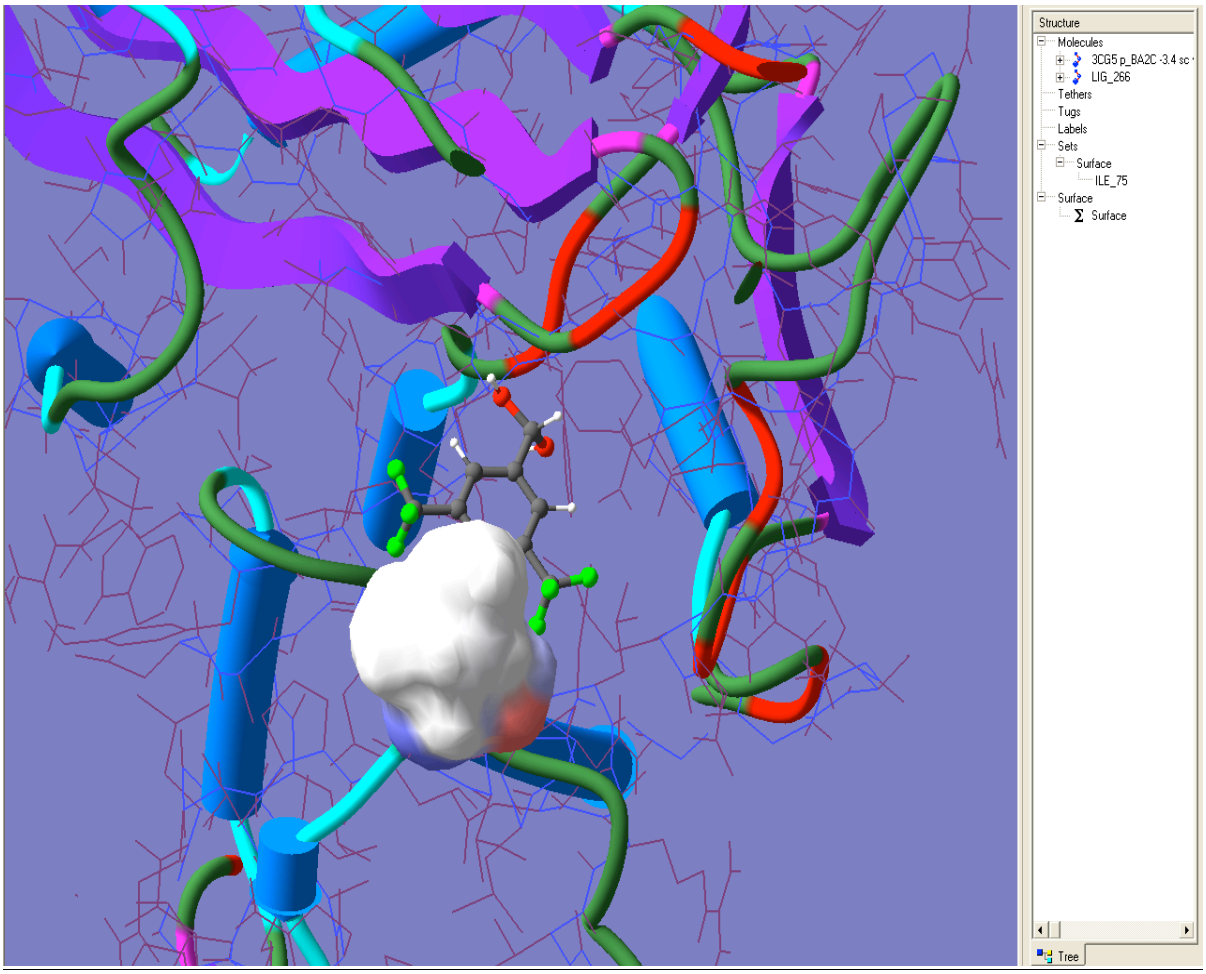

Figure 61: 3,5-Bis(trifluoromethyl)phenylboronic acid in BlaC. Ile75(105) is the closest amino acid at to the ligand at 5 Å away.

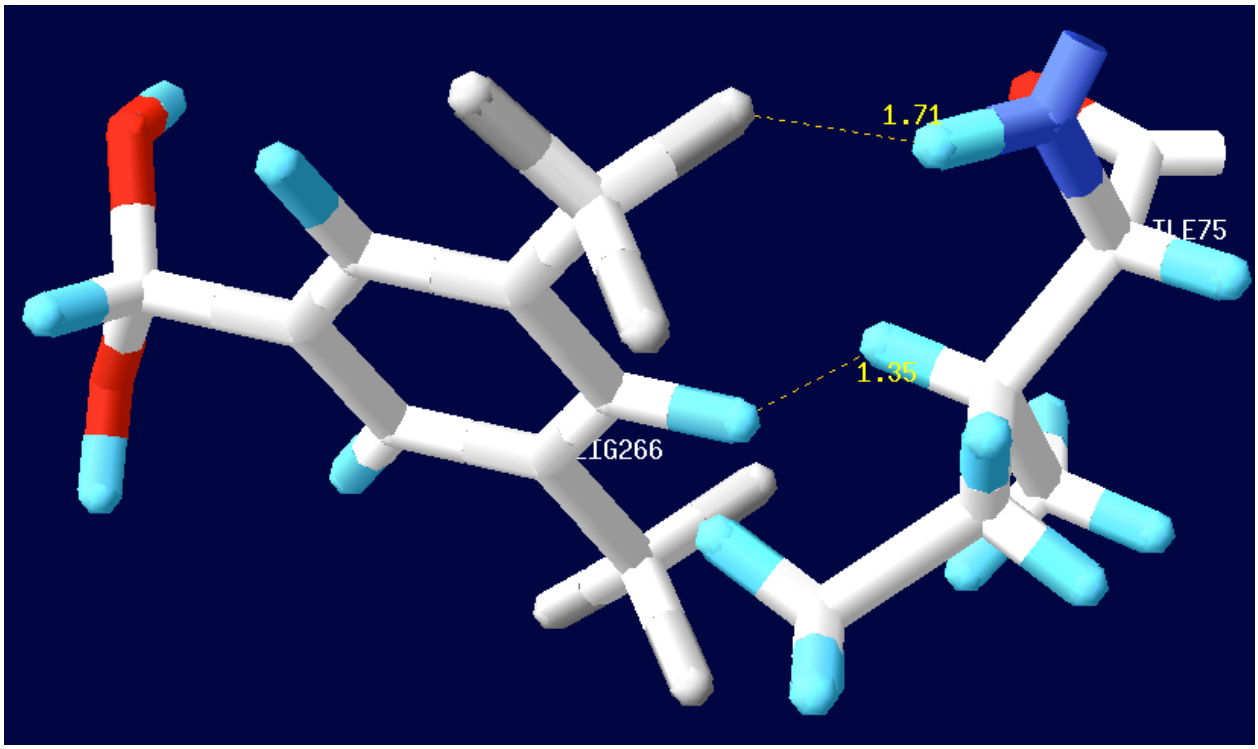

Figure 62: 3,5-Bis(trifluoromethyl)phenylboronic acid in BlaC. Ile75(105) is the closest amino acid at to the ligand at 5 Å away.

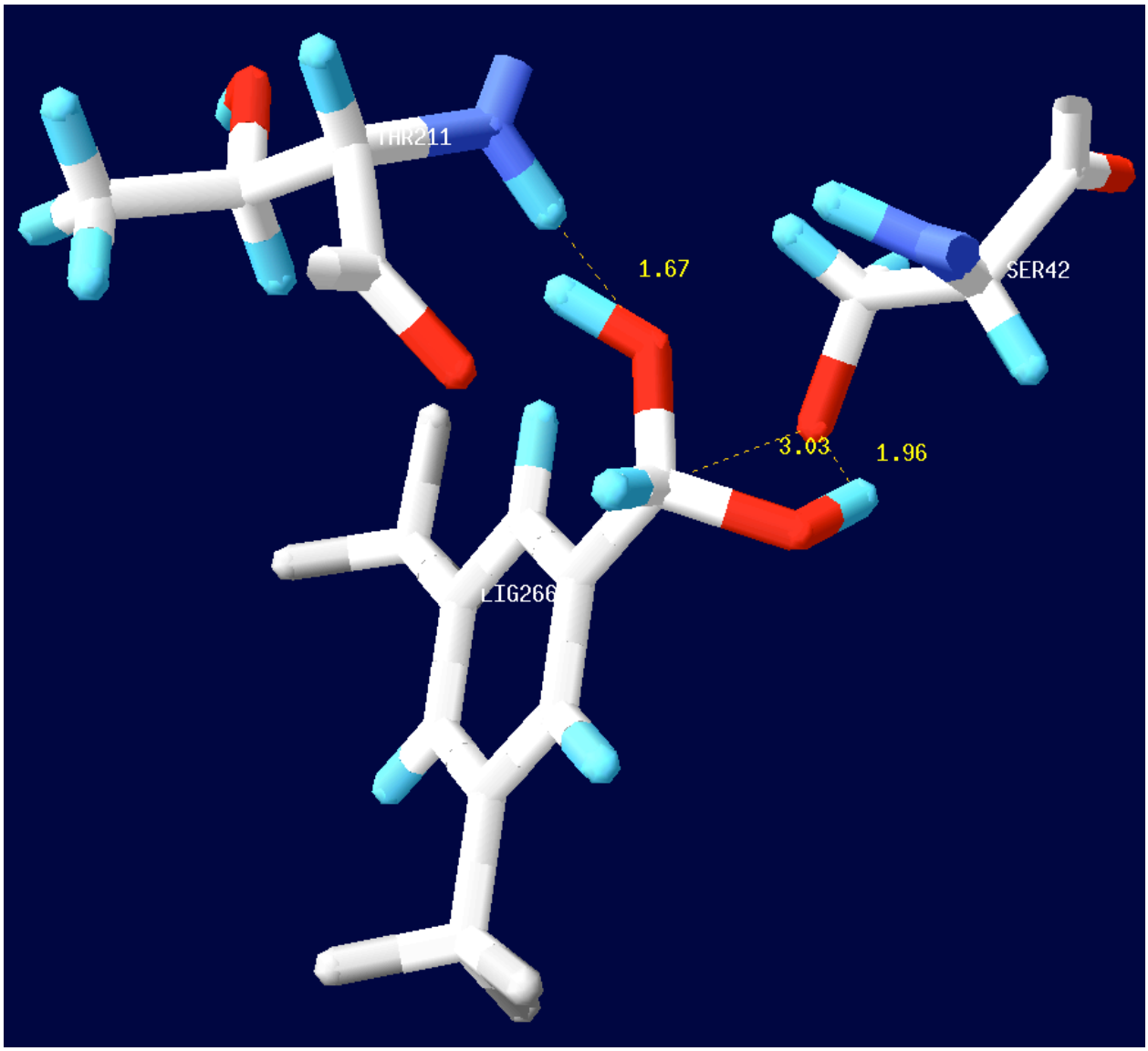

Figure 63: 3,5-Bis(trifluoromethyl)phenylboronic acid in BlaC. Thr211(237), Ser42(70) amino acids in the sphere within 6 Å from the inhibitor.

2-Carboxythiophene-5-boronic acid in the active site of BlaC and TEM-1

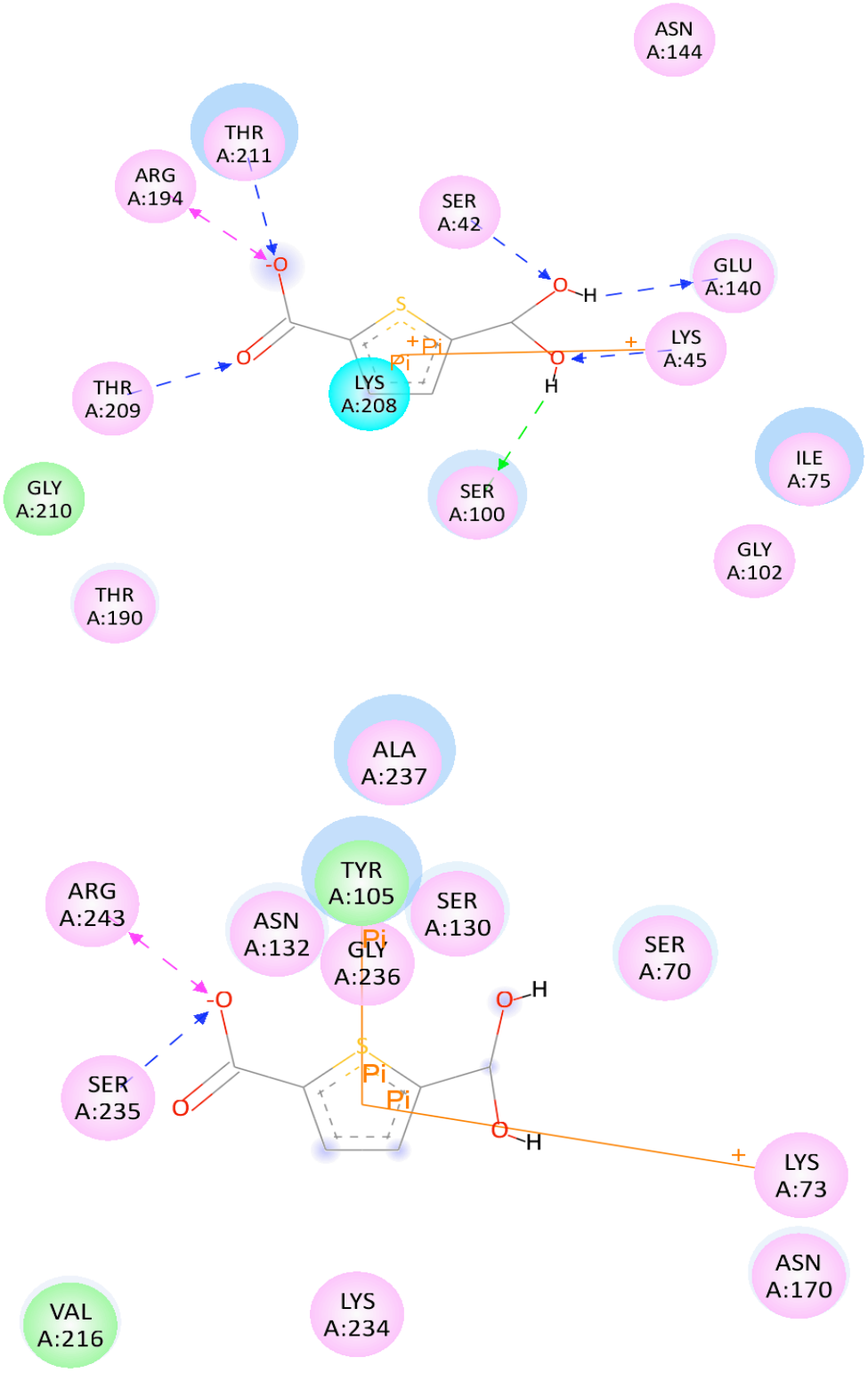

Figure 64: 2-Carboxythiophene-5-boronic acid in the active site of BlaC (top) and TEM-1 (bottom).

Table 9: 2-Carboxythiophene-5-boronic acid in the active site of BlaC and TEM-1.

2-Carboxythiophene-5-boronic acid			**BlaC**	**TEM-1**
3CG5(1ERO)	**BlaC**	**TEM-1**	**Å**	**Å**
Ser42(70)	Side chain Oxygen to Boron		3.66	4.45
	NH(H) to C(1)		3.93	
Lys45(73)	N(H) to OH(O) H-b		2.40	-
Ile75 (Tyr105)	NH(H) to C(4)	C'3 to C5	3.64	3.55
Ser100(130)	αCO(O) to OH(H) H-b		2.47	2.76
Gly102 (Asn132)		NH(H) to OH(O) H-b	-	2.52
Glu140(166)	OH(O) to OH(H)		2.26	-
Asn144(170)			-	-
Arg194 (Leu220)	NH(H) to CO(O)		4.10	-
Lys208(234)	N(H) to C(3)	NH(H) to CO(O) H-b	5.41	2.75
Thr209 (Ser235)	OH(H) to CO(O) H-b	OH(H) to CO(O) H-b	2.17	2.34
Thr211 (Ala237)	OH(H) to CO(O) H-b	αNH(H) to S	2.19	2.69
Ala217 (Arg243)	NH(H) to NO(O) H-b	NH(H) to CO(O) H-b		2.20

See page 82 (Table 8) for abbreviations.

Table 10: 2-carboxythiophen-5-boronic acid showing evidence of stacking.

2-Carboxythiophen-5-boronic acid in BlaC

[I]	Ki (M)	[Ez]	[I]/Ki
7.024E-03	4.925E-04	2.40E-05	14
2.489E-06	1.272E-06	1.20E-08	2

As the concentration of the inhibitor is lowered the Ki is lower. The lowest Ki that has been obtained without compromising the ratio [I]/Ki that should be greater than 1 is 1.272 μM.

Txuzuki *et al*., (2002) have determined the interaction energies of parallel and perpendicular thiophene dimer -1.71 and -3.12 kcal/mol respectively. Because of these interactions we may expect that some molecules of the inhibitor will not compete for the active site at high concentration.

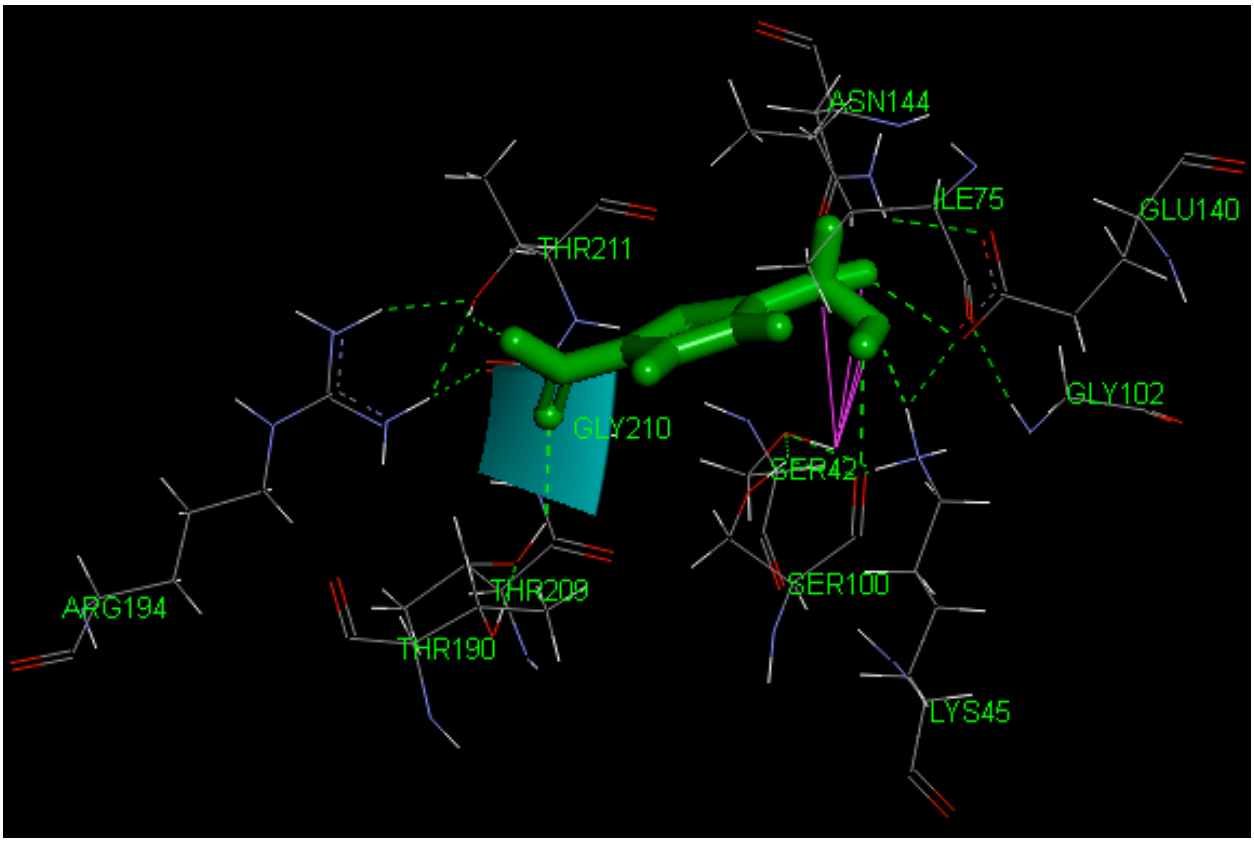

Figure 65: 2-Carboxythiophene-5-boronic acid in the active site of BlaC (3CG5). This picture in *DiscoveryStudio* suggests strong interactions between Thr209(235) and Thr211(237) and the carboxyl group of the thiophene. Also it suggests a strong interaction between the boronate moiety and Ser42(70), LYs45(73), Ser100(130), and Glu140(166).

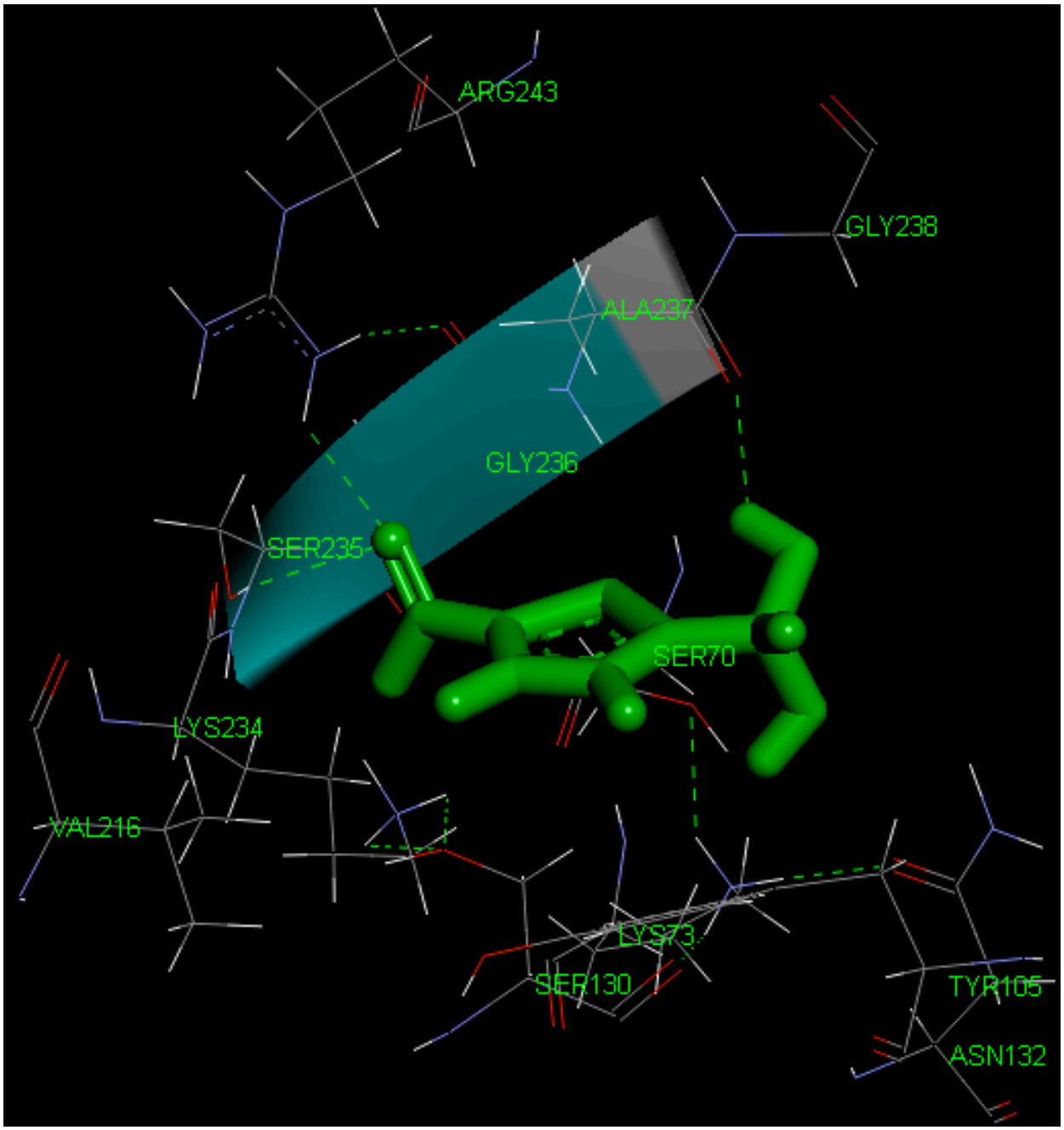

Figure 66: 2-Carboxythiophene-5-boronic acid in the active site of TEM-1 (1ERO). This picture in *DiscoveryStudio* shows strong interactions between the carboxyl group and Ser235, and Arg243; the boronate moiety is in strong interaction with the carboxyl end oxygen of Ala237 (Oxyanion hole).

2-Carboxythiophene-5-boronic acid in the active site of BlaC.

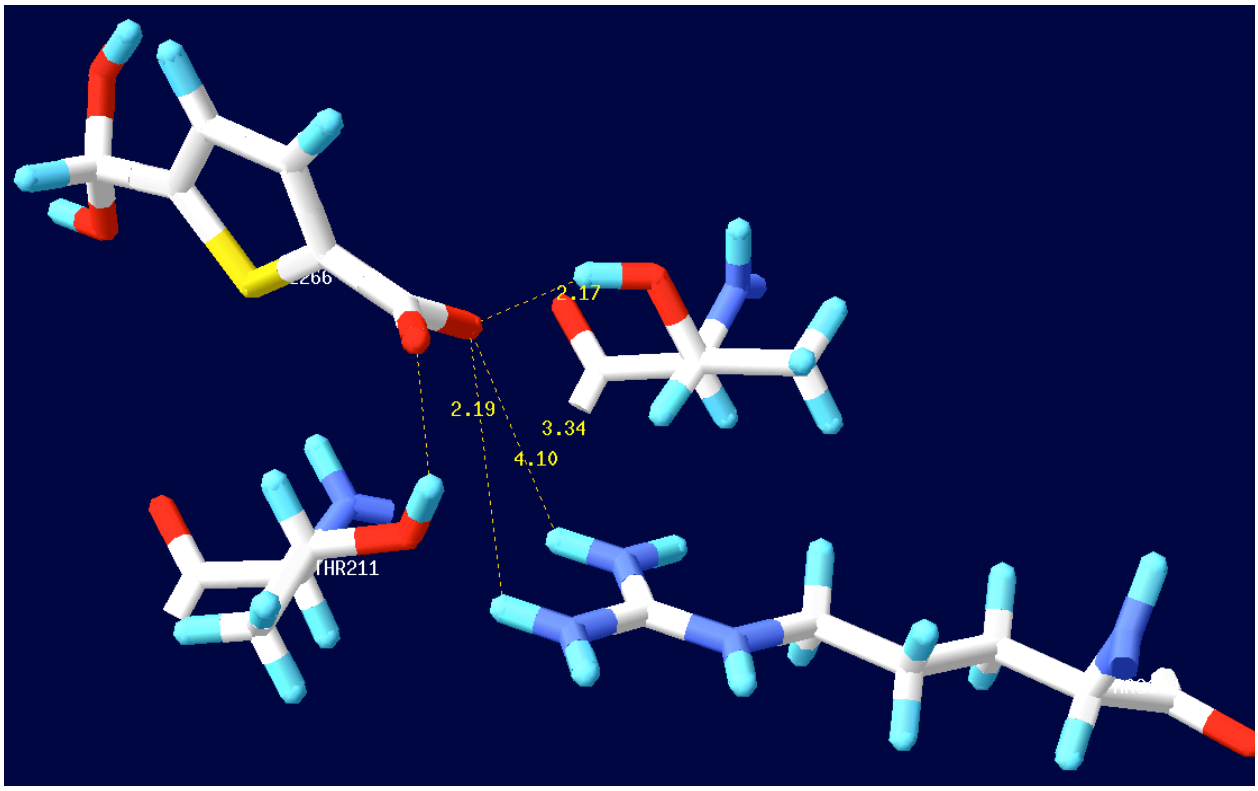

Figure 67: 2-Carboxythiophene-5-boronic acid in the active site of BlaC. Interactions between enzyme and the carboxyl moiety of the ligand. Thr209, Arg194, Thr211.

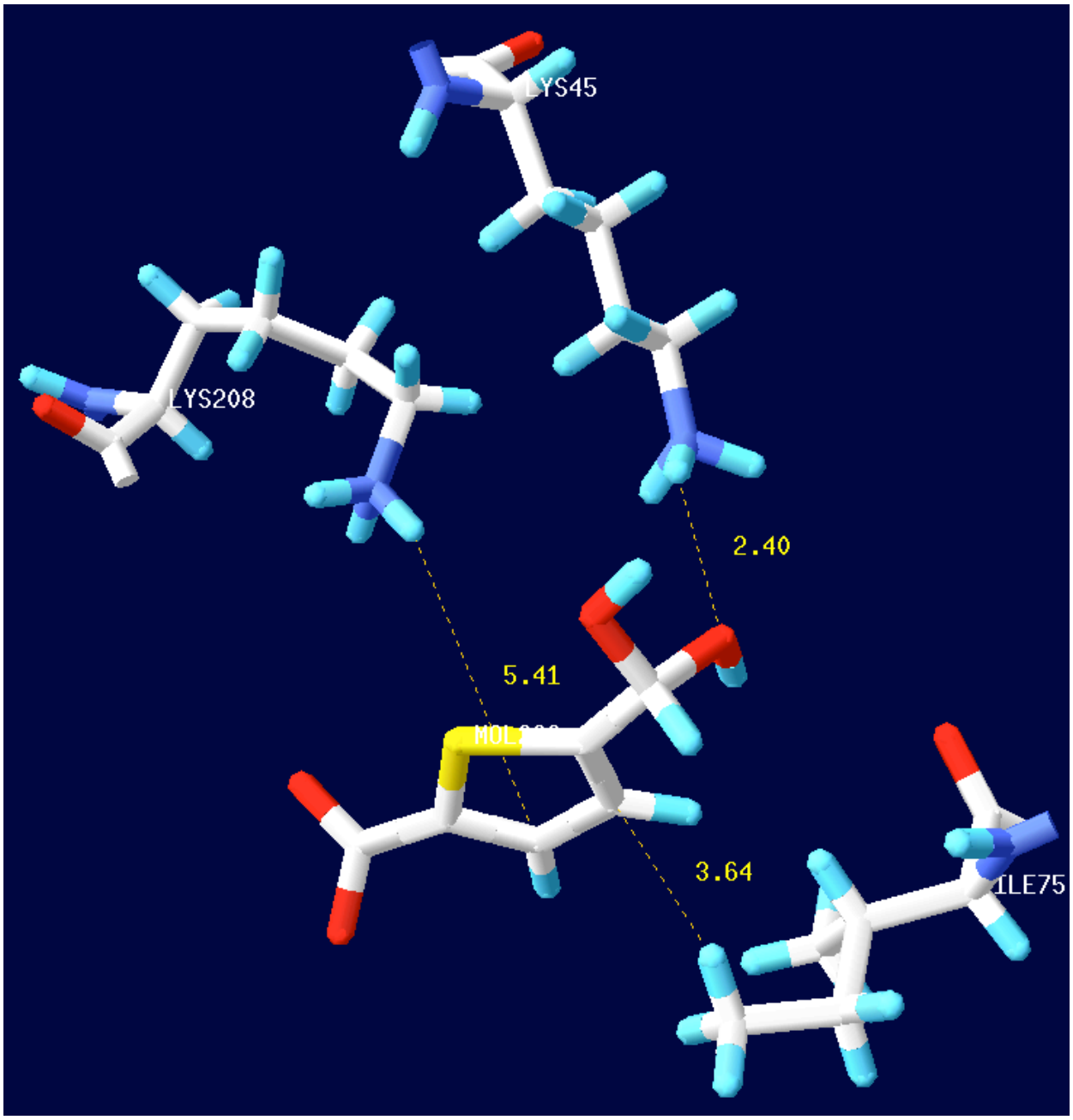

Figure 68: 2-Carboxythiophene-5-boronic acid in the active site of BlaC. Distances between Ile75, Lys45, and Ly208 and the inhibitor.

2-Carboxythiophene-5-boronic acid in the active site of TEM-1 (1ERO).

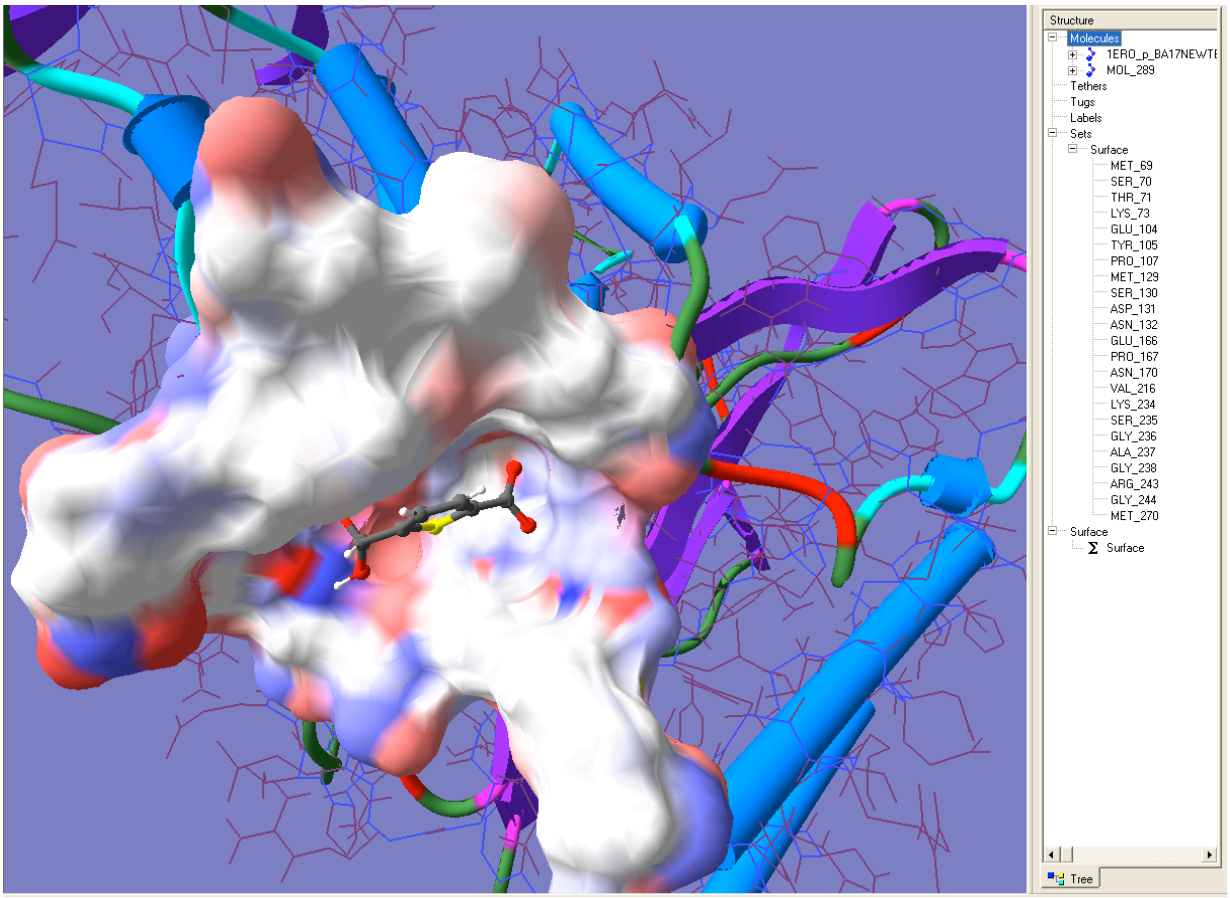

Figure 69: 2-Carboxythiophene-5-boronic acid in the active site of TEM-1 (1ERO). Surface on within 10.0 Å of the inhibitor. A list of amino acids in the 10.0 Å sphere from the inhibitor is shown in the window at the right.

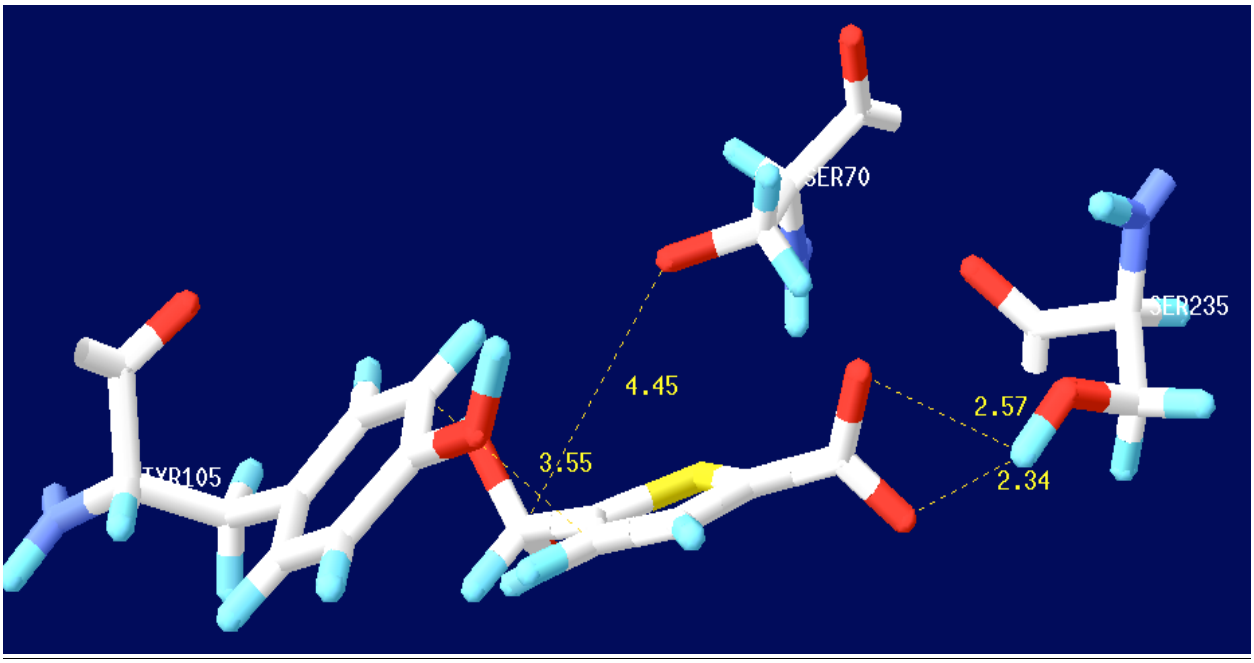

Figure 70: 2-Carboxythiophene-5-boronic acid in the active site of TEM-1.

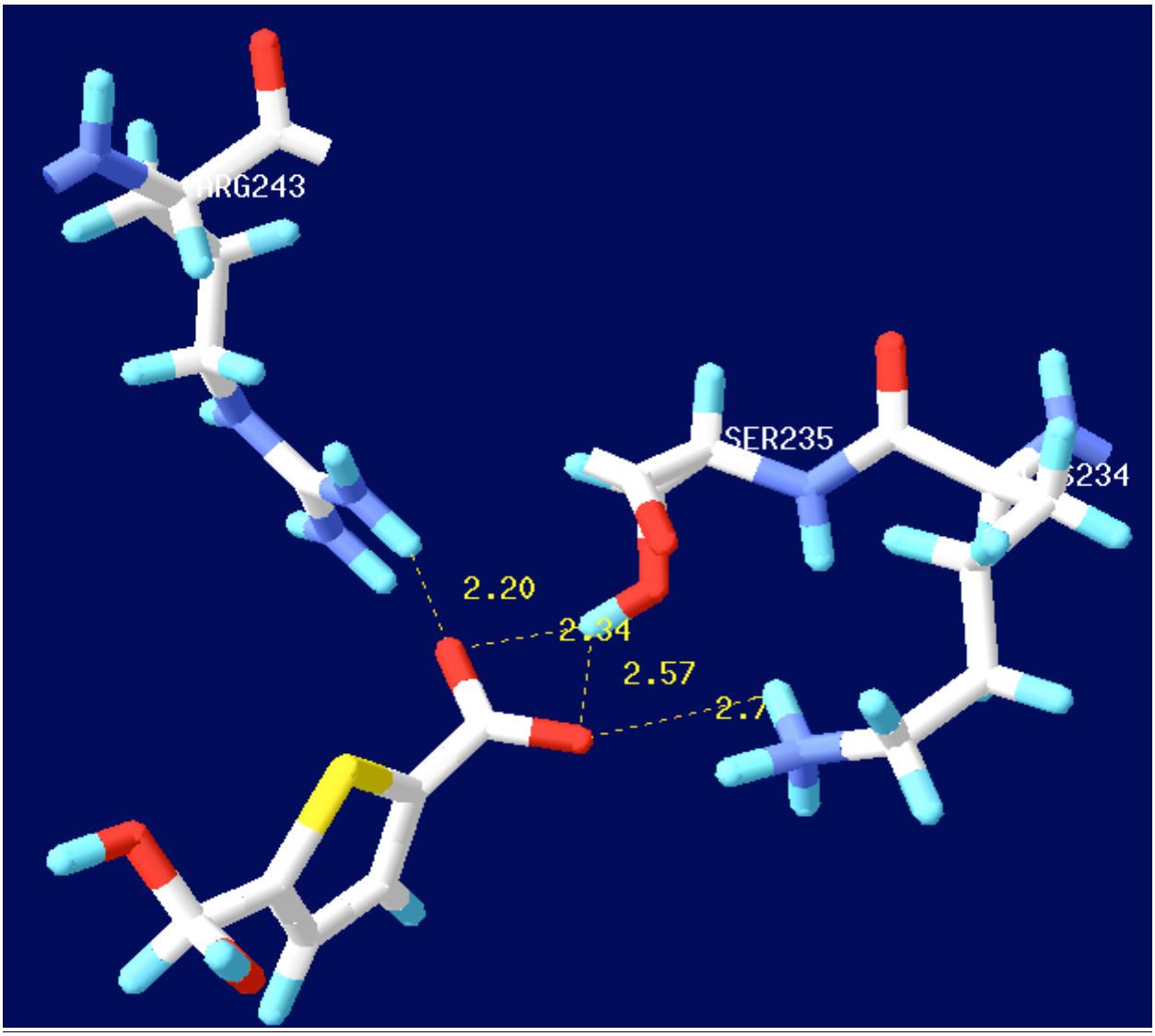

Figure 71: 2-Carboxythiophene-5-boronic acid in the active site of TEM-1. Interactions between the carboxyl group of the inhibitor and the nearest side chains in the active site.

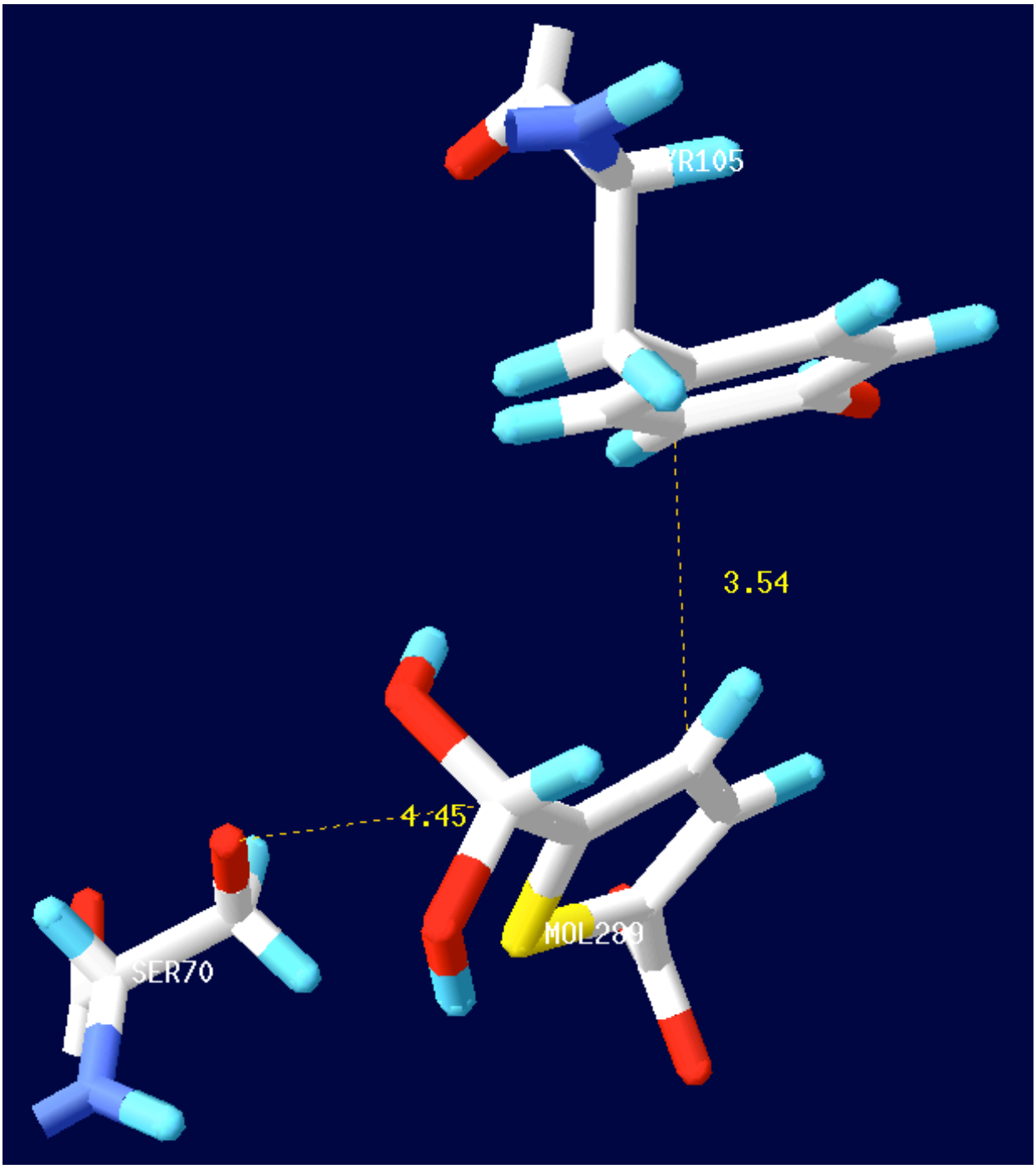

Figure 72: 2-Carboxythiophene-5-boronic acid in the active site of TEM-1. Possible ring stacking between the inhibitor and Tyr105.

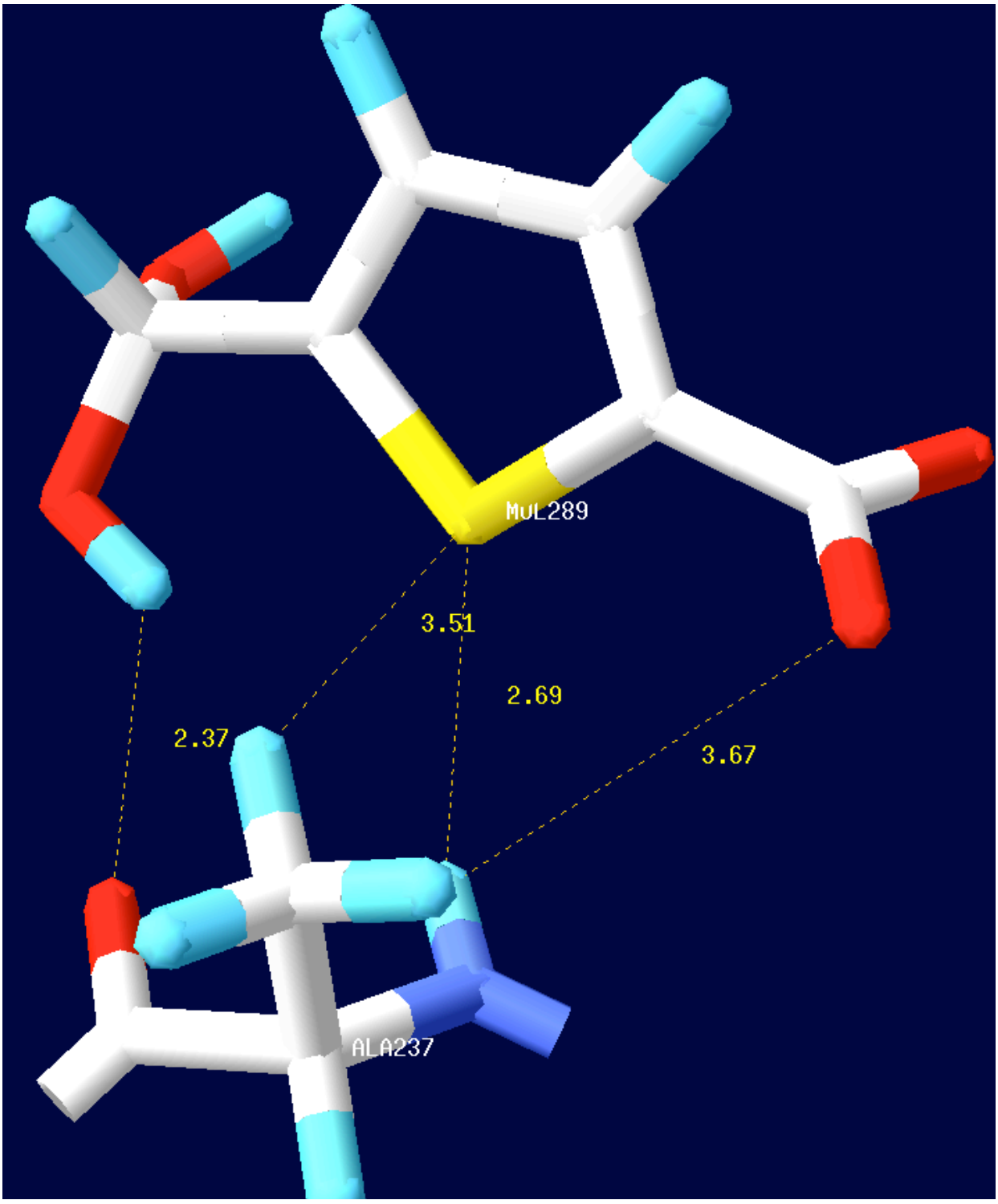

Figure 73: 2-Carboxythiophene-5-boronic acid in the active site of TEM-1. Ala237 and the inhibitor.

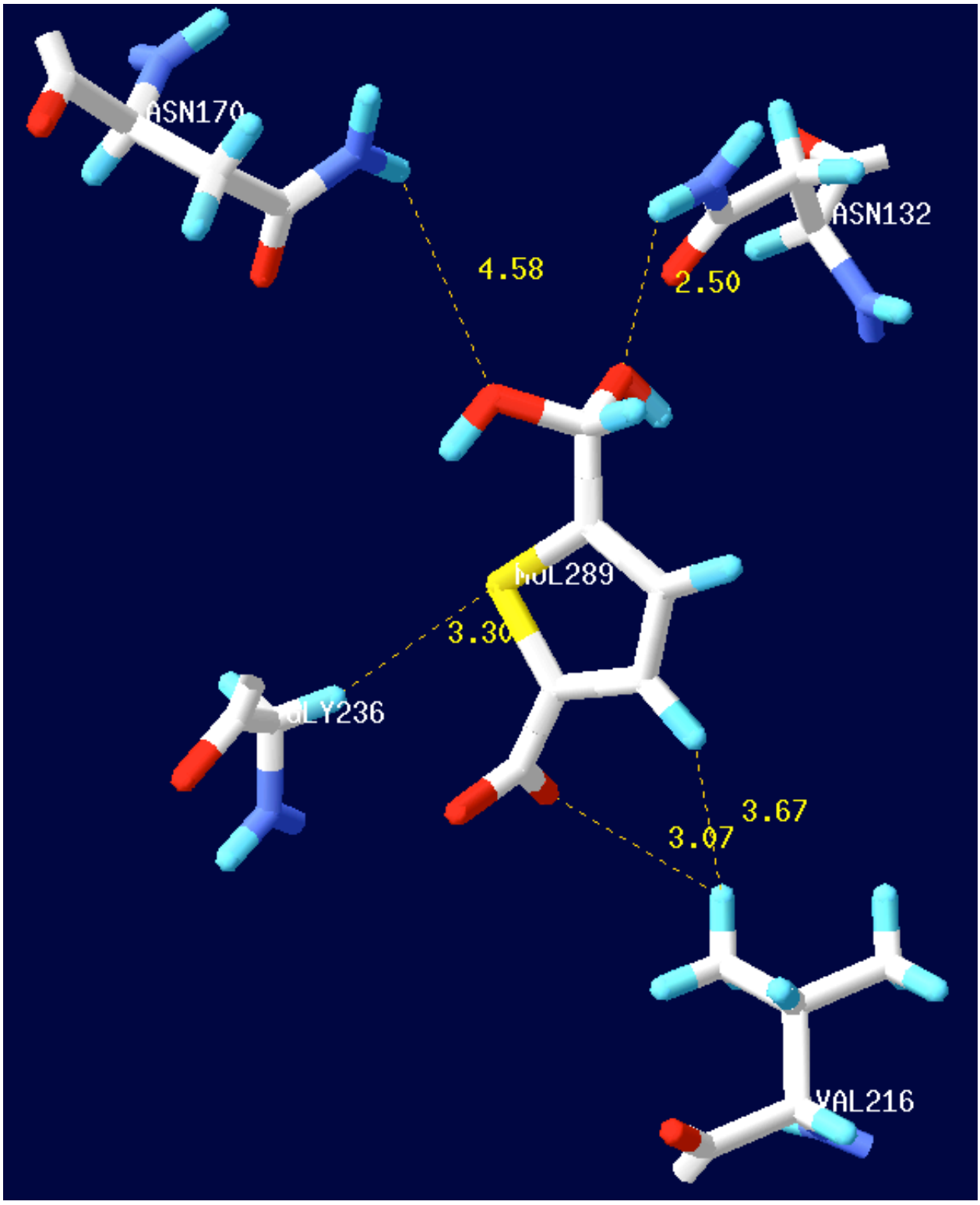

Figure 74: 2-Carboxythiophene-5-boronic acid in the active site of TEM-1.

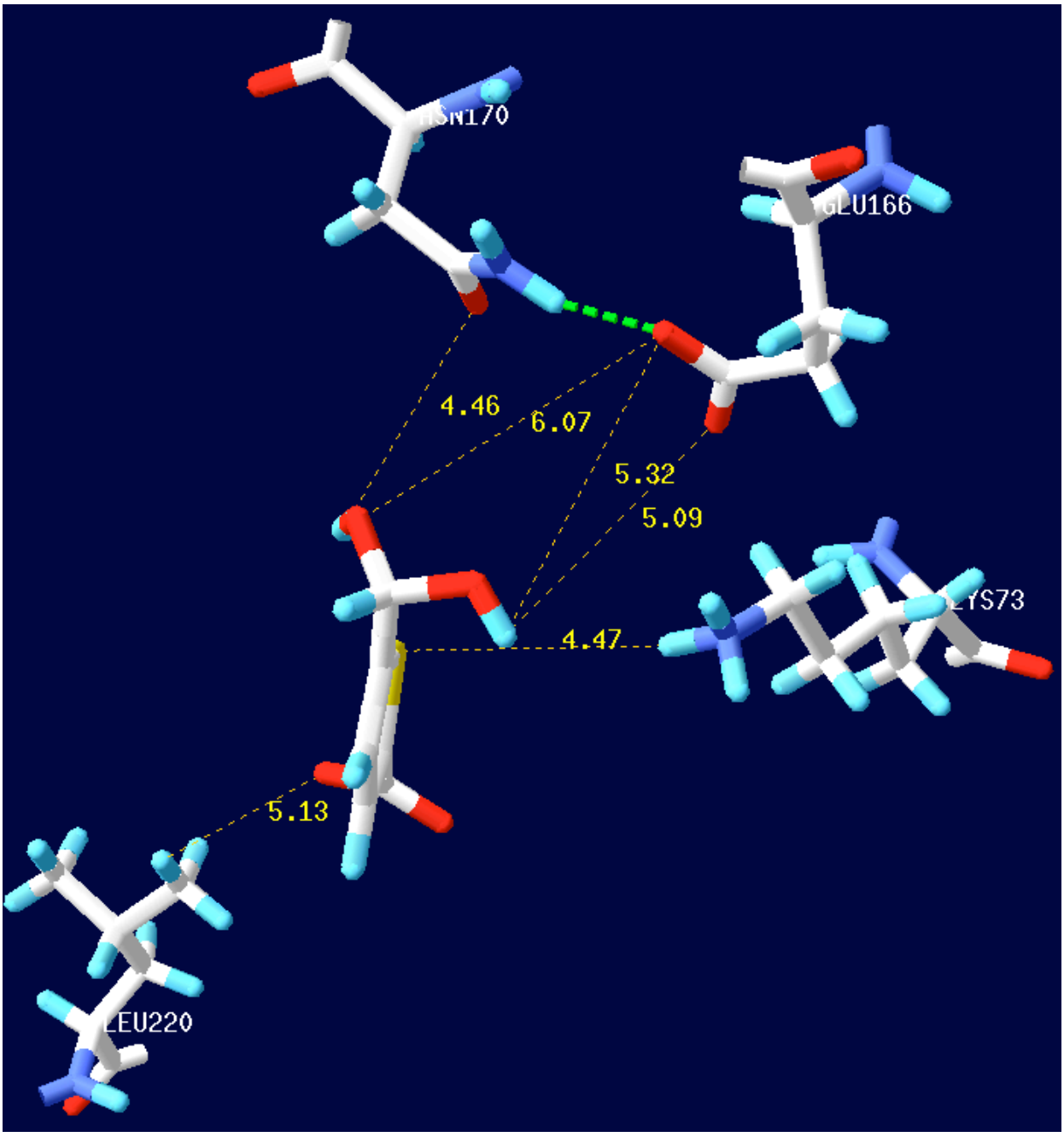

Figure 75: 2-Carboxythiophene-5-boronic acid in the active site of TEM-1. Lys73, Glu166, Asn170, Lys73, and Leu220 seem to be too far from the ligand to have meaningful interactions.

1,1,1- Trichloro-2,2-bis(4-chlorophenyl)ethane (4,4'-DDT) in the active site of BlaC (3CG5).

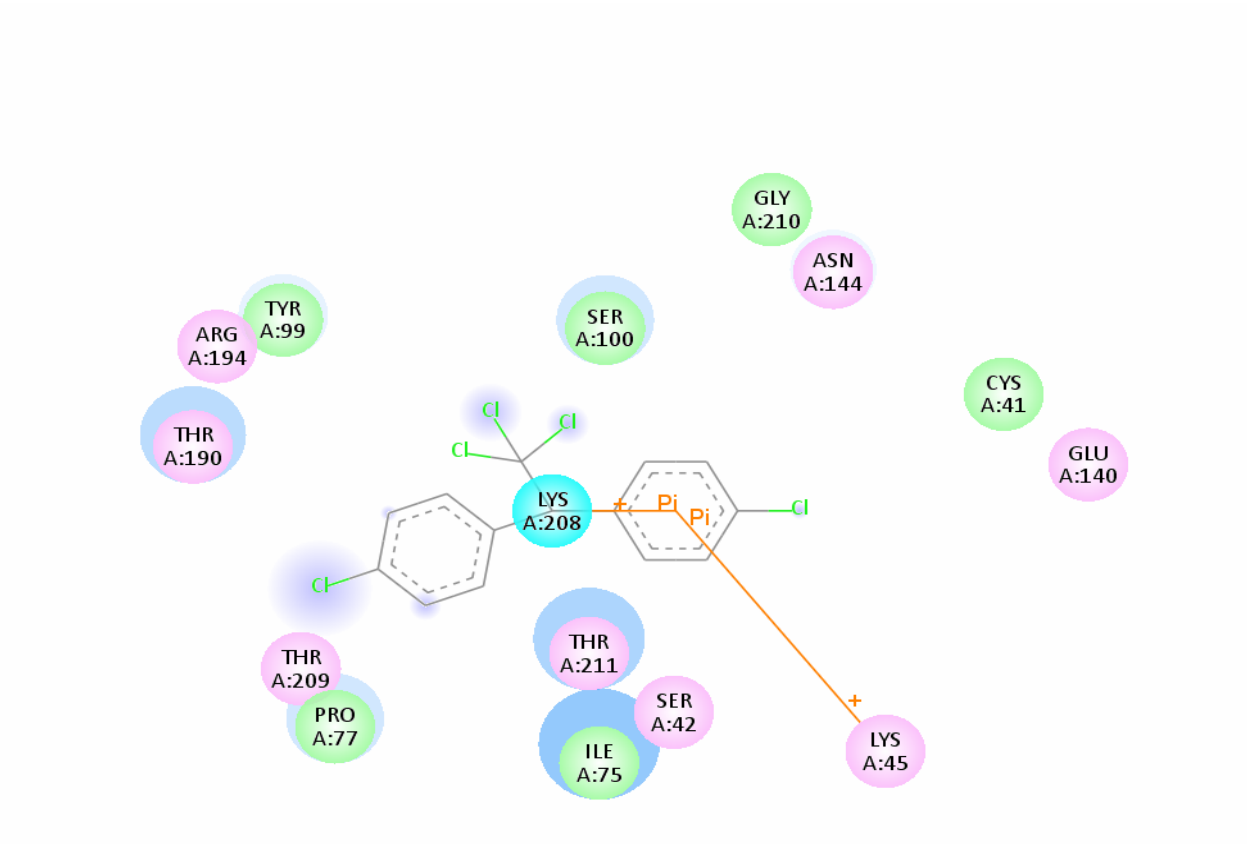

Figure 76: 4,4'-DDT in the active site of BlaC (3CG5).

Table 11: Important interactions for 4,4'-DDT in BlaC (3CG5) in the active site.

3CG5	Å	Enzyme Residue	Ligand	Hydrogen bond distance
Ile75	2.09	γH	C'2H	yes
Thr211	2.64	γH	mCl	yes
Thr209	2.77	γH	mCl	yes
Ser42	3.50	O	C'4F	yes
Lys45	3.73	εNH(H)	C'4Cl	yes
Ile75	3.80	H's	Rings	
Lys208	5.25	εNH(H)	C'3H	

See page 82 (Table 8) for abbreviations.

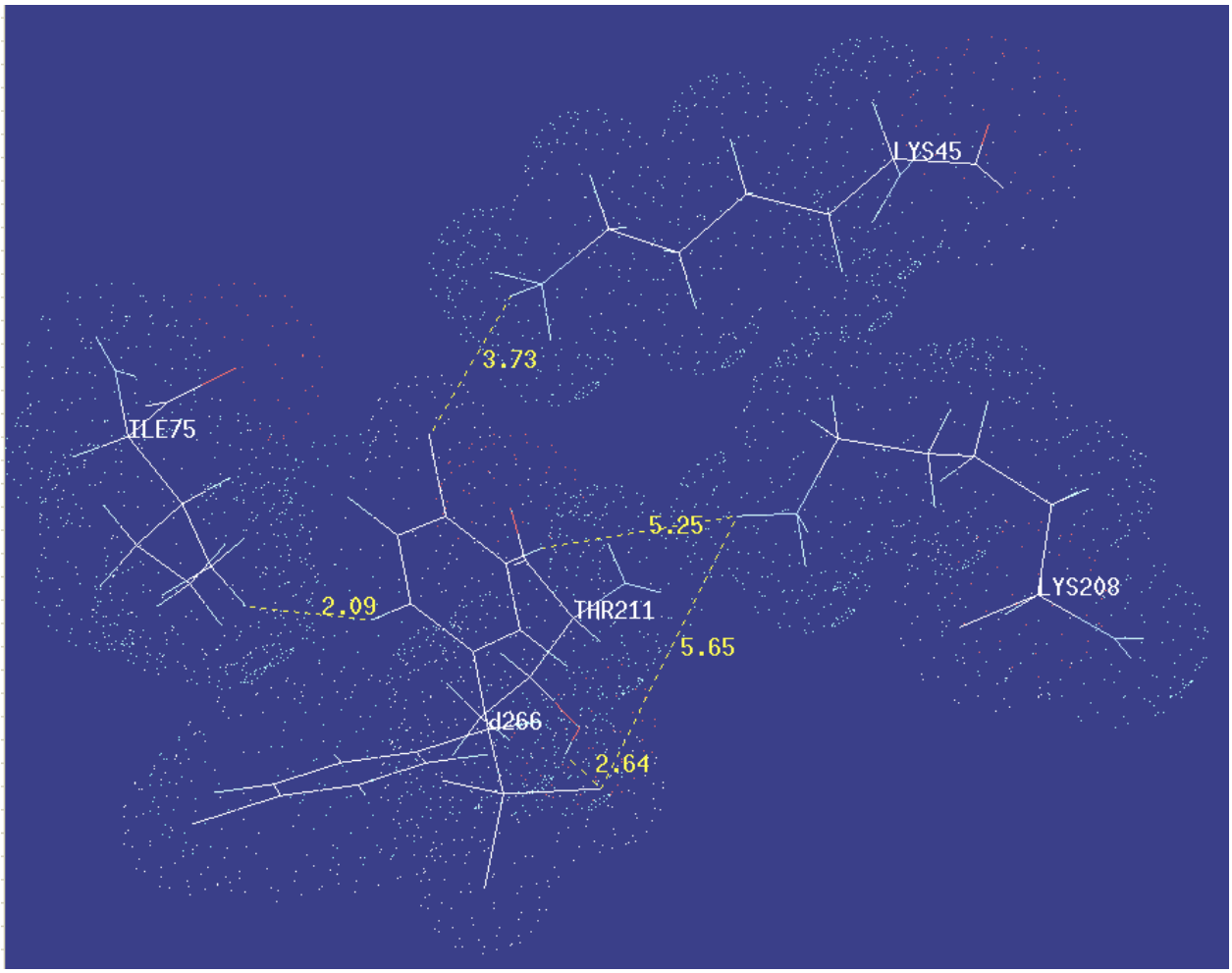

Figure 77: Residues Ile75, Lys208, Thr211 and Lys45 and DDT.

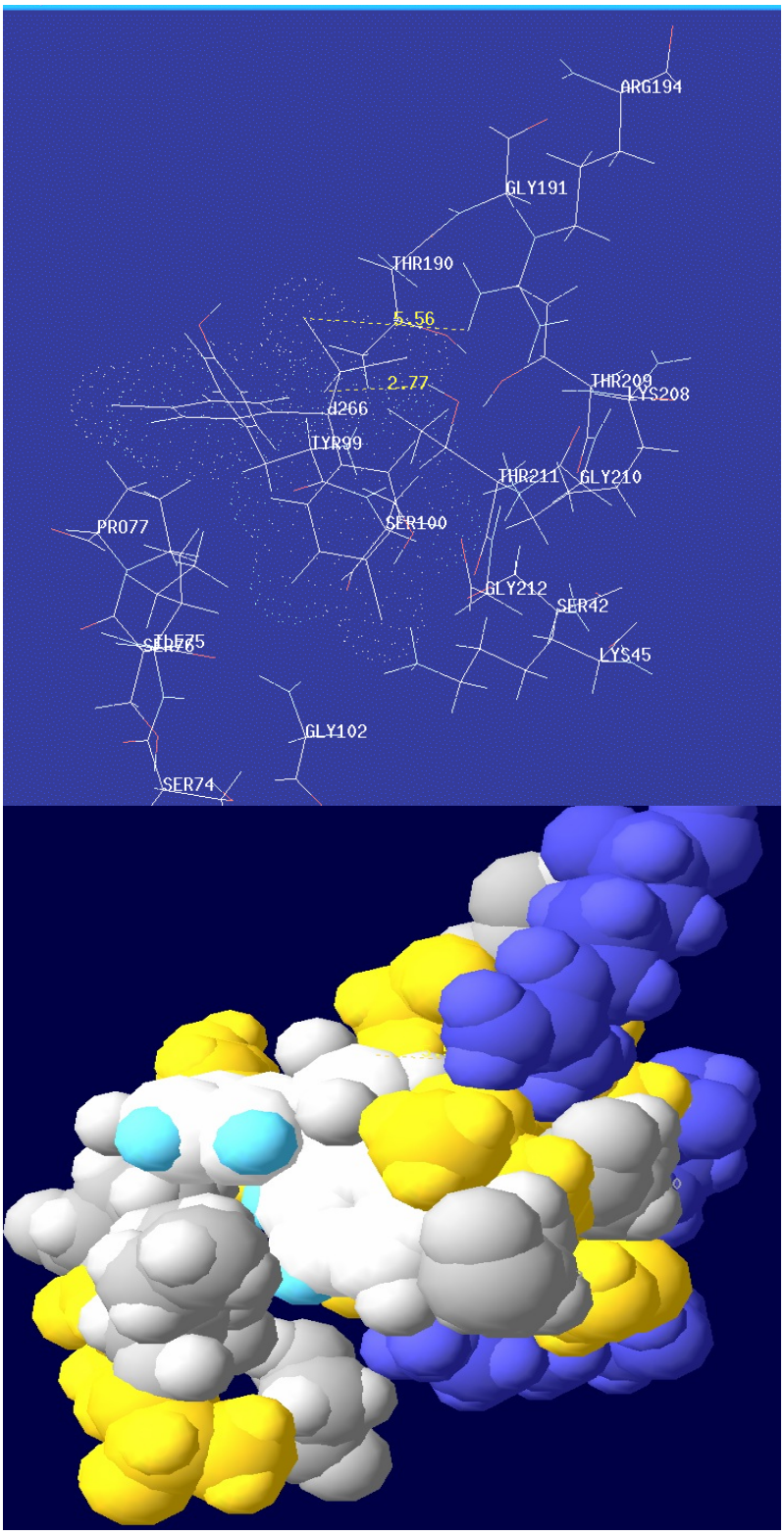

Figure 78: Wireframe model on top and space filling model in the bottom of the active site of BlaC (3CG5) with 4,4'-DDT.

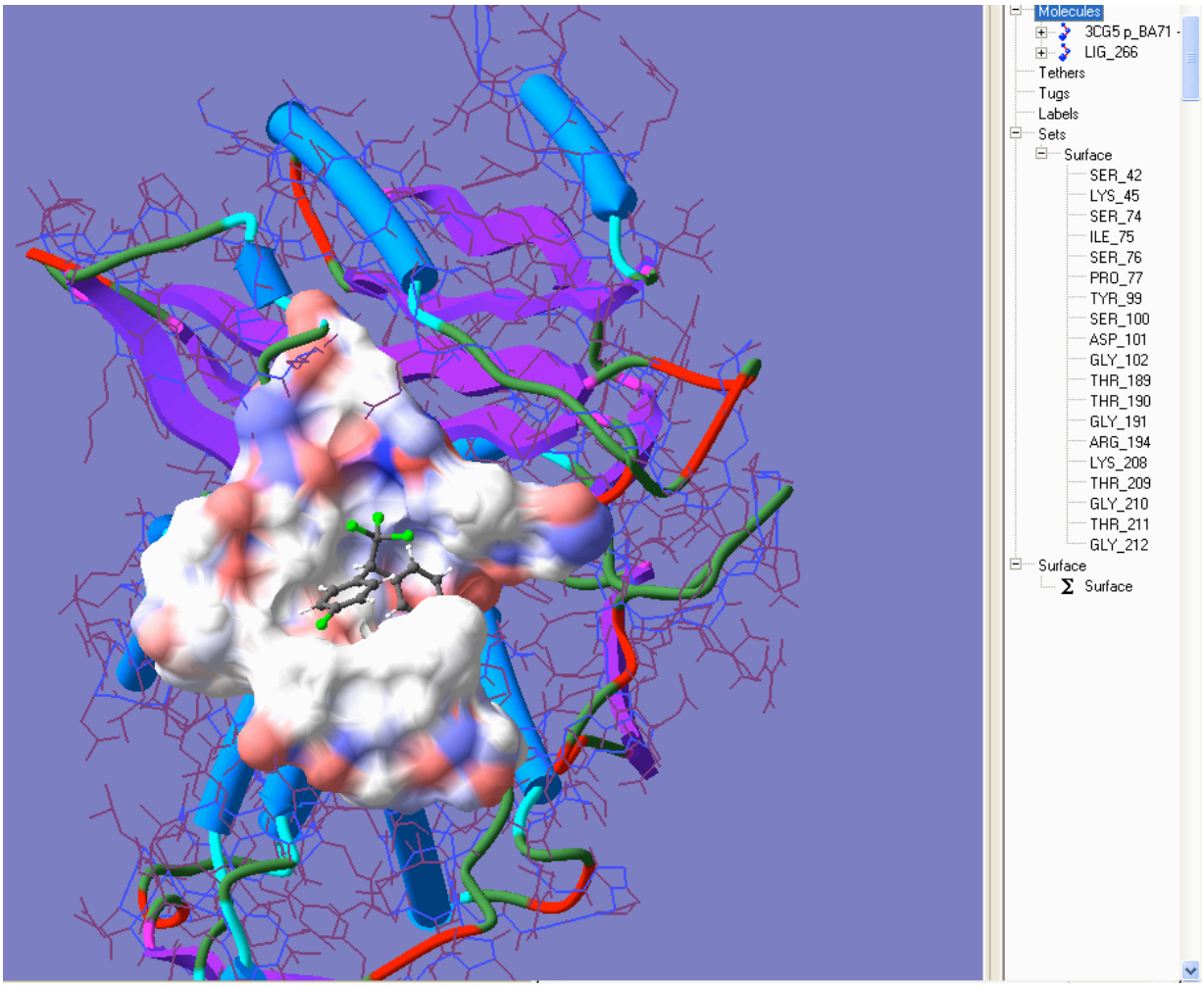

Figure 79: 4,4'-DDT in the active site of BlaC (3CG5). Surface on within 10.0 Å of the inhibitor. A list of amino acids in the 10.0 Å sphere from the inhibitor is shown in the window at the right. No coordinates were entered in *AutoDock Vina* for Ser42(70)-γO.

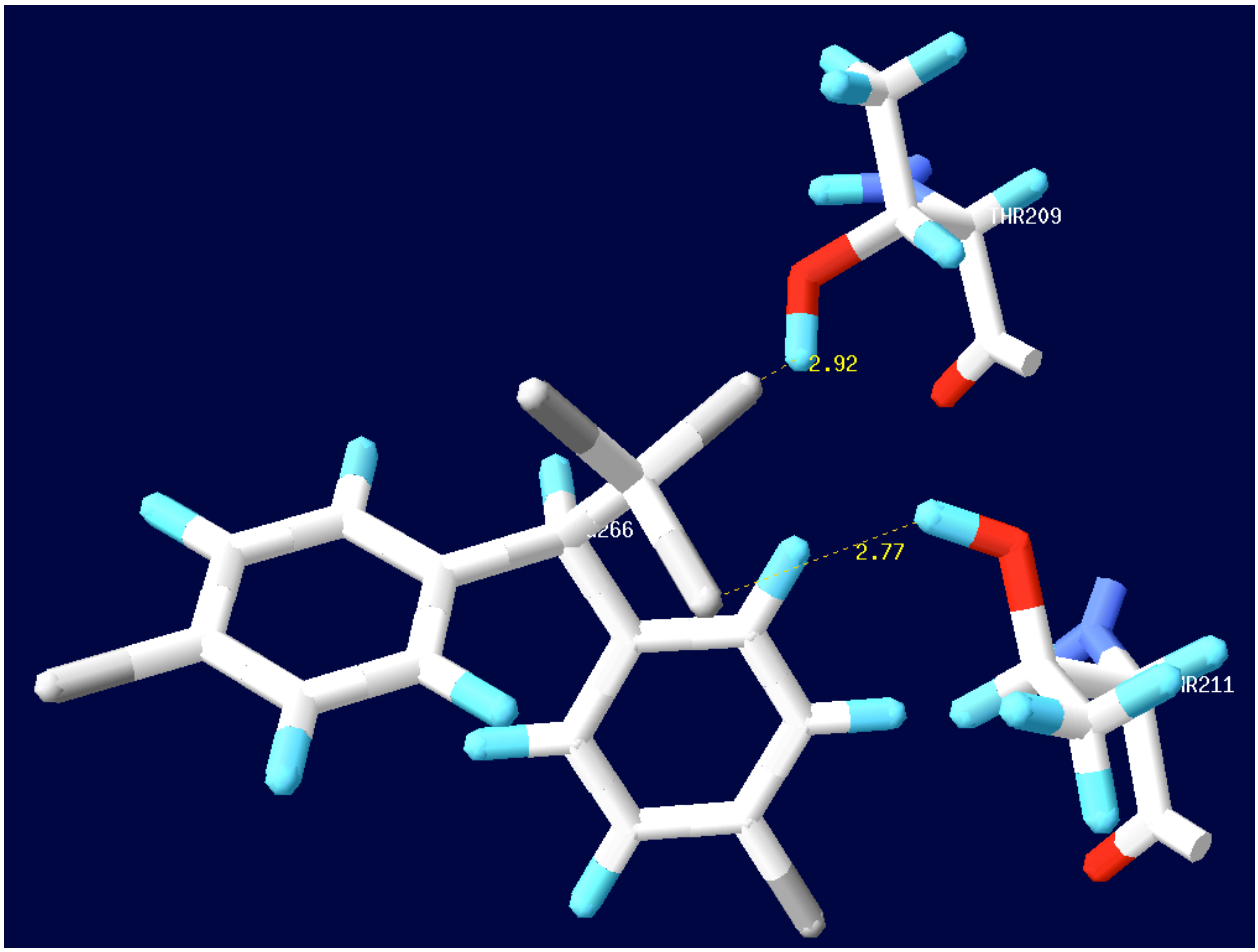

Figure 80: Hydrogen bonds for 4,4'-DDT in the active site of BlaC (3CG5). Possible hydrogen bonds between Thr209-γO and one of the methyl Chlorides in the small molecule. The same is observed for of Thr211-γO and the ligand.

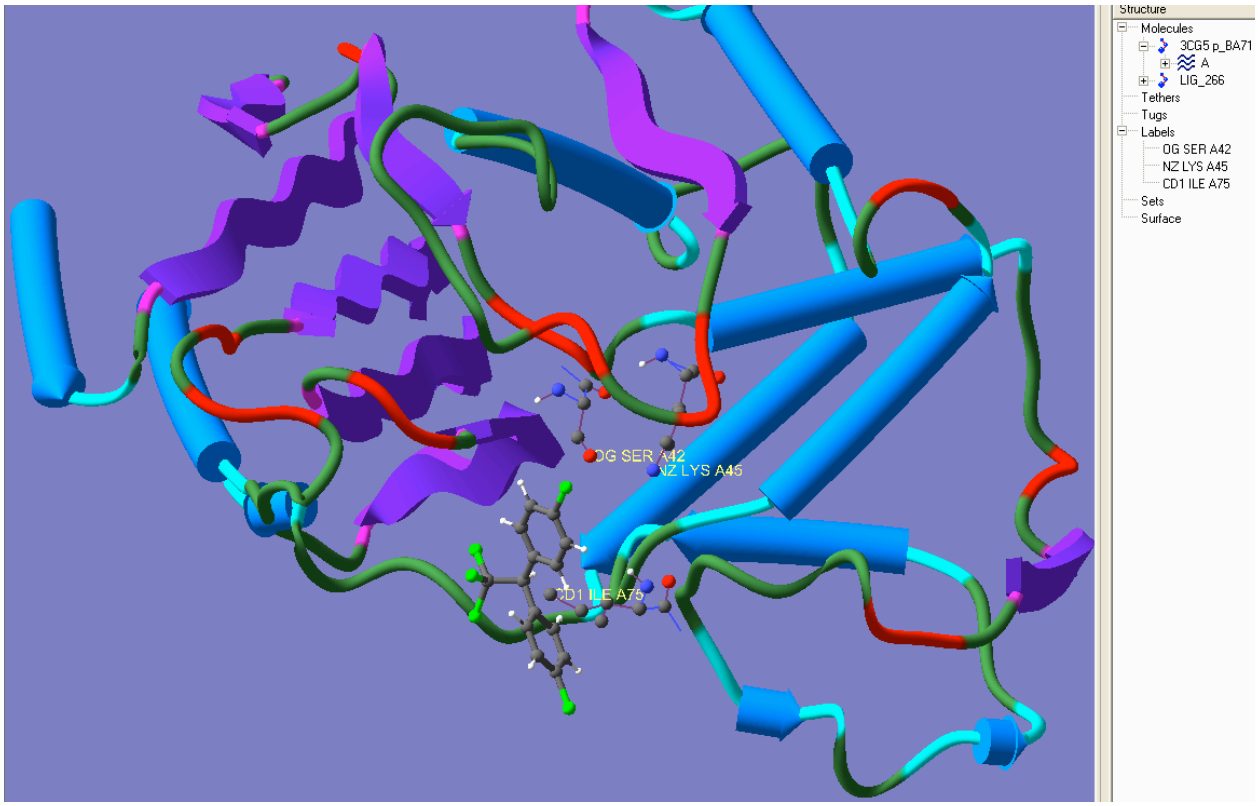

Figure 81: 4,4'-DDT in BlaC (3CG5) Active Site ball and sticks *(Sculpt).* The model shows Ser42(70)-γO opposite the trichloromethyl moiety of 4,4'-DDT.

Figure 82: Study of boronic acids with fluoride substituents inhibiting BlaC (3CG5). The pictures are in ascending order of Ki from kinetic experiments.

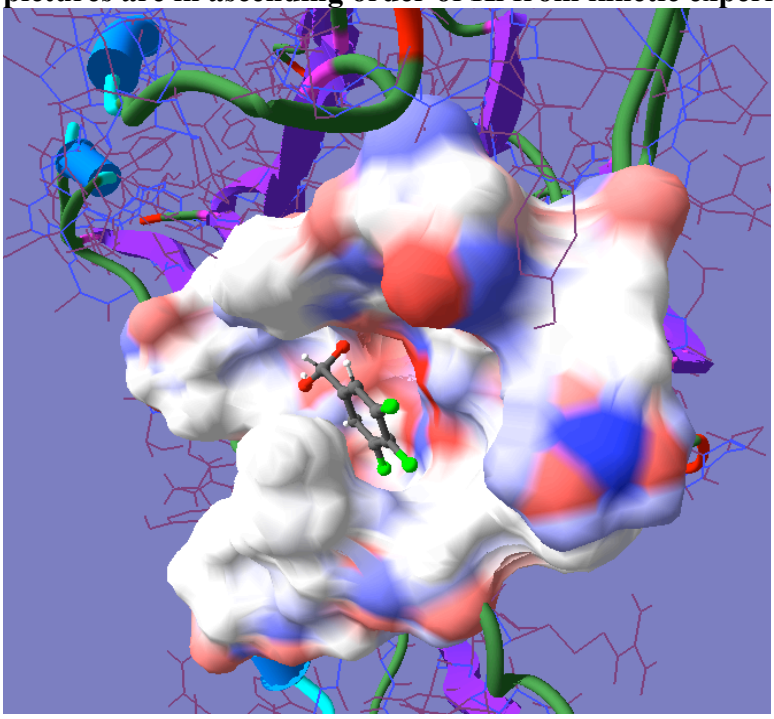

3,4,5-Trifluorophenylboronic acid
Ki, 175.7 µM

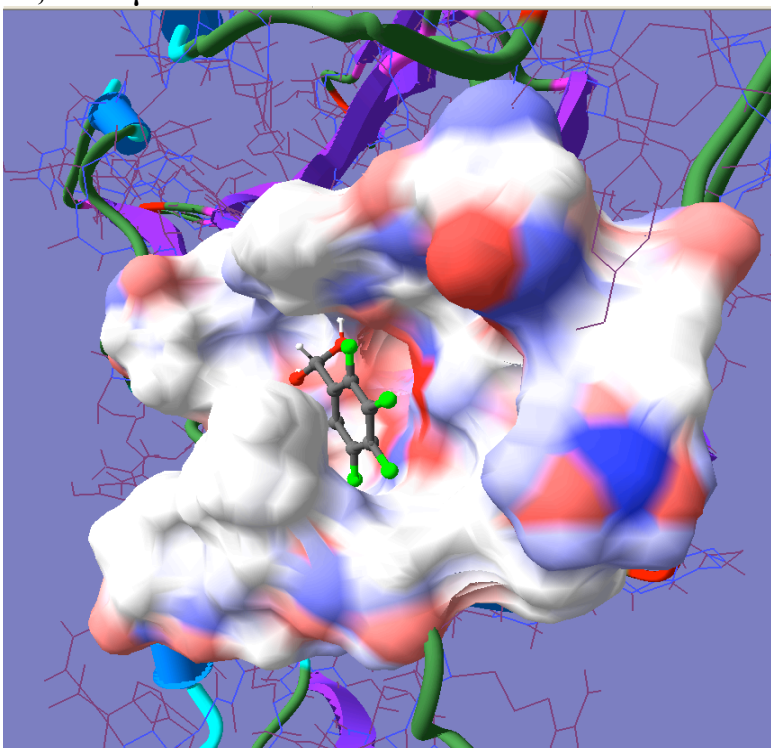

2,3,4,5-Tetrafluorophenylboronic acid
Ki, 228.6 µM

Figure 82: Study of boronic acids with fluoride substituents inhibiting BlaC (3CG5). The pictures are in ascending order of Ki from kinetic experiments (Continued).

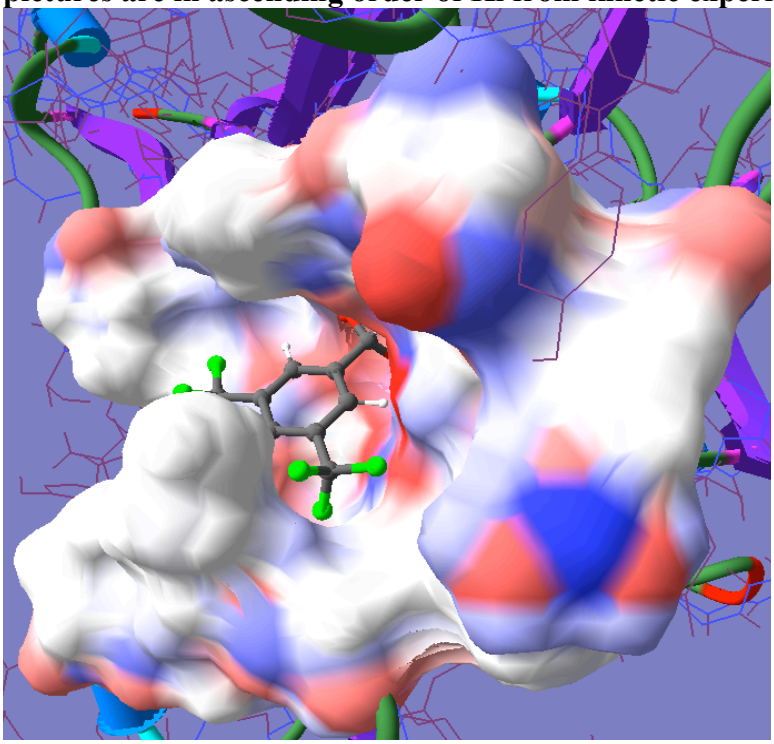

3,5-Bis(trifluoromethyl)benzylboronic acid
Ki, 302.3 µM

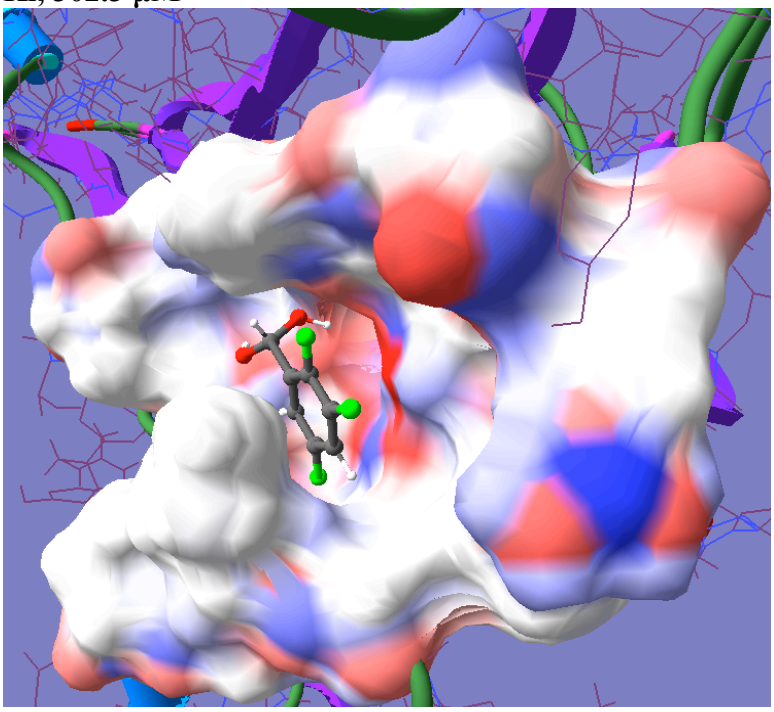

2,3,5-Trifluorophenylboronic acid
Ki, 477.2 µM

Figure 82: Study of boronic acids with fluoride substituents inhibiting BlaC (3CG5). The pictures are in ascending order of Ki from kinetic experiments (Continued).

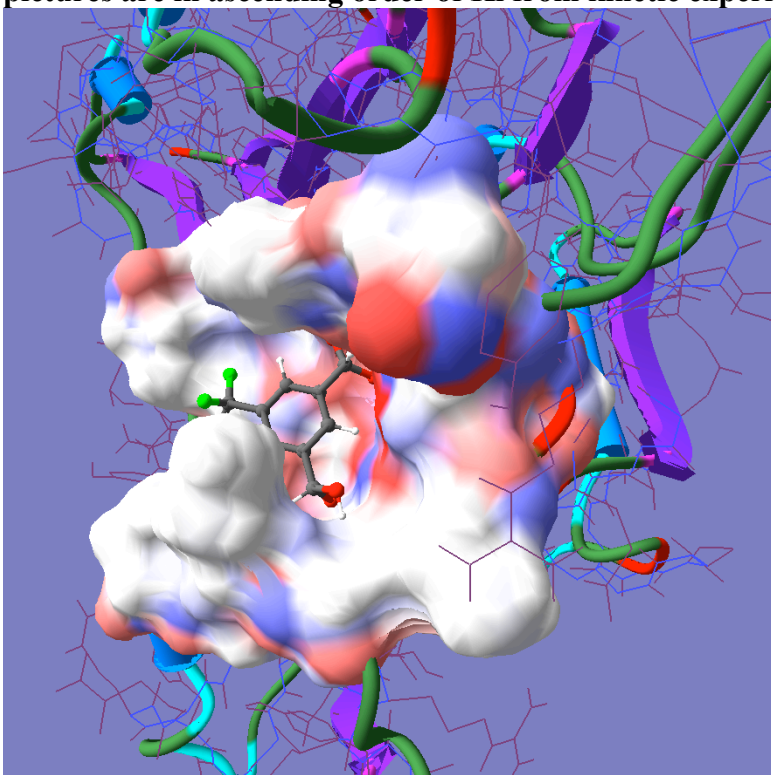

5-Trifluoromethyl-1,3-phenyldiboronic acid
Ki, 643.8 µM

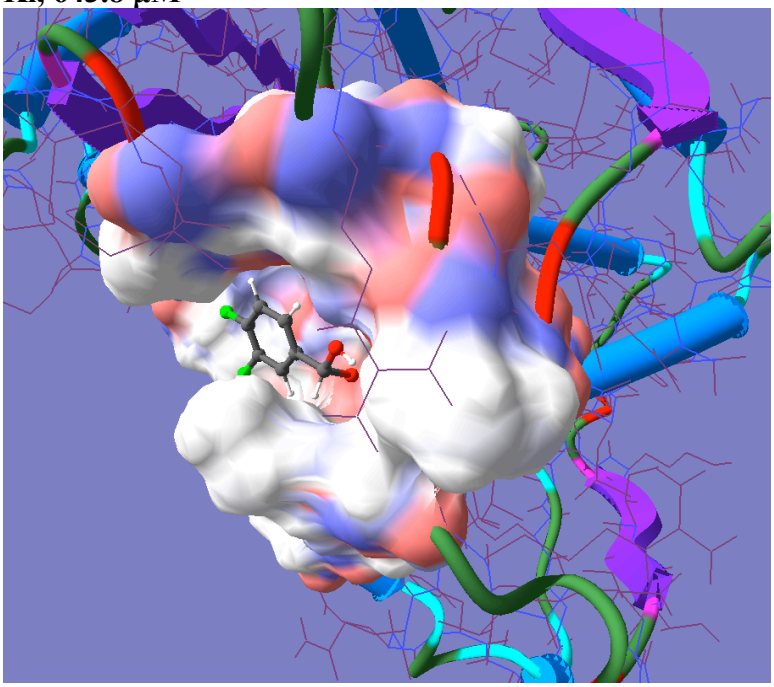

3-Chloro-4-fluorobenzeneboronic acid
Ki, 657.6 µM

Figure 82: Study of boronic acids with fluoride substituents inhibiting BlaC (3CG5). The pictures are in ascending order of Ki from kinetic experiments (Continued).

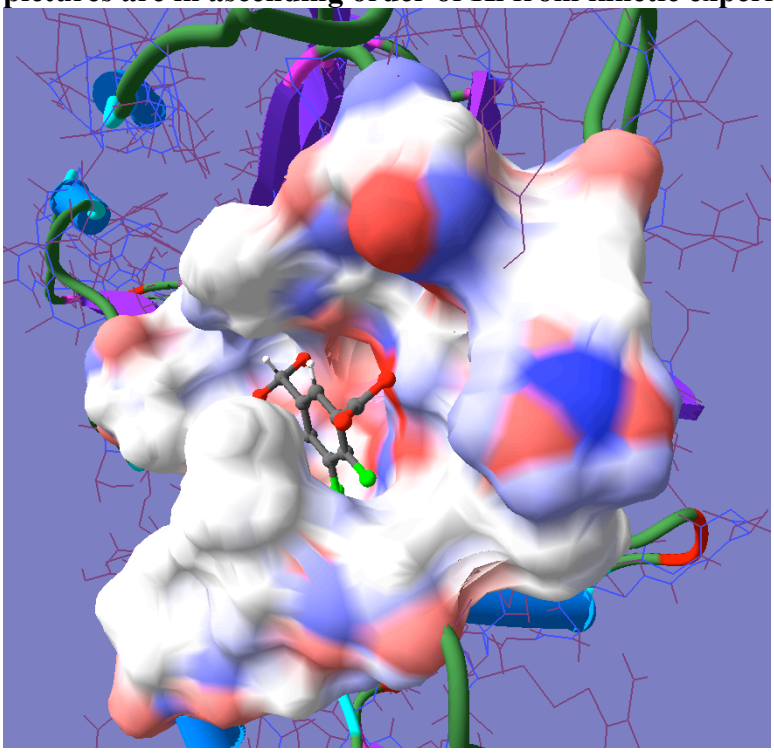

3-Carboxy-4,5-difluorophenylboronic acid
Ki, 1,468.7 µM

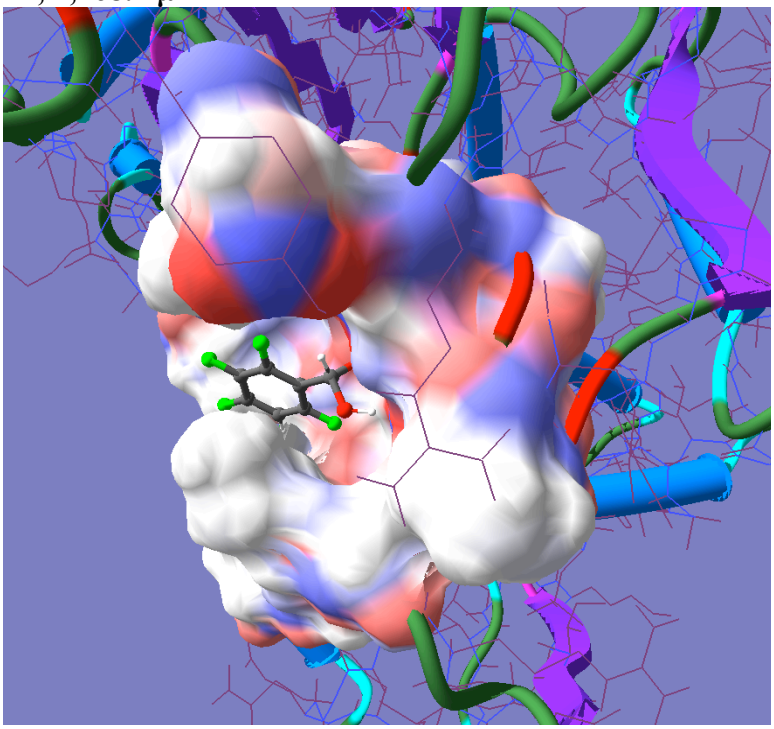

2,3,4,6-Tetrafluorophenylboronic acid
Ki, 2,183.6 µM

Figure 82: Study of boronic acids with fluoride substituents inhibiting BlaC (3CG5). The pictures are in ascending order of Ki from kinetic experiments (Continued).

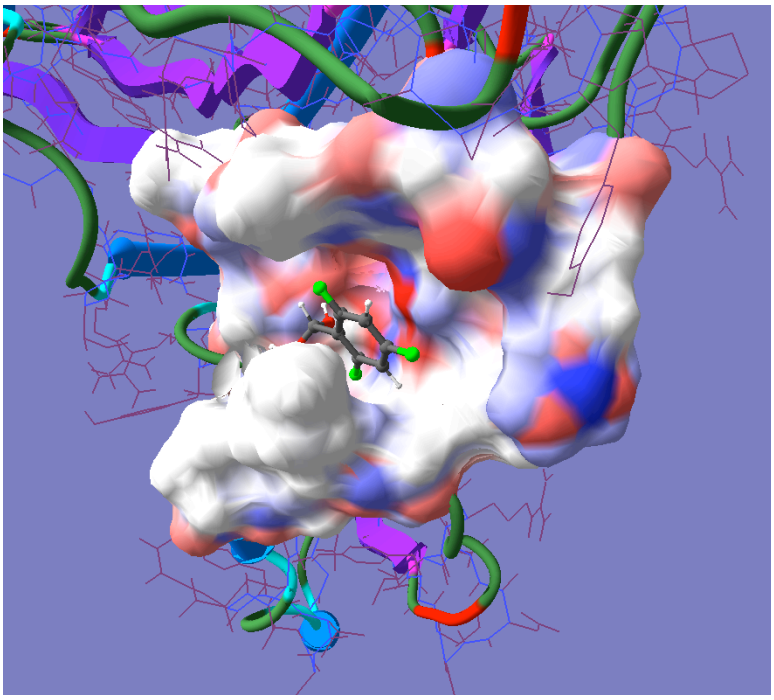

2,4,6-Trifluorophenylboronic acid
Ki, 5,998.6 µM

Figure 83: Study of boronic acids with polyatomic substituents at a *meta* position in the active site of BlaC (3CG5). The pictures are in ascending order of Ki from kinetic experiments.

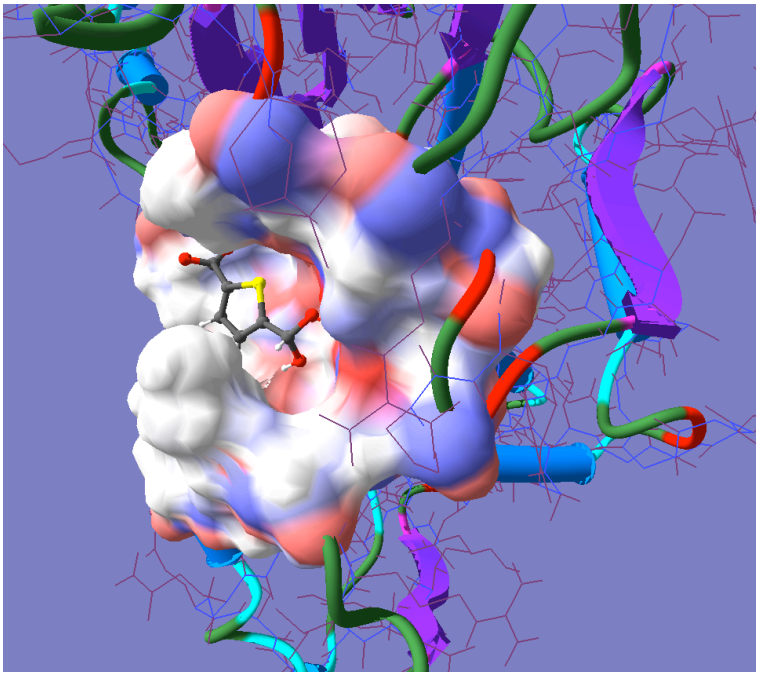

2-Carboxythiophene-5-boronic acid
Ki, 1.272 µM

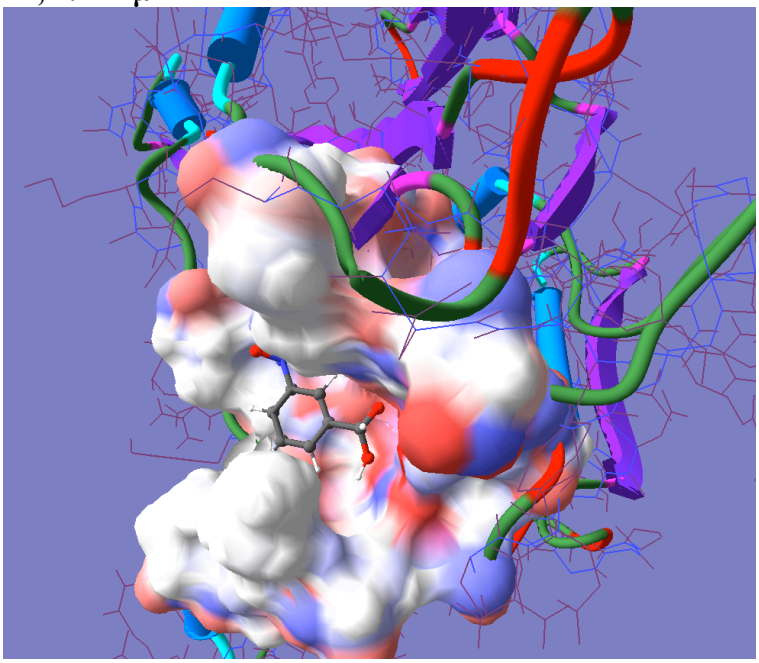

3-Nitrophenylboronic acid
Ki, 213.9 µM

Figure 83: Study of boronic acids with polyatomic substituents at a *meta* position in the active site of BlaC (3CG5). The pictures are in ascending order of Ki from kinetic experiments (Continued).

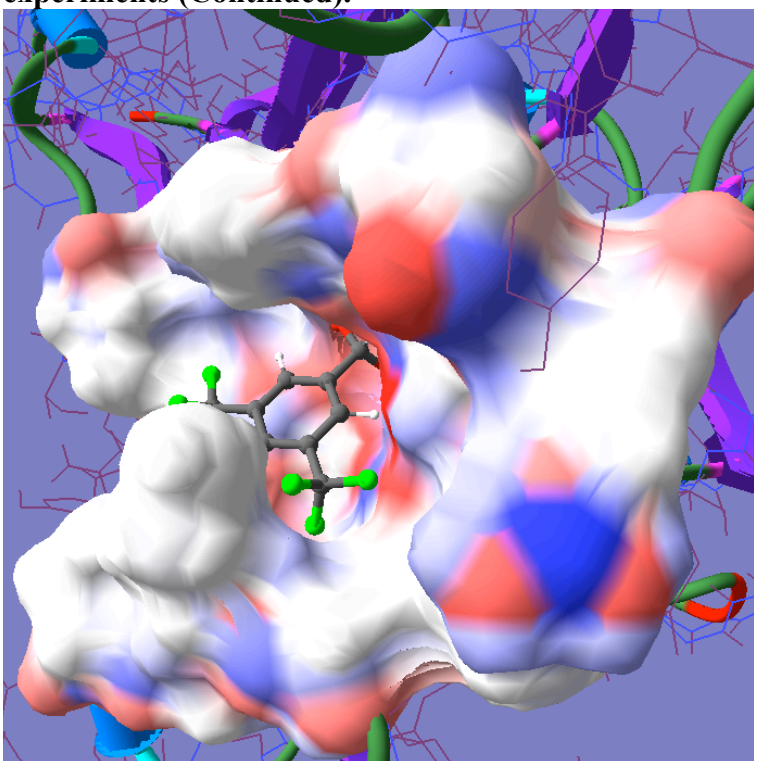

3,5-Bis(trifluoromethyl)benzeneboronic acid
Ki, 302.3 µM

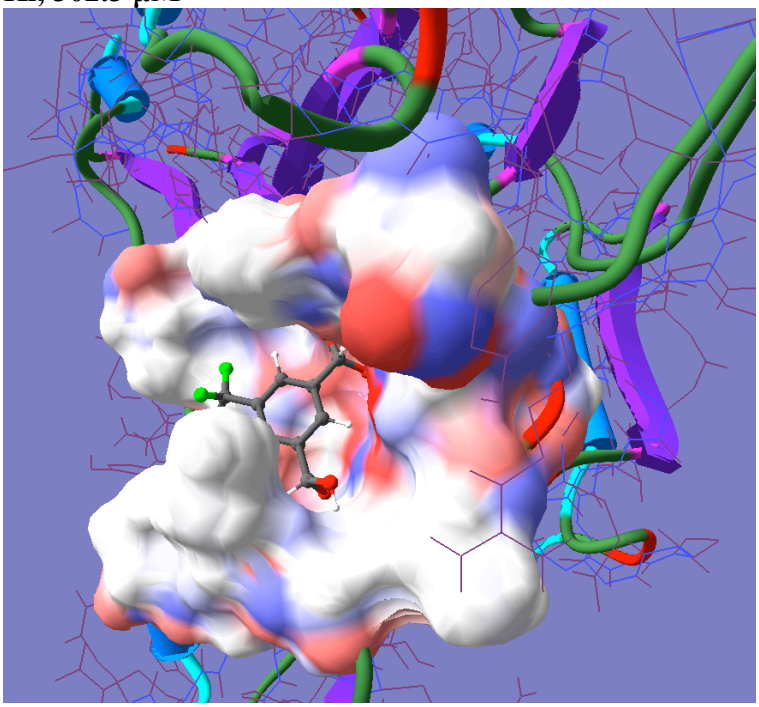

5-Trifluoromethyl-1,3-phenyldiboronic acid
Ki, 643.8 µM

Figure 83: Study of boronic acids with polyatomic substituents at a *meta* position in the active site of BlaC (3CG5). The pictures are in ascending order of Ki from kinetic experiments (Continued).

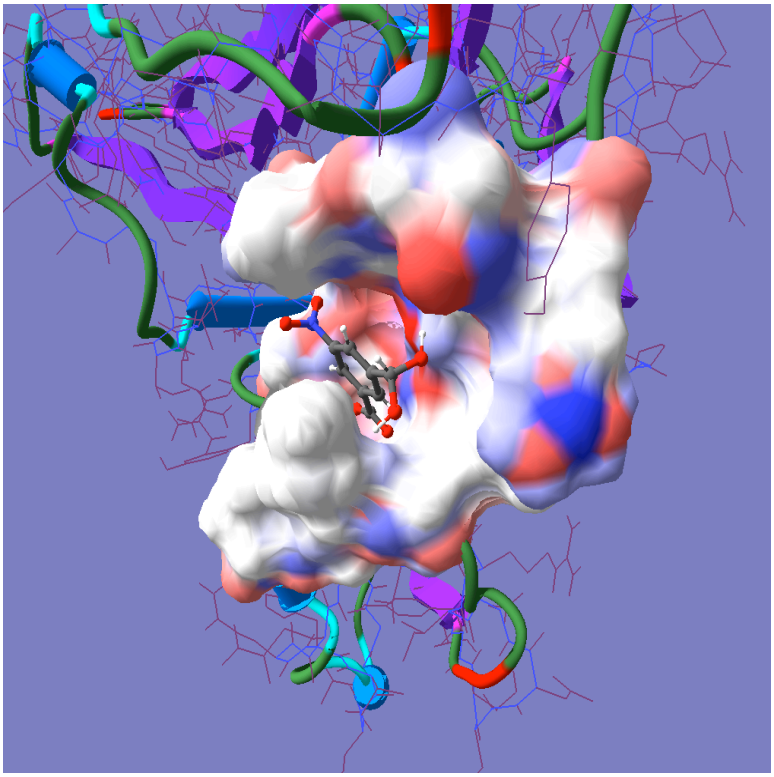

3-carboxy-5-nitrophenylboronic acid
Ki, 844.9 µM

Boronic acids as inhibitors of Bacillus cereus 569/H9 Beta-lactamase I

KI (uM)	*Compound name*	*Structure*
1.1	2-Carboxythiophene-5-boronic acid	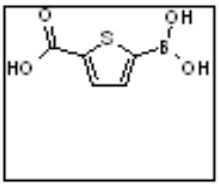
19.4	3-Carboxyphenylboronic acid	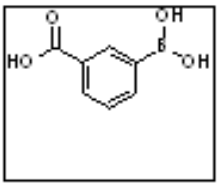
46.5	2-Carboxythiopehene-4-boronic acid	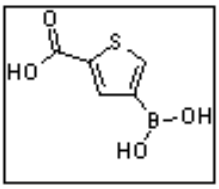
47.1	3-Carboxy-4-fluorophenylboronic acid	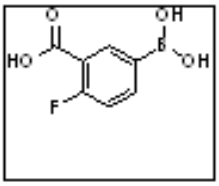
65.8	3-carboxy-5-nitrophenylboronic acid	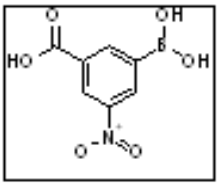

Figure 84: Study of structure activity relationship of boronic acids as inhibitors of *Bacillus cereus* β-lactamase I.

KI (uM)	*Compound name*	*Structure*
136.9	3-Amino-5-carboxylphehylboronic acid	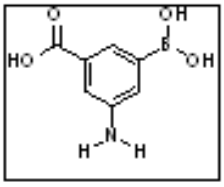
247.3	3-Nitrophenylboronic acid	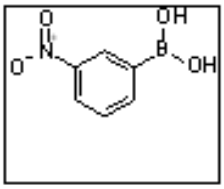
394.6	2,3,5-Trifluorophenylboronic acid	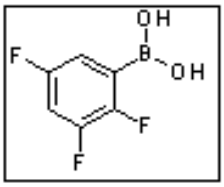
461.5	2,3,4,5,6-Pentafluorobenzeneboronic acid	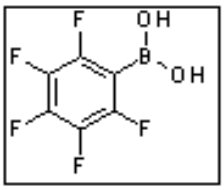
573.6	2,3,4,6-Tetrafluorophenylboronic acid	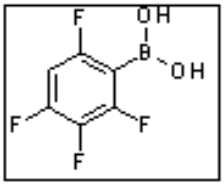
848.0	2-Phenyl-1-ethynylboronic acid pinacol ester	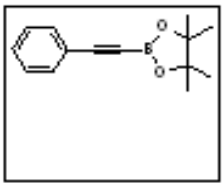

Figure 84: Study of structure activity relationship of boronic acids as inhibitors of *Bacillus cereus* β-lactamase I (Continued).

KI(uM)	Compound name	Structure
1,063.0	3-Pyridineboronic acid	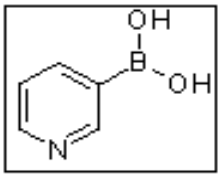
1,121.0	2,3,4,5-Tetrafluorophenylboronic acid	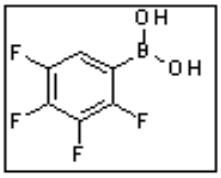
1,163.0	3-Chloro-4-fluorobenzeneboronic acid	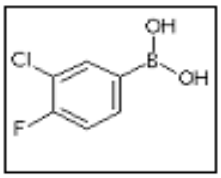
1,337.0	3-carboxytiophene-2-boronic acid	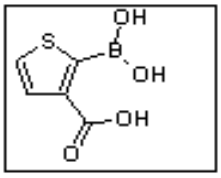
1,663.0	2,4,6-Trifluorophenylboronic acid	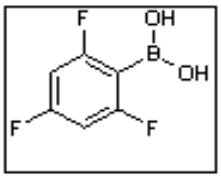
2,998.0	Phenylboronic acid	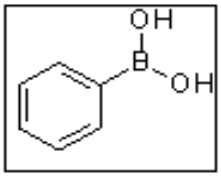

Figure 84: Study of structure activity relationship of boronic acids as inhibitors of *Bacillus cereus* β-lactamase I (Continued).

KI(uM)	*Compound name*	*Structure*
7,228.0	3,4,5-Trifluorophenylboronic acid	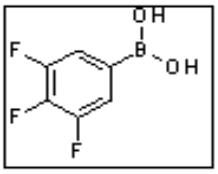

Figure 84: Study of structure activity relationship of boronic acids as inhibitors of *Bacillus cereus* β-lactamase I (Continued).

Discussion

As shown in tables 1, 2, and 3, there is no exact correlation between the Ki values obtained experimentally and the Ki obtained *in silico* by *AutoDock Vina*. There is however, a correlation in the sense that the Ki for a little more than half of the compounds fall in the micromolar range. The major drawback for docking is that there is no function that recognizes boron as an electron sink. In modeling, carbon was inserted instead of boron and was attached to two hydroxide groups and a hydrogen. The γO of Ser42(70) would then seek the hydrogens from these hydroxide groups for hydrogen bonding. The more hydrogen bonds we get the more likely this molecule will show low Ki by *in silico* analysis. Hydrogen bonds are easier to identify, whereas other types of interactions are less evident. Ile75 in BlaC (3CG5) and its counterpart Tyr(105) in TEM-1 (1ERO) are two side chains that seem of importance in stabilizing the inhibitor molecule in the active site via van der Waals interactions and ring stacking interactions respectively. What is of importance here is the relative position not the lowest Ki. The attempt is to find a pattern that would help us to predict the next best family of inhibitors. Introducing coordinates in the docking program produced a lower Ki depending on how well the ligand fit in the active site nevertheless the higher Ki should not be eliminated because the inhibitor can still work. Therefore, scanning solely in *in silico* to eliminate the worst or accept only the best is a mistake. Proof of the above is the case of 3,5-Bis(trifluoromethyl)benzeneboronic acid which showed a high Ki *in silico* but it shows a good position in the compounds tested in BlaC. Moreover, in BlaC the fluorinated aryl boronic acid are shown to tilt to the side of Ile75(105) as in a sigma pi interaction, the 3,5-Bis(trifluoromethyl)benzeneboronic acid however, engage Ile75(105) on both sides. The same happens with 5-trifluoromethyl-1,3-phenyldiboronic acid, 3-carboxy-5-nitrophenylboronic acid. The same happens also with DDT which has two phenyl groups

attached to trichloroethane moiety. In each of the aforementioned molecules two bulky groups sit on each side of the prominence of Ile75(105). It has been observed that whenever there are three bulky substituents including the boronate moiety two of them fall on each side of Ile75(105), the inhibitor does not tilt to the side as in molecules where all substituents are single atoms. It has been observed that when there are only two bulky substituents including the boronate moiety the other group would orient itself toward Thr209(Ser235), Thr211(Ala237), Lys208(234) and away from Ile75(105) and the aromatic ring may be in sigma pi stacking interaction with Ile75(105).

In the case of 4,4'-DDT the experimental Ki and the *AutoDock Vina's* Ki are close, experimental 48 μM and *Vina's* 40 μM. For the DDT *Vina's* docking was done without centering the molecule in the active site, *AutoDock Vina* was allowed to choose another active site. As a result a better Ki was obtained. The rationale for this is that the chlorines from the trichloromethyl moiety of the 4,4'-DDT would not look for of Ser42(70)- γO because this oxygen is deprotonated and would evade chlorine atoms. The model shows that the tricholomethyl moiety is in fact far away from Ser42(70)- γO. The ligand is in the active site, however. Most of the interactions are van der Waals weak interactions, Ile75 being a key player since the two phenyl groups of 4,4'- DDT interact on each side of the Ile75 side chain. The thiophenes seem to be of particular importance in BlaC as well as in TEM-1. In this case it should be noticed that the compound second in effectiveness to 2-carboxy-5-thipheneboronic acid is 3-carboxyphenylboronic acid. Both compounds have a carboxyl group on the *meta* position to the boronate moiety. According to Beesley (1983) in studying class C β-lactamases, the affinity falls in the order *meta* > *para* > *ortho* in boronic acid inhibitors for class C β-lactamases. This may hold true for the class A β-lactamase enzymes and that the thiophenes may have an advantage over the phenylboronic acid in that the angle is different between the boronate

and the carboxyl group, it seems wider in the thiophene than in the phenylboronic acid. The key for a better inhibitor may be in changing the angle between these two moieties but maintaining their angles between 120˚ and 180˚. Thus we count with several elements for more exploration, the boronate moiety remains unchanged, the thiophene, the carboxyl group *meta* to boronate, leaving positions 3 and 4 of the thiophene free to experiment with. Hydrophobic are called for in this two positions so that the solvent would drive the molecule inwards into the active site since the driving force for boronic acid interaction with the serine enzymes is the hydrophobic effect (Weston *et al*., 1998)

Conclusions

1) Boronic acids are inhibitors of *Mycobacterium tuberculosis* β-lactamase (BlaC) and *Bacillus cereus* 569/H9 β-lactamase I TEM-116.
2) The thiophene ring is needed because is aromatic, it can enter into sigma pi interactions with Tyr105 in the TEMs enzymes and it shows that it may a better angle somehow wider than the 120˚ observed in 3-carboxyphenyl boronic acid.
2) 2-Carboxythiophen-5-boronic acid and possible its derivatives are of interest; 2-carboxythiophen-5-boronic acid binds tightly to both enzymes studied in this research.
3) Two bulky groups at *meta* position to each other and to the boronate moiety bind in a way that both sit at each side of Ile75 in BlaC.
4) Combining the features that a carboxyl group *meta* to the boronate moiety binds away from Ile75 and that two bulky groups engulf Il75 would lead to a better inhibitor in BlaC.
6) 2-Carboxythiophene-5-boronic acid and 4,4'-DDT are the key for better inhibitors in BlaC.
7) 2-Carboxythiophen-5-boronic acid and 4,4'-DDT are also the key for better inhibitors of the TEMs. In this case the thiophene group is in pi-pi stacking interaction with Tyr105 and the usual carboxyl group and the boronate moiety look for their appropriate interactions Ser235 for the carboxyl group and the Ser70 for the boronate moiety. *In silico* experiments favored the inhibition of TEM-1 (1ERO) with a Ki of 17 μM. Therefore the combinations of these two molecules should also be considered for designing inhibitors of the TEMs.

Appendix A

Interactions of clavulanate in the active site of BlaC as is in the crystal structure 3CG5 compared to results from *AutoDock Vina* non-hydrolyzed and hydrolyzed clavulanic acid.

ΔG for the non-hydrolyzed structure of clavulanic acid (Figure 69) produced by *AutoDock Vina* is -6 kcal/mol which would translate to a Ki of 40 µM which is compatible with the ΔG *Vina* returned for the boronic acid tested and DDT. Therefore *Vina* results should be trusted.

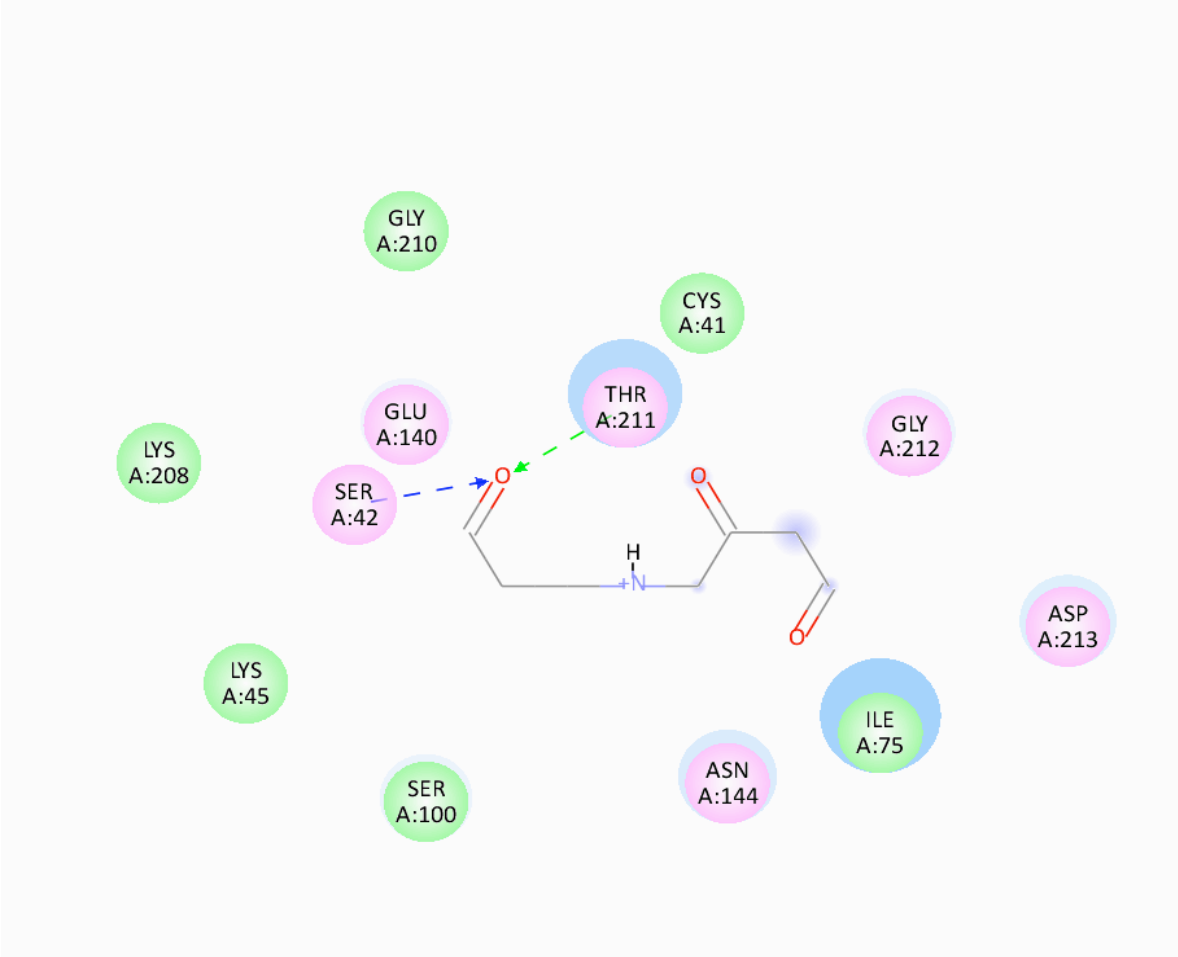

Figure 85: Interactions in the active site of BlaC (3CG5) and clavulanate as is in the crystal structure from NCBI. No docking was performed therefore no ΔG from *AutoDock Vina* was obtained.

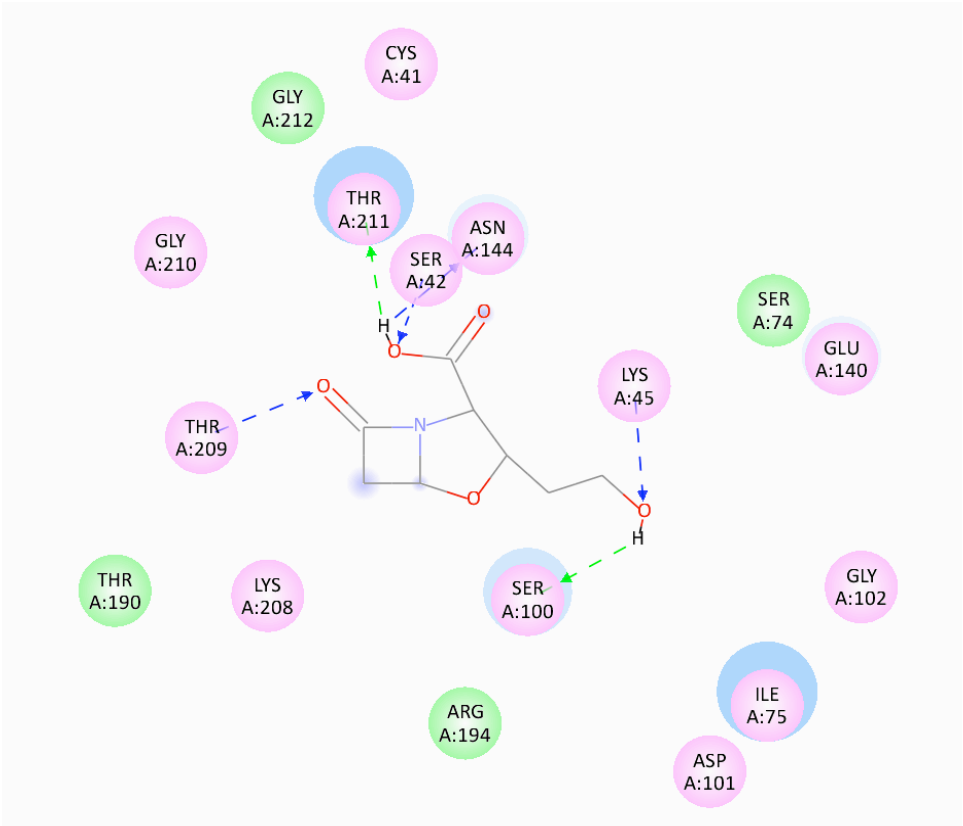

Figure 86: Interactions of clavulanate in the active site of BlaC (3CG5) before hydrolysis. This was done by docking with *AutoDock Vina*. *Vina's* ΔG = -6

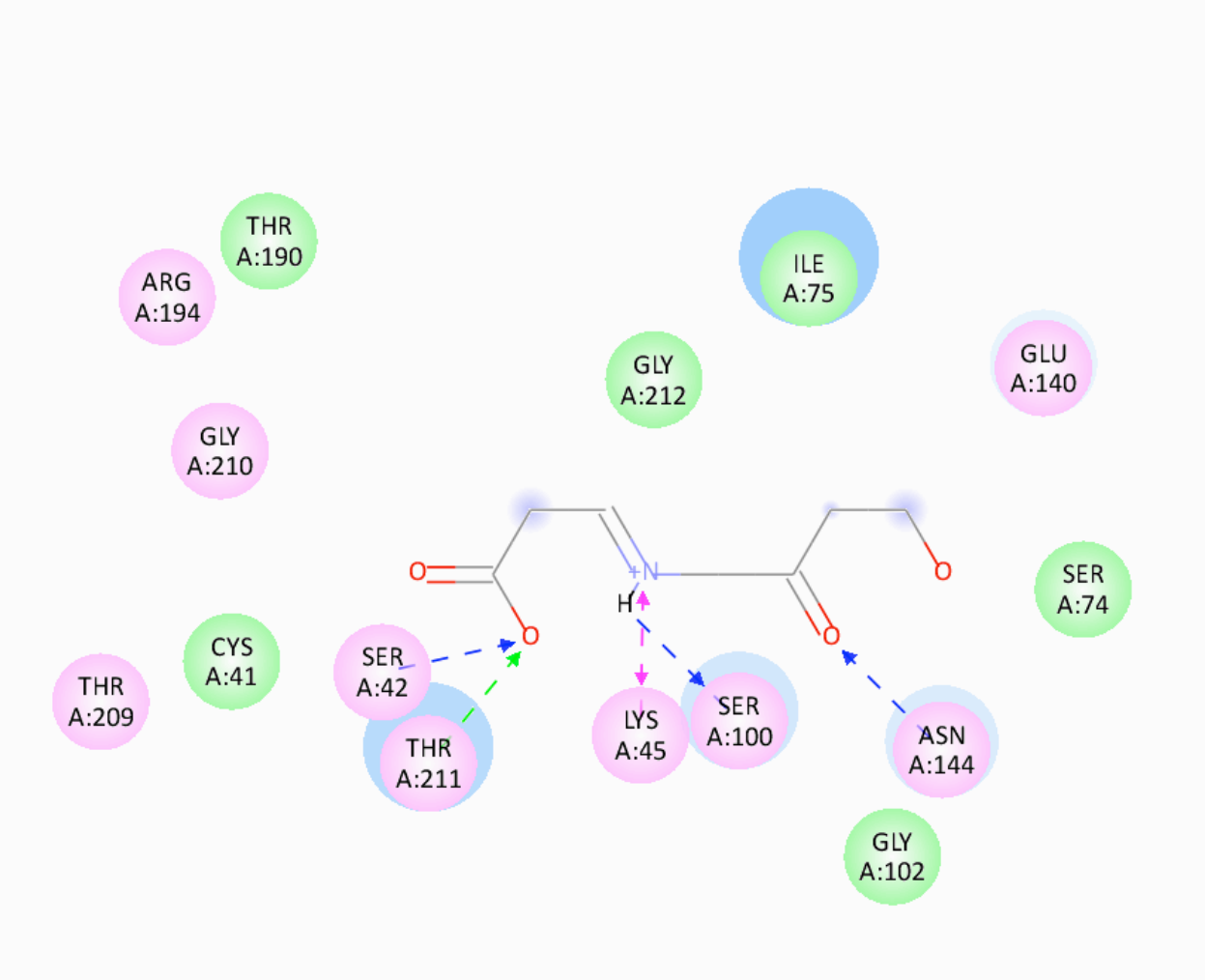

Figure 87: Interactions of clavulanate in the active site of BlaC (3CG5) after hydrolysis. A carboxyl group was placed in position 7 of the oxapenam (clavam) (See figure 1) so that Ser42(70)-γO would get attracted to this end of the molecule and not the hydroxyl in the hydroxyethyledene moiety. Compare this figure with figure 68. *Vina's* ΔG = -5.3

Appendix B

Effect on docking when no coordinates are set for the active site in VcPpt *AutoDock Vina*.

The effect of not limiting the binding of the inhibitor to the active site is that the inhibitor binds far from the active site.

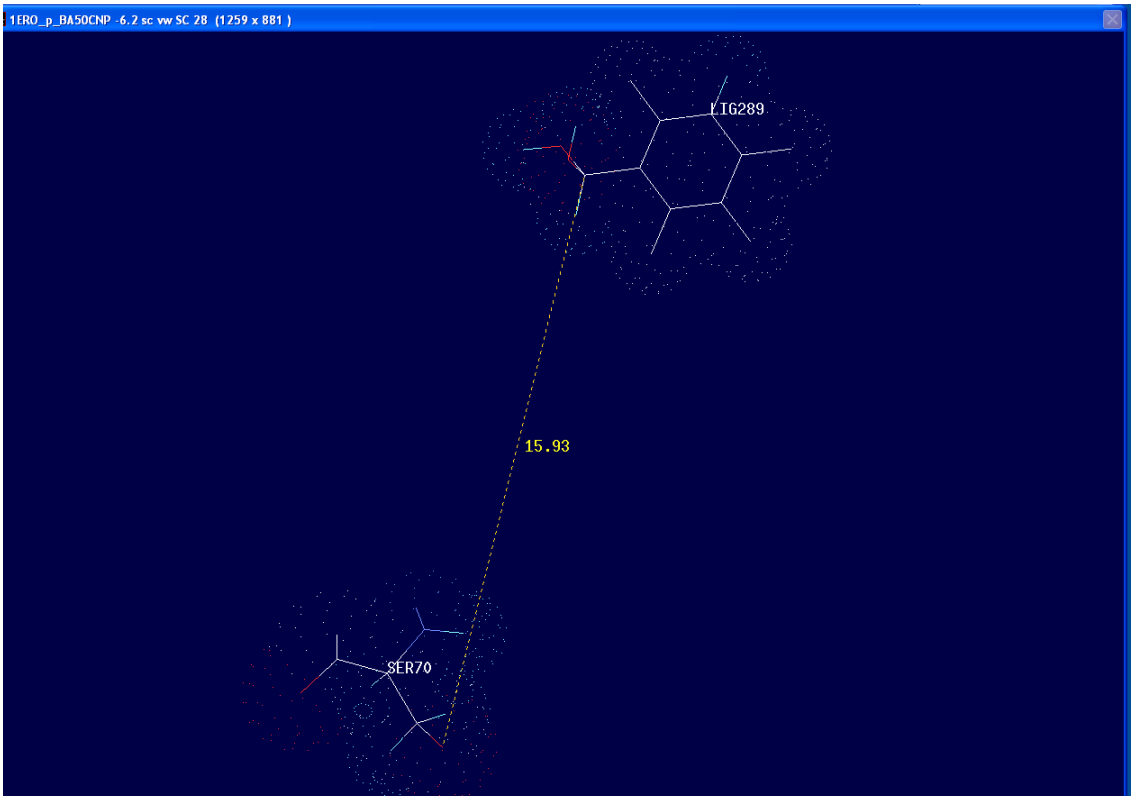

Figure 88: Effect on ducking if no coordinates are set for the active site in VcPpt *AutoDock Vina*. The picture shows 2,3,4,6-Tetrafluorurophenylboronic acid in TEM-1 (1ERO) which is located more than 15 Å away from Ser70-γO.

Appendix C

Programs used for modeling.

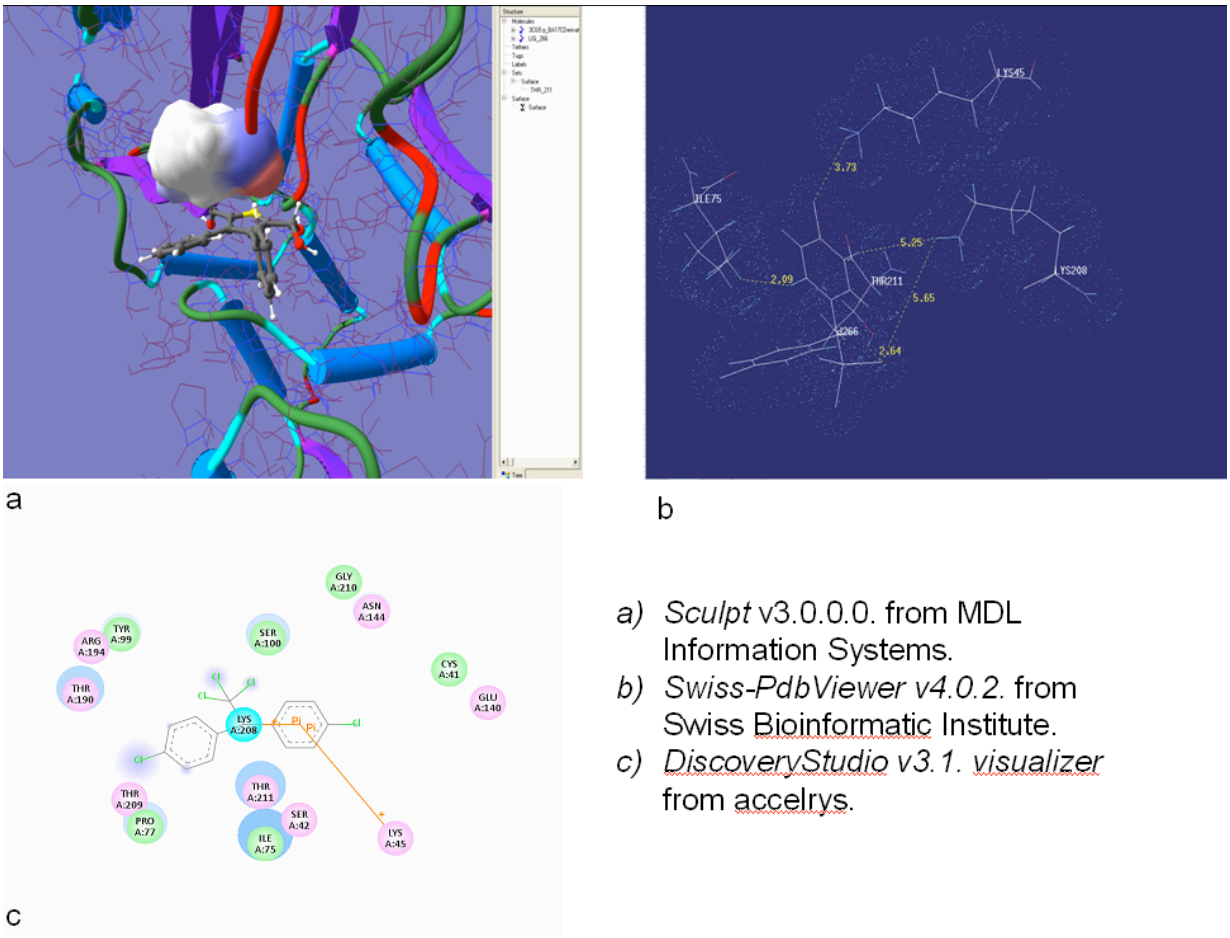

Figure 89: Programs used for modeling Sculpt, *Swiss-PdbViewer, and DiscoveryStudio*.

Appendix D

Database created to account for all trials with boronic acids versus β-lactamase from *Bacillus cereus* 569/H9

KI(uM)	*BA - #*	*Compound name*	*Structure*
219.8	51	4-(9H-carbozol-9-yl)phenylboronic acid	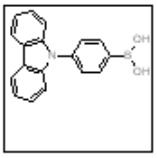
244.2	55	Dimesitylborinic acid	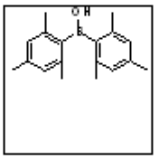
268.3	10	3-Nitrophenylboronic acid	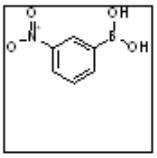
394.6	32	2,3,5-Trifluorophenylboronic acid	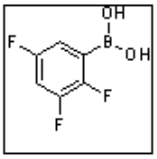
501	41	2,3,4,5,6-Pentafluorobenzeneboronic acid	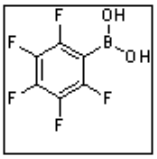
591.1	50	2,3,4,6-Tetrafluorophenylboronic acid	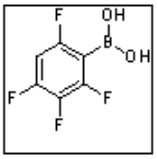

Figure 90: *Access* database from Microsoft was used in the analysis of boronic acids and their Ki for SAR.

Appendix E.

Element	Description
	Residues involved in hydrogen-bond, charge or polar interactions are represented by pink circles.
	Residues involved in van der Waals interactions are represented by green circles.
	Water molecules are represented by aquamarine circles.
	Metal atoms are represented by gray circles.
	Covalently bonded residues are represented by magenta-colored circles.
	The solvent accessible surface of an interacting residue is represented by a blue halo around the residue. The diameter of the circle is proportional to the solvent accessible surface.
	The solvent accessible surface of an atom is represented by a blue halo around the atom. The diameter of the circle is proportional to the solvent accessible surface.
	Hydrogen-bond interactions with non-amino acid residues are represented by a black dashed line arrow directed towards the electron donor.
	Hydrogen-bond interactions with amino acid main chains are represented by a green dashed arrow directed towards the electron donor.
	Hydrogen-bond interactions with amino acid side-chains are represented by a blue dashed arrow directed towards the electron donor.
	Charge interactions are represented by a pink dashed arrow with heads on both sides.
	Pi interactions are represented by an orange line with symbols indicating the interaction.

Figure 91: Color code used by *DiscoveryStudio Visualizer* program in the 2D representation of the enzyme-ligand interactions.

Bibliography

1. Ambler, R. P. The structure of β-lactamases. *Phil. Trans. R. Soc. Lond.* [Online] **1980**, *B 289*, **321-331**.

2. Andries, K.; Verhasselt, P.; Guillemont, J.; Gohlmann, H. W. H.; Neefs, J. M.; Winkler, H.; Gestel, J. V.; Timmerman, P.; Zhu, M.; Lee, E.; Williams, P.; DeChaffoy, D.; Huitric, E.; Hoffner, S.; Cambau, E.; Truffot-Pernot, C.; Lounis, N.; Jarlier, V. A Diarylquinoline Drug Active on the ATP Synthase of *Mycobacterium tuberculosis*. *Science* [Online] **2005.** *14 January. Vol. 307*. **223-227**.

3. AutoDock Vina utility for windows website. www.biochemlabsolution.com (accessed July 2013)

4. Barlow, M.; Hall, B. G.; Experimental Prediction of the Evolution of Cefepime Resistance From the CMY-2 AmpC β-Lactamase, *Genetics* [Online] **2003**. *164*: **23-29**.

5. Beesley, T.; Gascoyne, N.; Knott-Hunziker, V.; Petursson, S.; Waley, S. G.; Jaurin, B.; Grundstrom, T. The inhibition of class C β-lactamases by boronic acids. *Biochem. J.* [Online] **1983**. *209*, **209-233**.

6. Carnegie Mellon University website. Lecture 15: Enzyme Inhibition https://www.bio.cmu.edu/courses/03231/LecF04/Lec15/lec15.pdf (accessed June 2013).

7. Chakraborty, D.; Basu, S.; Das, S. A Study on Infections Caused By Metallo Beta Lactamase Producing Gram Negative Bacteria in Intensive Care Unit Patients. *American Journal of Infectious Diseases* [Online**] 2010**, *6 (2),* **34-39**.

8. Clement, C. Cristina Ph. D. Thesis, The Graduate School and University Center, The City University of New York, New York, NY. 2006.

9. Clustal Omega website, EMBL-European Bioinformatic Institute, Cambridgeshire, UK http://www.ebi.ac.uk/Tools/msa/clustalw2/ (accessed June 2013).

10. DeSoyza, Tushini V. Ph.D. thesis, The Graduate Center/CUNY, New York, NY. 1990.

11. Deshpande, A. D.; Baheti, K. G.; Chatterjee, N. R. Degradation of β-lactam antibiotics. *Current Science*. [Online] **2004**, *December 25, Vol. 87, No 12*. **1684-1695**.

12. Eisenberg D. *Physical Chemistry with Applications to the Life Sciences*. The Benjamin/Cummings: Menio Park, CA. 1979; pp 149-153.

13. Essack, S. Y., The Development of β-lactam Antibiotics in Response to the Evolution of β-Lactamases. *Pharmaceutical Research* [Online] **2001,** *18,* **1391-1399**.

14. Fisher, J. F.; Meroueh, S. O.; Mobashery, S. Bacterial Resistance to β-lactam Antibiotics: Compelling Opportunism, Compelling Opportunity. *Chem. Rev*. [Online] **2005**, *105*, **395-424**.

15. Flores, A. R.; Parsons, L. M.; Pavelka, M. S. Jr. Genetic analysis of the β-lactamases of *Mycobacterium tuberculosis* and Mycobacterium smegmatis and susceptibility to β-lactam antibiotics. *Microbiology* [Online] **2005**, *151*, **521-532**.

16. Foye, W. O.; Lemke, T. L.; William, D. *Principles of Medicinal Chemistry*, 4th ed.; Wilkins: 1995; pp 759-802.

17. González, Janet. Ph.D. Thesis, The Graduate School and University Center, The City University of New York, New York, NY. 2012.

18. Hall, D. G., *Boronic Acids*; Wiley-Vch: Edmonton, AB, 2005; pp 1-16.

19. Hall, B. G.; Barlow, M. Evolution of the Serine β-lactamases: past, present and future. *Drug Resistance Update* [Online] **2004,** *7*, **111-123**

20. Hall, B. G.; Barlow, M. Revised Ambler classification of β-lactamases. *Journal of Antimicrobial chemotherapy*. [Online] **2005**, **1050-1051**.

21. Hata, M.; Fujii, Y.; Tanaka, Y.; Ishidawa, H.; Ishii, M.; Neya, S.; Tsuda, M.; Hoshino, T. Substrate Deacylation Mechanisms of Serine β-lactamases. *Biol. Pharm. Bull*. [Online] **2006**, *29(11),* **2151-2159**.

22. Hu, G. Z.; Chen, H. Y.; Si, H. B.; Deng, L. X.; Wei Z. Y.; Yuan, L.; Kuang, X. H. Phenotypic and molecular characterization of TEM-116 extended-spectrum β-lactamase produced by *Shigella flexneri* clinical isolate from chickens. *FEMS Microbiol. Lett.* [Online] **2008**. *279,* 162-166.

23. Hugonnet J. E.; Blanchard, J. Irreversible Inhibition of the Mycobacterium truberculosis β-Lactamase by Clavulanate. *Biochemistry* [Online] **2007**, *46*, **11998-12004**.

24. Jacoby, G. A. AmpC β-Lactamases. *Clinical Microbiology Reviews* [Online] **2009.** *Jan.* **161-182**.

25. Lahey Clinic website http://www.lahey.org/Studies/te (accessed on August 2013).

26. Lamotte-Brasseur, J.; Lounnas, V.; Raquet, X.; Wade, R. pKa Calculations for class A β-lactamases: Influence of substrate binding. *Protein Science* [Online] **1999***, 8***, 404-409.**

27. Lee, M.; Hesek, D.; Mobashery, S.; A Practical Synthesis of Nitrocefin. *J. Org. Chem*. [Online] **2005**, *70*, **1.**

28. Long, D. *Biochemists' handbook*. Van Nostrand: Princeton, N. J., 1961.

29. Meroueh, S. O.; Fisher, J. F.; Schlege, B.; Mobashery, S.. Ab Initio: Q/MM Study of Class A β-Lactamases Acylation: Dual Participation of Glu166 and Lys73 in a Concerted Base Promotion of Ser70. *J. Am. Chem. Soc*.[Online] **2005**, *127*, **15397-15407**.

30. Matagne, A.; Lamotte-Brasseur, J.; Frere, J. Catalytic properties of class A β-lactamases: efficiency and diversity. *Biochem.* [Online] **1998**. *330*, **581-598.**

31. Nelson, D. L.; Cox.; Lehninger: *Principles of Biochemistry*, 5th ed.; Freeman: New York, 2008; pp 183-233.

32. OpenBabel website. www.openbabel.org. (accessed on August 2013).

33. Peimbert, M.; Segovia, L. Evolutionary engineering of a β-Lactamase activity on a D-Ala D-Ala transpeptidase fold. *Protein Engineering* [Online] **2003**, *vol. 16 no.1*. **27-35**.

34. Philipp, M.; Bender, M. L. Inhibition of Proteases by Arylboronic Acids. *National Academy of Science* [Online] **1971,** *68*, **478-480**.

35. Pubmed website. http://www.ncbi.nlm.nih.gov/sites/entrez (Accessed July 2008)

36. Salverda, M. L. M; Visser, A. G. M.; Barlow, M. Natural evolution of TEM-1 β-lactamase: experimental reconstruction and clinical relevance. *FEMS Microbiolo Rev.* [Online] **2010**. *34*, **1015-1036**.

37. Sculpt Users Guide. MDL Information Systems, Inc. (1999).

38. SDS CD-EMC. University La Sapienza of Rome. http://schubert.bio.uniroma1.it/CEMC/ (accessed July 2013).

39. Sigma Aldrich.com website. http://www.sigmaaldrich.com/catalog/search/ProductDetail/SIGMA/P7794 (accessed July 2008)

40. Steinberg, H.; McCloskey, A. L. *Boron Chemistry*. The Macmillan Company, New York, 1964 Vol. 1.

41. Swiss Institute of Bioinformatics website. Swiss-PdbViewer,. www.expasy.org/spdbv/ (accessed July 2013).

42. Tortora, G. J.; Funk, B. R.; Case, C. L. *Microbiology, An Introduction*, 6th ed.; Wesley: 1998; pp 85-91, 311-317.

43. Tremblay, L. W.; Hugonnet, J.E.; Blanchard, J. S., Structure of the Covalent Adduct Formed between *Mycobacterium tuberculosis* β-Lactamase and Clavulanate. *Biochem*. [Online] **2008**, *47*, **5312-5316**.

44. Tsuzuki, S.; Honda, K.; Azumi, R.. Model Chemistry Calculations of Thiophene Dimer Interactions: Origin of π-Stacking. *J. Am. Chem. Soc*. [Online] **2002**, *124*. **12200-12209**.

45. University of Oulu website. Physical Biochemistry Protein-ligand binding. Slide 41. http://www.biochem.oulu.fi/Biocomputing/juffer/Teaching/PhysicalBiochemistry/PhysBiochem-protein-ligand.pdf (Accessed on July 2013).

46. University of Virginia Website http://cti.itc.virginia.edu/~cmg/Demo/compInh.html (accessed January 2013).

47. Usher, K. C.; Blaszczak, L. C.; Weston, G. S.; Shoichet, B. K.; Remington, S. J.. Three-Dimensional Structure of AmpC β-Lactamase from *Escherichia coli* Bound to a Transition-State Analogue: Possible Implications for the Oxyanion Hypothesis and for Inhibitor Design. *Biochem*. [Online] **1998**, *37*, **16082-16092**.

48. Verna, D.; Jacobs, D. J.; Livesay, D. R. Variations within Class-A β-Lactamase Physiochemical Properties Reflect Evolutionary and Environmental Patterns, but not Antibiotic Specificity. *Computational Biology* [Online] **2013**. *July. Vol. 9, Issue 7.* **1-16**.

49. Villacorta, M.; Arriaga, P.; Laynez, J.; Menendez, M. Interaction of β-lactamases I and II from Bacillus cereus with semisynthetic cephamycins. *Biochem, J.* [Online] **1991**, *279*, **111-114**.

50. Voladri, R. K. R.; Lakey, D. L.; Kernodle, D. Recombinant Expression and Characterization of the Major β-Lactamase of *Mycobacterium tuberculosis*. *Antimicrobial Agents and Chemotherapy* [Online] **1998**, *42*, **1375-1381**.

51. Weston, G. S.; Blazquez, J.; Baquero, F.; Schoichet, B. K. Structure-Based Enhancement of Boronic Acid-Based Inhibitors of AmpC β-lactamase. J. Med. *Chem*. [Online] **1998**, *41*, **4577-4586**.

52. World Heath Organization website http://www.who.int/tb/challenges/xdr/facts_nov (accessed August 2008).

Other readings.

1. Ambler, R. P.; Coulson, A. F. W.; Frere, J. M. Ghuysen; Joris, B.; Forsman, M.; Levesque, R.C.; Tiraby, G.; Waley, S. G. A standard numbering scheme for the Class A β-lactamases. *Biochem. J.* [Online] **1991, 276-272**.

2. Crompton, I. E.; Cuthbert, B. K.; Lowe, G.; Waley, S. G.; β-Lactamase inhibitors – The inhibition of serine β-lactamases by specific boronic acids. *Biochem J.* [Online] **1998**, *251*, **453-459.**

3. Davies, R. B.; Abraham, E. P. Separation, Purification and Properties of β- Lactamase I and β-Lactamase II from Bacillus cereus 569/H/9. *Biochem. J.* [Online] **1974**, *143*, **115-127.**

4. Evans Group website. An Introduction to Hydrogen Bonding. http://www2.lsdiv.harvard.edu/labs/evans/pdf/smnr_2009_Kwan_Eugene.pdf (Accessed July 2013).

5. Garland, C. W.; Nibler, J. W.; Shoemaker, D. P.; *Experiments in Physical Chemistry*, 7th ed.; Mc Graw Hill: Boston, 2003; pp 42-43, 689.

6. Joule, J. A.; Mills, K.; *Heterocyclic Chemistry at a Glance*, 2nd ed.; Wiley: 2013; pp 23, 157, 177.

7. Lammert, John M. *Techniques in Microbiology*. Prentice Hall, Upper Saddle River, NJ. 2007; pp 1-60.

8. Massova, I.; Kollman, P. A. pKa, MM, and QM Studies of Mechanisms of β-Lactamases and Penicillin-Binding Proteins: Acylation Step. *Journal of Computational Chemistry*. [Online] **2002**, *Vol. 23, No. 16*, **1559-1576.**

9. Organic chemistry portal http://www.organic-chemistry.org/namedreactions/suzuki-coupling.shtm (accessed July 2008).

10. Prague, C. N.; Access 97 Bible. Foster City CA 1997.

11. Protein science org website https://www.proteinscience.org (Accessed July 2008).

12. Surles, M. C.; Richardson, J. S.; Richardson, D. C.; Brooks Jr., F. P. Sculpting proteins interactively: Continual energy minimization embedded in a graphical modeling system. *Protein Science* [Online] **1994**, *3,* **198-210**.

13. Tafi, A.; Agamennone, M.; Tortorella, P.; Alcaro, S.; Gallina, C. AMBER force field implementation of the boronate function to simulate the inhibition of β-lactamases by alkyl and aryl boronic acids. *European Journal of Medicinal Chemistry* [Online] **2005,** *40*. **1134-1142**.

14. Tremblay, L. W.; Fan, F.; Blanchard, J. S. Biochemical and Structural Characterization of *Mycobacterium tuberculosis* β-Lactamase (BlaC) with the Carbapenem and Doripenem. *Biochemistry* [Online] **2010**, *May 4, 49(17),* **3766-3773**.

15. Wang, F.; Craig, C.; Sacchettini, J. C. Crystal Structure and Activity Studies of the *Mycobacterium tuberculosis* β-Lactamase Reveal Its Critical Role in Resistance to β-lactam Antibiotics. *Antimicrobial Agents and Chemotherapy*. [Online] **2006**. *August.* **2762-2771**.